

**Phosphatidylinositol-specific phospholipase C interaction with G-proteins in
relation to the environmental stress response in wheat (*Triticum aestivum*)**

Hala Badr Abdel-Sadek Khalil

**A Thesis in the Department of
Biology**

**Presented in Partial Fulfillment of the Requirements for the
Degree of Master of Science at**

**Concordia University
Montreal, Quebec, Canada**

September 2009

© Hala Badr Abdel-Sadek Khalil, 2009



Library and Archives
Canada

Published Heritage
Branch

395 Wellington Street
Ottawa ON K1A 0N4
Canada

Bibliothèque et
Archives Canada

Direction du
Patrimoine de l'édition

395, rue Wellington
Ottawa ON K1A 0N4
Canada

Your file *Votre référence*
ISBN: 978-0-494-63021-1
Our file *Notre référence*
ISBN: 978-0-494-63021-1

NOTICE:

The author has granted a non-exclusive license allowing Library and Archives Canada to reproduce, publish, archive, preserve, conserve, communicate to the public by telecommunication or on the Internet, loan, distribute and sell theses worldwide, for commercial or non-commercial purposes, in microform, paper, electronic and/or any other formats.

The author retains copyright ownership and moral rights in this thesis. Neither the thesis nor substantial extracts from it may be printed or otherwise reproduced without the author's permission.

In compliance with the Canadian Privacy Act some supporting forms may have been removed from this thesis.

While these forms may be included in the document page count, their removal does not represent any loss of content from the thesis.

AVIS:

L'auteur a accordé une licence non exclusive permettant à la Bibliothèque et Archives Canada de reproduire, publier, archiver, sauvegarder, conserver, transmettre au public par télécommunication ou par l'Internet, prêter, distribuer et vendre des thèses partout dans le monde, à des fins commerciales ou autres, sur support microforme, papier, électronique et/ou autres formats.

L'auteur conserve la propriété du droit d'auteur et des droits moraux qui protègent cette thèse. Ni la thèse ni des extraits substantiels de celle-ci ne doivent être imprimés ou autrement reproduits sans son autorisation.

Conformément à la loi canadienne sur la protection de la vie privée, quelques formulaires secondaires ont été enlevés de cette thèse.

Bien que ces formulaires aient inclus dans la pagination, il n'y aura aucun contenu manquant.


Canada

CONCORDIA UNIVERSITY

School of Graduate Studies

This is certify that the thesis prepared

By: Hala Badr Abdel-Sadek Khalil

Entitled: Phosphatidylinositol-specific phospholipase C interaction with G-proteins in relation to the environmental stress response in wheat
(Triticum aestivum)

and submitted in partial fulfillment of the requirements for the degree of

Master of Science (Biology)

Complies with the regulations of the University and meets the accepted standards with respect to originality and quality.

Signed by the final examining committee:

-----Chair

-----Examiner

-----Examiner

-----Examiner

-----Supervisor

Approved by

Chair of Department or Graduate Program Director

10 September 2009

Dean of Faculty

ABSTRACT

Phosphatidylinositol-specific phospholipase C interaction with G-proteins in relation to the environmental stress response in wheat (*Triticum aestivum*)

Hala Badr Abdel-Sadek Khalil

Tolerance to environmental stress in plants is controlled by several internal factors and environmental signals. In this study, we have focused on phosphatidylinositol-specific phospholipase C (TaPI-PLC) and phosphoglycerol-specific phospholipase C (TaPG-PLC) in wheat, *Triticum aestivum*. Three homologs of TaPG-PLCs were identified as cDNA with high sequence similarity to rice and Arabidopsis PG-PLC1. TaPG-PLC3 was mapped on the distal part of the long arm of chromosome 5A, whereas TaPG-PLC1 and TaPG-PLC2 like genes appear to be duplicated in two of hexaploid wheat 3 three genomes. A TaPG-PLC1::Green fluorescent protein (GFP)-fusion was localized on endoplasmic reticulum (ER), golgi and plasma membrane (PM). Important protein-protein interactions were found for wheat PI-PLCs. The PI-PLC1::GFP fusion was localized on ER and PM. *In vivo* interactions between TaPI-PLC1 and two classes of G-proteins, the heterotrimeric G protein subunit TaG α and a non-canonical G-protein J822, were detected using Bimolecular Fluorescent Complementation (BiFC). The interactions were detected in both the ER and PM. In contrast, TaPI-PLC2::GFP fusion was localized only on PM and was not found to interact with TaG α or J822. Since both TaPI-PLC1 and J822 are up-regulated by cold stress and it is possible that they play an important role in signaling during cold acclimation.

ACKNOWLEDGMENTS

First of all, I would like to express my deepest thanks to my God, the most merciful who give me the ability in all my entire life.

I would like to like to express my gratitude to my supervisors Dr. Patrick Gulick for his incredible patience to guide me through this research. It has been excellent opportunity for me to work in his lab. I also truly appreciate his endless morale and his ability to help his students.

My warmest grateful also goes to my committee members Dr. Varin Luc and Dr. Bill Zerges who gave me suggestions, constructive criticism, and excellent advice in my research.

I would also like to thank Dr. Jean Danyluk, from Université du Quebec a Montréal (UQAM), Dr. Francois Laliberté, Institute Armand Frappier, Laval and Dr. Alan M. Jones, University of North Carolina, for providing me with wheat cDNA libraries, tobacco seeds and BiFC vectors, respectively.

My appreciation goes to my colleagues, Zhejun Wang who cloned G α protein and made it available to me for my work, Ariel Denajo who did a great job to clone PI-PLC1 and Nesreen Abdel Mageed who did the bioinformatics analysis for PI-PLC2.

I would like to express my sincere appreciation to all my laboratory members who contributed to this wok for their help and advice in many situations. I deeply appreciate them and I hope we can keep in touch.

Many thanks to the Biology and Biochemistry departments at Concordia University for the knowledge I gained from the professors, staffs and graduate students.

My last, but not least gratitude is for my family members and especially to my dear parents who have given me so much and who have encouraged me so much.

My warmest gratitude goes to all my friends, roommates and colleagues have helped and supported.

TABLE OF CONTENT

LIST OF FIGURES.....	IX
LIST OF TABLES.....	XI
PART I. INTRODUCTION.....	1
1. Polyploidization in wheat genome.....	2
1.1. Nulisomic, ditelosomic and chromosome bin mapping in wheat gene.....	3
2. Phospholipid structure and phospholipase activities.....	4
2.1. PI-PLC and Signal transduction in eukaryotes.....	5
2.2. PG-PLC and Phosphatidylglycerol hydrolysis.....	6
2.3. GTP-binding proteins activate PLCs during signal transduction	8
3. Signal transduction during cold acclimation in plants.....	9
3.1. Phospholipid and phospholipase dynamics during cold accumulation	10
3.2. GTP-binding proteins in signal transduction during cold accumulation..	11
4. Subcellular localization of desired protein	12
4.1. GFP	13
4.2. GFP Applications in plants.....	14
5. Protein-protein interaction studies	15
5.1. Bimolecular fluorescent complementation (BiFC).....	16
PART II. MATERIALS AND METHODS	17
1. Bioinformatic resources.....	17
2. Plant materials.....	17
3. Plant growth conditions.....	18
3.1. Soil preparation.....	18

3.2. Triticum, Aegilops and Tobbaco growth conditions	18
4. Chinese spring Triticum aestivum cytogenetic stocks.....	18
5. Fluorescent organelle markers	20
6. Modified plant genomic DNA extraction using CTAB	20
6.1. Buffers	20
6.2. DNA extraction procedure.....	21
7. Agarose gel electrophoresis.....	22
8. Gateway cloning system.....	22
8.1. BP Reaction	22
8.2. LR Reaction.....	23
9. TaPG-PLC cDNA sequencing and analysis.....	24
10. TaPG-PLC homolog mapping.....	24
10.1. TaPG-PLC homolog genome mapping	24
10.2. Chromosome assignment and bin map of TaPG-PLC1-3	28
11. TaPI-PLC1 full length cDNA cloning.....	28
12. Subcellular localization of fluorescent protein and in vivo p.....	30
12.1. Generating entry clones	30
12.2. Plant expression clones.....	31
12.3. Agrobacterium transformation	32
12.4. Agroinfiltration.....	32
12.5. Confocal laser scanning microscopy	33
PART III. RESULTS.....	34
1. PG-PLC1 sequence analyses.....	34

2. Mapping of TaPG-PLC homologs.....	37
2.1. TaPG-PLC genome mapping.....	37
2.2. Chromosome assignment and bin map of TaPG-PLC3.....	38
3. <i>Triticum aestivum</i> full-length TaPI-PLC1 cDNA clone isolation...41	
4. Generating Gateway TaPI-PIC and TaPG-PLC fluorescent fusion..44	
5. Subcellular localization of TaPG-PLC and TaPI-PLCs.....	46
5.1. Subcellular localization of TaPG-PLCs	46
5.2. Subcellular localization of TaPI-PLCs	51
6. <i>In vivo</i> interactions between wheat PLC genes and GTP-binding ...56	
6.1. <i>In vivo</i> interactions between wheat PLC genes and G α using BiFC.....	56
6.2. <i>In vivo</i> interactions between wheat PLC genes and the wheat J822	57
PART IV. DISCUSSION.....	60
1. TaPG-PLC annotation.....	60
2. TaPG-PLC mapping on wheat genome.....	61
3. TaP1-PLC sequence analyses	64
4. The relation between some isoforms of PI-PLC and the envir.....	65
5. The localization of TaPG-PLC in plants.....	67
5.1. TaPG-PLC localized in ER, Golgi and PM.....	67
5.2. TaPG-PLC homologs and secretion pathway.....	67
6. Subcellular localization of TaPI-PLCs in plants.....	69
6.1. TaPI-PLC1 and TaPI-PLC2 were localized on ER and PM, respectively	69
6.2. The effect of EF-hand and C2-2 domains on TaPI-PLC2 trageting to ...	71

7. TaPI-PLC1 and TaG α and their relations in signal transduction...	71
8. TaPI-PLC1 and j822 non canonical GTP-binding protein inter.....	73
9. Future studies.....	73
REFERENCES.....	75
APPENDICES.....	84

LIST OF FIGURES

Figure 1:	Common phospholipids structure and phospholipase hydrolysis.....	7
Figure 2:	Signal transduction pathway in eukaryotic cells.....	7
Figure 3:	Scheme of Gateway BP and LR recombination reactions.....	23
Figure 4:	The multiple amino acids sequence alignments for the three homo....	35
Figure 5:	Phylogram of PG-PLCs in wheat (Ta), Arabidopsis (At) and rice	37
Figure 6:	Genome mapping of TaPG-PLC1, TaPG-PLC2 and TaPG-PLC3.....	39
Figure 7:	Mapping of TaPG-PLC1-3 using cytogenetic stocks of hexaploid C..	40
Figure 8:	Nucleotide sequence of TaPI-PLC1 full length cDNA and predicted .	42
Figure 9:	Multiple alignments between Ta (<i>Triticum aestivum</i>) PI-PLC1, Os (<i>Oryza sativa</i>) PI-PLC1, Zm (<i>Zea mays</i>) PI-PLC, and At (<i>Arabidopsis thaliana</i>) PI-PLC6.....	45
Figure 10:	PCR products of PG-PLC1 homologs and their truncations.....	45
Figure 11:	PCR products of TaPI-PLC1 and TaPI-PLC2 and some truncations...	45
Figure 12:	Endoplasmic reticulum like structure of TaPG-PLC::GFP fusions in epidermic tobacco tissues.....	49
Figure 13:	Co-localization of TaPG-PLC1::GFP with sex mCherry organelle markers.....	50
Figure 14:	Subcellular localization of TaPG-PLC1 Δ NT::GFP truncation in epidermic tobacco tissues.....	52
Figure 15:	Endoplasmic reticulum like structure of TaP1-PLC1::GFP fusion in epidermic tobacco tissues.....	52
Figure 16:	Plasma membrane like structure of TaP1-PLC2::GFP fusion in epidermic tobacco tissues.....	52
Figure 17:	Co-localization of TaPI-PLC1::GFP with six mCherry organelle markers.....	53
Figure 18:	Co-localization of TaPI-PLC2::GFP with Six mCherry organelle marks.....	54

Figure19:	Co-localization of TaPI-PLC2 Δ EF-hand::GFP with PM (Plasma Membrane) mCherry marker in epidermic tobacco tissues.....	55
Figure 20:	Co-localization of TaPI-PLC2 Δ C2-2::GFP with ER (Endoplasmic Reticulum) mCherry marker in epidermic tobacco tissues.....	55
Figure 21:	BiFC visualization of TaPI-PLC1 and TaGa in epidermic tobacco tissues.....	58
Figure 22:	BiFC visualization of TaPI-PLC1 and J822 in epidermic tobacco tissues.....	59
Figure 23:	Chromosome bin map of 5A in wheat the predicted position of TaPG-PLC1-3 in wheat the colinearity between chromosome 5A in wheat and its relative to rice genome.....	63

LIST OF TABLES

Table 1:	<i>Triticum</i> and <i>Aegilops</i> species used for genome designation.....	18
Table 2:	Chinese <i>Triticum aestivum</i> cytogenetic stocks used for chromos.....	19
Table 3:	Organelle markers as red fluorescent-protein fusions.....	20
Table 4:	Oligo nucleotide PCR primers were used in this study.....	25
Table 5:	PG-PLC annotation in Arabidopsis and rice.....	36
Table 6:	The Gateway entry clones and GFP fusion constructs for expression in <i>N. benthamiana</i>	47
Table 7:	The prediction of subcellular localization of candidate proteins with 4 prediction algorithms.....	48
Table 8:	PI-PLCs of wheat, rice and Arabidopsis involvement in environmental stress.....	66
Table 9:	The deduced amino acid sequences of TaPG-PLC signal peptides.....	68
Table 10:	The localization of higher plant PI-PLCs.....	70

PART I. INTRODUCTION

Sequencing of the model plant genomes, such as those of *Arabidopsis thaliana* and rice (*Oryza sativa*), has revolutionized our understanding of plant biology but it has yet to translate into the improvement of major crop species such as wheat (*Triticum aestivum*), maize (*Zea mays*), or barley (*Hordeum vulgare*). The genome size of hexaploid wheat (16,979 Mbp) is the largest among all cereal crops, including maize (2671 Mbp), sorghum (*Sorghum bicolor*; 735-1642 Mbp) and rice (490 Mbp) (Huang *et al.*, 2002). Because of the large size of the hexaploid wheat genome, the complete sequencing has not been feasible. However, the large scale expressed sequence tag (EST) sequencing and comparison to the rice genome has given an important insight into the gene content of wheat (Peng *et al.*, 2004). Moreover, cytogenetic studies and gene mapping in wheat have allowed the identification and characterization of the different homeologous genomes and have demonstrated the utility of studying wheat genome evolution as a model for the analysis of polyploidization, a major force in the evolution of the eukaryotic genomes (Feuillet and Muehlbauer, 2009).

In general, plants have an outstanding ability to cope with highly variable environmental stresses, including cold, drought, salinity and nutrient availability. These stresses together represent the primary cause of crop loss worldwide (Boyer 1982). Low temperature and freezing tolerance are polygenic traits involving a large number of genes, whose expressions are controlled by low temperature. Alterations in the expression levels of these genes lead to the numerous molecular and physiological changes characteristic of the cold acclimation process. The complexity of the acclimation

process is reflected in the number of genes that are affected by low temperature, which according to a recent estimate is up to 25% of the transcriptome in *Arabidopsis* (Krebs *et al.*, 2002).

Many reports have identified cold acclimation-induced genes from many plant species including winter wheat. Microarray analysis led to the discovery of 43 novel genes that are differentially regulated between spring and winter cultivars. The genes include C86, F29, J822, J900 and J925 whose BLAST-based annotations are glycine rich protein, a receptor-like kinase, GTP binding regulatory protein, calcium binding EF-hand and Ras-related GTP-binding protein, respectively (Gulick *et al.*, 2005). Such stress regulated candidate genes serve as a starting point for further investigation of regulatory and signaling elements that control the coordinated gene expression that is essential for understanding cold acclimation and the genetic basis of cold tolerance.

1. Polyploidization in wheat genome

Common bread wheat is an allohexaploid with 42 chromosomes and a basic chromosome number of 7 groups; each group contains a set of three homeologous chromosome pairs belonging to the A, B, and D genomes. The genus *Triticum* includes several groups of polyploids such as tetraploid *T. turgidum* and *T. timopheevii* with genomes AB and AG, respectively, in addition to hexaploid *T. aestivum* (genome ABD). The source of the A genome may be two diploid species, *T. monococcum* (A_m) and *T. urartu* (A_u); the latter species is thought to be most closely related to the A genomes of *T. turgidum* and *T. aestivum*. The potential donor of the hexaploid wheat D genome is *Aegilops tauschii*. The origin of the B and G genomes is still under discussion. The most probable donors of these genomes may be extinct relatives of *Ae. speltoides*, *Ae. bicornis*,

Ae. searsii, *Ae. longissima*, and *Ae. sharonensis*. *Ae. speltoides* genome is most closely related to both B and G genomes (Shcherban *et al.*, 2004).

1.1. Nullisomic, ditelosomic and chromosome bin mapping in wheat genes

Because of triplication of genetic material, wheat can tolerate the loss of whole chromosomes, and chromosome arms and segments (Sears, 1966; Endo and Gill, 1996). The use of nullisomic-tetrasomic, ditelosomic, and deletion lines missing successive terminal segments allows for the mapping of molecular markers to chromosomes, arms, and chromosome bins within arms. Aneuploids and deletion lines have been used extensively in mapping studies (Gill *et al.*, 1993). Recently, taking advantage of gametocidal chromosome introduced from *Ae. cylindrica* host, wheat stocks containing terminal chromosomal deletions of various lengths have been developed and 436 deletion lines involving all 21 wheat chromosomes have been isolated (Endo and Gill, 1996). These cytogenetic stocks have been exploited for large-scale mapping of molecular markers into chromosomal bin regions delineated by neighboring deletion breakpoints (Werner *et al.*, 1992; Qi and Gill, 2001). The deletion stocks have been used extensively in mapping genes controlling phenotypic traits (Endo *et al.*, 1991; Mukai and Endo, 1992) and biochemical markers (Yamamori *et al.* 1994). The deletion stocks are ideally suited for mapping co-dominant biochemical and DNA markers. The most of the DNA markers are located in parallel positions on all three homeologous chromosomes of the A, B and D genomes. This fact enables the construction of a consensus map for each homeologous group of wheat, a hypothetical map comprising all the DNA markers of the three homeologues (Endo and Gill, 1996). There has also been extensive mapping of the wheat genome using classical crosses and recombinant populations (Singh *et al.*, 2007).

2. Phospholipid structure and phospholipase activities:

The common phospholipids are membrane components represented in Figure (1). The structure of phospholipids consists of two fatty acyl chains esterified to glycerol backbone at sn-1 and sn-2 positions, a phosphate at sn-3 position (creating the “phosphatidyl” moiety), to which a variable head group (R) is attached (Munnik *et al.*, 1998). Phospholipases are a diverse set of enzymes that hydrolyze phospholipids. Multiple forms of phospholipase D, C, and A have been characterized in plants. These enzymes are involved in a broad range of functions in cellular regulation, lipid metabolism, and membrane remodelling. Phospholipid-signaling systems are grouped according to the phospholipases that initiate the formation of the messenger molecules. Phospholipase D (PLD) releases the head group from PA (Phosphatidic acid); phospholipase C (PLC) cleaves the head group and the sn-3 phosphate from Diacylglycerol (DAG), which usually is rapidly phosphorylated by DAG-kinase to form Phosphatidic acid (PA) (Lundberg and Sommarin, 1992). Phospholipase A₁ (PLA₁) cleaves the fatty acid residue from the sn-1 position and PLA₂ cleaves the fatty acid residue from the sn-2 position of the phospholipids (Meijer and Munnik, 2003). The products of PLA₁, A₂, C, or D activity have been implicated in signaling cascades (Laxalt and Munnik, 2002; Meijer and Munnik, 2003; Wang *et al.*, 2000; Wang, 2002), which have been shown to regulate stress tolerance partly through modulation of stress-responsive gene expression (Zhu 2002). Hence, activation of phospholipases often is an initial step in generating second messengers.

PLCs hydrolyze the glycerolphosphate ester linkage of phospholipids to DAG and phosphorylated head group. According to substrate specificity and cellular function, PLCs

in plants can be divided into three groups: (a) the phosphoinositide specific phospholipase (PI-PLC) that hydrolyzes phosphoinositides, (b) the nonspecific-PLC that acts on the common phospholipids such as phosphatidylglycerol and phosphatidylcholine (PtdCho) and some other phospholipids and (c) the glycosylphosphatidylinositol (GPI)-PLC that hydrolyses GPI-anchor on proteins (Wang, 2001). This study concentrates on two groups of PLCs; PI-PLC and phosphoglycerol specific phospholipase (PG-PLC) and their relation with the signal transduction in hexaploid wheat.

2.1. PI-PLC and Signal transduction in eukaryotes

PI-PLC is better understood than other PLCs. The PI-PLCs in mammalian systems comprise at least ten different isoenzymes, which are divided into three classes PLC β , γ and δ based on the sequence homology and mechanism of activation (Williams, 1999). Multiple PLCs have been cloned from plants, such as Arabidopsis (Hartweck *et al.*, 1997), soybean (Shi *et al.*, 1995) and potato (Kopka *et al.*, 1998). Plant PI-PLCs are closely related to mammalian PLC δ (Munnik *et al.*, 1998). Plant PI-PLCs all contain X domain and Y domain that are necessary for the phosphoesterase activity, and a C2 domain toward the C terminus which is a Ca^{2+} - binding domain. PI-PLCs hydrolyze the glycerolphosphate ester linkage on the phospholipid to release DAG and phosphorylated inositol. Plant PI-PLCs lack the Pleckstrin homology domain which is found in mammalian PI-PLCs, which has a lipid binding function thought to play a role in directing PI-PLCs to specific membranes.

The increase in cytosolic Ca^{2+} is often preceded by hydrolysis of phosphatidylinositol 4,5-bisphosphate (PIP₂), a phospholipid found in plasma membrane.

The binding of hormones to their receptor triggers activation of a specific G protein, which activates phospholipase C (PLC). PI-PLC hydrolyses PIP₂ to DAG and inositol 1,4-triphosphate (IP₃) (Figure 2). IP₃ diffuses in the cytosol where it triggers the release of calcium from intracellular stores, while DAG remains in the membrane. In the animal cells, DAG activates certain members of the protein kinase C (PKC) family, but in plants these enzymes do not seem to exist, as they are not encoded in Arabidopsis genome (Meijer and Munnik, 2003). DAG is immediately phosphorylated to PA by DAG kinase (DGK) (Munnik, 2001).

2.2. PG-PLC and Phosphatidylglycerol hydrolysis

Phosphatidylglycerol (PG) is found in almost all organisms and it is essential for oxygenic photosynthesis in plants and cyanobacteria. Thylakoid membranes in the chloroplasts are composed predominantly of glycerolipids, such as monogalactosyldiacylglycerol (MGDG), digalactosyldiacylglycerol (DGDG) and sulfoquinovosyldiacylglycerol (SQDG) (Siegenthaler, 1998). By contrast, PG is the only phospholipid found in thylakoid membranes which are the site of photosynthetic light reactions and electron transport (Joyard *et al.*, 1998). In higher plants, PG is synthesized in at least three subcellular compartments; plastids, endoplasmic reticulum and mitochondria (Ohlrogge and Browse, 1995).

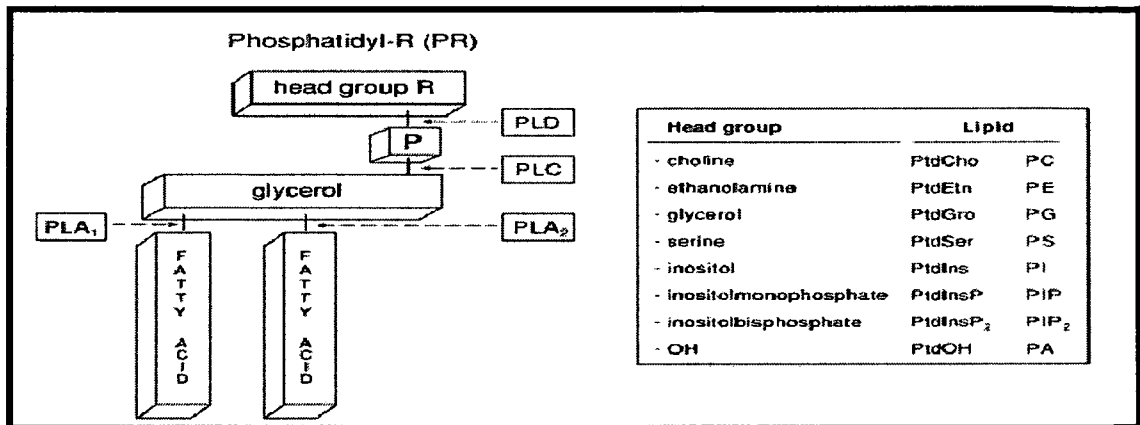


Figure (1): Common phospholipids structure and phospholipase hydrolysis. There are multiple forms of phospholipases; ie; D, C and A. These enzymes are involved in a broad range of functions in cellular regulation, lipid metabolism and membrane remodeling. Phospholipases are classified into five major groups: phospholipase D (PLD), C (PLC), A2 (PLA2), A1 (PLA1), and B (PLB) according to their sites of hydrolysis on phospholipids (The figure is taken from Meijer and Munnik, 2003).

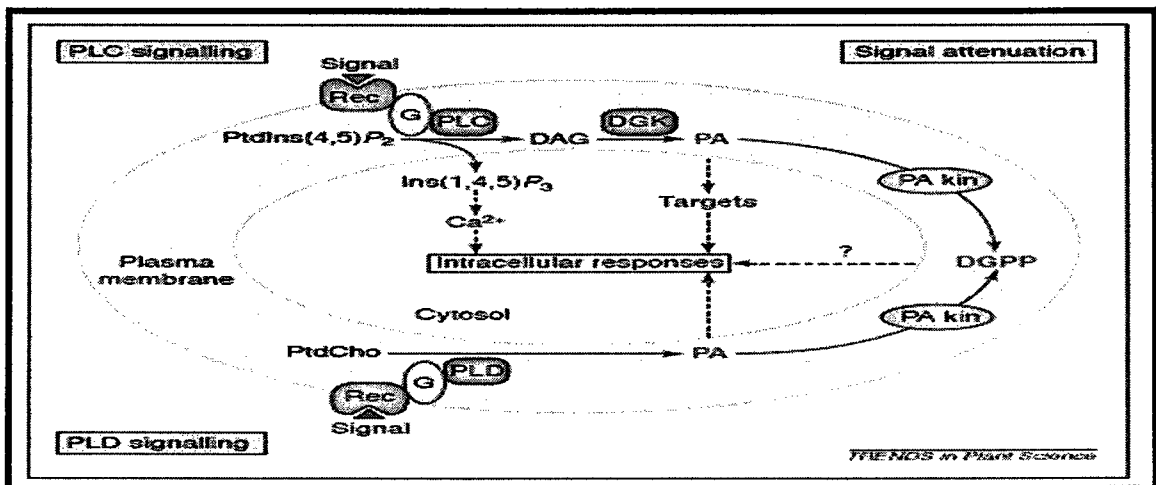


Figure (2): Signal transduction pathway in eukaryotic cells. The main character in the pathway is PA . PA is produced directly via activation of phospholipase D (PLD) enzyme which hydrolyzes Phosphatidyl Choline (PC). PI-PLC hydrolyzes phospholipids (PIP₂) to generate IP₃ and DAG. IP₃ diffuses into cytosol for releasing Ca²⁺ from intracellular stores. DAG remains in membrane where it is phosphorylated to phosphatidic acid (PA) by DAG kinase (DGK) (The figure is taken from <http://home.medewerker.uva.nl/t.munnik/>).

2.3. GTP-binding proteins activate PLCs during signal transduction

In the animal model of PLC, the signaling is initiated from a receptor. This receptors activates G proteins, which activate intracellular effector enzymes such as PLC and PLD to produce second messengers (IP₃, DAG or PA). A common mechanism of signal transduction in animal cells involves the activation of heterotrimeric G proteins which behave as molecular switches that can rapidly change from an active GTP bound form to the inactive GDP bound form (Hepler and Gilman, 1992). The existence of homologous genes for these proteins suggests that similar signaling also functions in plants. Biochemical and molecular analyses have demonstrated that heterotrimeric G proteins are present in plants and their activation has been shown to stimulate effector enzymes and induce physiological responses (Bolwell *et al.*, 1991). In recent years, much has been learned about the diversity of signal transduction through plant G proteins. The identification and mutation of genes in Arabidopsis and rice play an important role in the analysis of G-protein signaling. The α , β and γ subunits of G protein heterotrimer have been identified in several plant species. The Arabidopsis genome contains only one canonical $G\alpha$ gene, GPA1 (Ma *et al.*, 1990). GPA1 is a single copy gene in Arabidopsis, but some polyploid species such as soybean have been shown to have two closely related GPA1 genes (Kim *et al.*, 1995).

Solubilization of a receptor-G-protein-PLC complex has been achieved, indicating a physical association of these components (Aiyar *et al.*, 1999). Misra *et al.*, (2007) presented the first direct evidence in plants that phospholipase C (PLC) functions as an intracellular effector molecule for the α -subunit of pea (*Pisum sativum*)

heterotrimeric G protein and regulates its activities. Protein-protein interaction studies using *in vitro*, yeast two hybrid system and *in vivo* co-immunoprecipitation showed that $G\alpha$ protein interacts with the calcium-binding domain (C2) of the pea phospholipase C (PLC δ).

3. Signal transduction during cold acclimation in plants

The response of plants to any environmental signal is mediated by a series of reactions, collectively referred to as signal transduction. Low temperature signal transduction starts with the perception of the cold signal by a yet unidentified receptor located presumably at the plasma membrane. A putative sensor protein has been proposed to detect physical phase transitions in microdomains of the plasma membrane as a result of temperature shifts (Murata and Los, 1997). Ding and Pickard (1993) have shown that the tension-dependent activity of a mechanosensitive Ca^{2+} channel in onion increases when temperature is lowered. The reason for this enhancement is not known, but they proposed that changes in membrane properties or properties of the channel itself are important. The elevation in cytosolic Ca^{2+} from extracellular spaces is an early event in the response to cold. This cytosolic Ca^{2+} is suggested as an important second messenger in low temperature signal transduction and developing cold acclimation. A positive correlation between cold-induced Ca^{2+} influx and accumulation of cold-induced transcripts has been shown for alfalfa (Monroy and Dhidsa, 1995) and Arabidopsis (Henriksson and Trewavas, 2003). Knight *et al.*, (1991) used a transgenic approach to demonstrate a transient increase in cytosolic Ca^{2+} in response to cold. Transgenic plants of Arabidopsis and tobacco, which expressed the calcium-sensitive luminescent protein aequorin demonstrated a rise in cytosolic Ca^{2+} concentration in response to low

temperature. In addition to cold, cytosolic Ca^{2+} influx was also observed with other environmental stresses, which suggests that, there is a specific signature of the cytosolic Ca^{2+} for different stresses. Ca^{2+} signature can be described in terms of the characteristics of the time course of changes in cytosolic Ca^{2+} (Evans *et al.*, 2001; Plieth, 2005). Various abiotic stress responses use Ca^{2+} from different subcellular sources, including the extracellular compartment, vacuole and mitochondria (Knight *et al.*, 1996; Subbaiah *et al.*, 1998).

3.1. Phospholipid and phospholipase dynamics during cold accumulation

Changes in phospholipids in plants responding to cold temperature have been investigated many times from a structural viewpoint. It has been shown repeatedly that the total phospholipid content increased during cold acclimation of wheat plants (Willemot and Pelletier, 1980). In Arabidopsis, drought and low temperature increased the mRNA levels of AtPLC1, but the AtPLC2 gene was expressed constitutively (Hirayama *et al.*, 1995). Moreover, lipid profiling has been applied to analyze changes in lipid molecular species of Arabidopsis under low temperature stresses. Significant changes in membrane lipid molecular species occurred when Arabidopsis plants were cold-acclimated at 4°C (Welti *et al.*, 2002). De Nisi and Zocchi, (1996) showed that in the roots of maize plantlets, a cold exposure induced a decrease in the level of membrane polyphosphoinositide. In addition, Vergnolle *et al.*, (2005) analyzed the transcriptome of cold treated Arabidopsis suspension cells in presence of inhibitors of PLCs and PLDs and reported that the expression of most cold responsive genes was affected by the inhibitors. Their results suggest that both the PLCs and PLDs are elements of two distinct cold signaling pathways. Changes in IP₃ levels have often been linked with changes in activity

of PI-PLC (Krinke *et al.*, 2007). Moreover, RT-PCR results showed the different cold induction patterns between PI-PLC and PG-PLC. Both genes were strongly induced from day 1 to day 14 of cold acclimation (Liu, 2005).

3.2. GTP-binding proteins in signal transduction during cold accumulation

Some G proteins have been identified in plants to be involved in stress regulation. G protein-associated receptors might also serve as membrane-bound receptors for regulating ion channels and abscisic acid (ABA) signaling in Arabidopsis guard cells. In Arabidopsis, the GPA1 gene encodes the α subunit of a G protein. Mutants of GPA1 have disrupted stomatal regulation, are insensitive to ABA, and the rate of water loss from *gpa1* mutants is greater than that from wild-type plants (Wang *et al.*, 2001).

J822 is a novel cold regulated gene in wheat which encodes a predicted guanine nucleotide binding protein based on high sequence similarity to GTP binding domain of known G-protein was identified in a previous study of gene expression by microarray analyses (Gulick *et al.*, 2005). J822 does not have significant sequence similarity to heterotrimeric G proteins and was hypothesized to be a non canonical G-protein (Liu, 2005). RT-PCR was carried out to analyze the effect of cold acclimation on J822 in winter and spring wheat cultivars. The results showed that J822 was more strongly induced in the highly freezing tolerant winter wheat cultivars and in cold sensitive spring wheat cultivars and those J822 transcripts were induced within the first 24 hours of cold acclimation (Gulick *et al.*, 2005). Yeast two-hybrid screening and Bimolecular Fluorescent Complementation (BiFC) showed that J822 interacts with proteins derived from partial length cDNA clones of PI-PLC1 and PG-PLC1 (Tardif *et al.*, 2007).

4. Subcellular localization of proteins

Protein subcellular localization, consequent to protein trafficking is a key functional characteristic of proteins. Therefore, comprehensive knowledge on the subcellular localization of proteins is essential for understanding their roles and interacting partners in cellular metabolism (Garg *et al.*, 2008).

Computational approaches to predict protein localization are helpful but not conclusive. These methods for predicting subcellular localization can be broadly divided into two types: predictions on the basis of finding homology to annotated proteins and machine learning approaches for making predictions. The former method attempts to classify an unknown protein to a subcellular class on the basis of homology (Marcotte *et al.*, 2000) or conserved motifs (Scott *et al.*, 2004). A major limitation of this method is its inability to correctly classify a protein which has insufficient homology to a known protein. The other approach, i.e. machine learning techniques, infers a predictive model from proteins with a known localization pattern in which pattern conservation is refined by reiterative comparison to proteins of known function. This approach requires the conversion of the amino acid sequence to indices that characterize the biochemical properties of the protein (Garg *et al.*, 2008).

A recent and potentially powerful tool for studying the *in vivo* subcellular localization of a protein is the Green Fluorescent Protein (GFP). Fusion of the GFP coding sequence to coding regions of genes of unknown location has therefore become an extremely valuable tool for determining the localization of proteins for giving insight into biochemical or regulation process within the plant cell (Galvez *et al.*, 1998).

4.1. GFP

The importance of GFP was recognized in 2008 when the Nobel committee awarded Osamu Shimomura, Marty Chalfie and Roger Tsien the Chemistry Nobel Prize for the discovery and development of GFP. Wild type GFP originally isolated from jellyfish (*Aequorea victoria*) consists of 238 amino acids (Prasher *et al.*, 1992). Residues 65-67 (Ser-Tyr-Gly) in the GFP sequence form the fluorescent chromophore (Heim *et al.*, 1994). Wild type GFP has a major excitation peak at a wavelength of 395 nm and a minor one at 475 nm and its emission peak is at 509 nm (Tsien, 1998). GFP is the only well-characterized example of a protein which displays strong visible fluorescence without any additional substrates or co-factors (Heim and Tsien, 1996) and it is not necessary to destroy the tissue to visualize the fluorescent emission. In addition, GFP has a broad range of pH stability, retaining conformation from pH 5.5–12.0, and is extremely thermostable, surviving temperatures up to 65°C (Bokman and Ward, 1981). Therefore, GFP provides a universal protein tag that can be used to visualize a virtually unlimited number of spatial and temporal processes in all living systems.

GFP retains fluorescence when fused to another protein both on the N- and C-terminal ends. This makes it an attractive fluorescent tag to monitor number of phenomena in living cells and organisms (Sheen *et al.*, 1995). Because the fluorescence emission of wild-type GFP is poorly detectable in a number of plant species including tobacco, several GFP mutants have been created to make this protein a suitable marker in plant systems (Ward *et al.*, 1982) and (Yang *et al.*, 1996). Such modifications have been carried out by Chiu *et al.*, 1996 and the resulting [sGFP(S65T)] gives a 120-fold brighter signal than the original GFP in plant cells. This result has led to several examples of

brightly fluorescent transgenic tobacco lines transformed with a modified GFP (Kohler *et al.*, 1997).

4.2. GFP Applications in plants

The fact that GFP does not need any additional substrates or cofactors to fluorescence and its ability to be expressed in a variety of organisms has made it a universal reporter gene for scientific research. At the cellular level, GFP has been used in plants mainly as a subcellular targeting tool in living cells for protein localization (Kohler *et al.*, 1997) dynamics, protein trafficking, protein-protein interactions (Heinlein *et al.*, 1995), cell division (Gu and Verma, 1997), chromosome replication and intracellular transport pathways (Grebenok *et al.*, 1997). Beyond subcellular studies, GFP is being used as an *in vivo* reporter to assess frequency of transient and stable transformations (Chalfie *et al.*, 1994). Moreover, using GFP instead of a β -glucuronidase (GUS) as a marker for transformation reduced the cost of screening transformants (Niedz *et al.*, 1995).

GFP is the first truly *in vivo* reporter system useful in whole plants. For instance, viral infections in plants have been studied using GFP by replacing coat-protein genes from Potato Virus X (PVX) with the fluorescent fusion protein and monitoring virus-infected tissue with the microscope to study virus movements and by fusing the protein to movement proteins to determine how the virus spreads through and among host cells (Baulcombe *et al.*, 1995). Staci *et al.*, (1997) engineered tobacco plants using mgfp4, a mutagenized version of GFP that retains UV excitation, expressed under the control of the 35S promoter. When a transgenic plant mgfp4 expression was excited using long wave UV light (365 nm), the plant appeared green compared to non transgenic plants,

which appeared red due to the red autofluorescence of chlorophyll. In order to detect GFP expression in the plant, the level of expression of protein must be high enough to mask this red autofluorescence.

4.2.1. Studying PLC subcellular localization in plants

Based on the results from in vitro enzyme activity assays, two kinds of PI-PLC have been identified in cells of higher plants; one is predominantly present in the cytosolic fraction and the other is localized in the plasma membrane (Kim et al., 2004; Huang et al., 1995). Otterhag et al., (2001) found that a polyclonal antibody raised against a synthetic polypeptide specific for Arabidopsis AtPLC2 isoform detected a 66 KDa protein that was significantly enriched in plasma membrane fraction as compared with the intracellular membrane and microsomal fractions of Arabidopsis cells. These results suggest that the plasma membrane is a major cellular site for the presence of AtPLC2 enzyme. Kim et al., (2004) conducted an in vivo targeting experiment using *Vigna radiata* PI-PLC3 fused GFP as a fluorescent marker in a transient transfection assay. They demonstrated that Vr-PLC3 is predominantly present in the plasma membrane of transgenic Arabidopsis protoplasts.

5. Protein-protein interaction studies

The interactions between proteins are important for various biological functions. Most proteins function through interaction with other molecules, and often these are other proteins. Many proteins have multiple functions that depend on their cellular context. The cell-type-specific and signaling-dependent functions of these proteins are often determined by their interaction partners in particular cell (Hu and Kerppola, 2005). Some enzymes and other complexes are folded in specific way to be functional, and the

interactions between the different peptides are necessary for the whole complex to function. Since interactions are so essential, protein-protein interactions are an important topic of study. There are also a large number of transient protein-protein interactions, which in turn control a large number of cellular processes (Phizicky and Fields, 1995). As protein-protein interactions are so important, there are a multitude of *in vitro* and *in vivo* methods to detect them, including co-immunoprecipitation, co-purification as well as *in vitro* interaction methods (Zhang *et al.*, 2005; Joung *et al.*, 2000). Each method has its own strengths and weaknesses, especially with regard to the sensitivity and specificity of the method. The signals from the exterior of a cell are mediated to the inside of that cell by protein-protein interactions of the signaling molecules. Protein-protein interactions are likely to play an important role in response to abiotic stress, in the signal transduction cascade. Therefore, the interaction network will provide a new view on how cells identify and transduce stress signal to trigger genetic responses responsible for appropriate plant response (Tardif *et al.*, 2007).

5.1. Bimolecular fluorescent complementation (BiFC)

Because interaction with different partners can occur in different subcellular locations, determination of the location of a protein complex can provide insight into its functional roles and regulation. The BiFC approach is based on the formation of a fluorescent complex when two fragments of a fluorescent protein are brought together by an interaction between two proteins fused to the fluorescent protein fragments. This fluorescence is detected via fluorescence microscopy. This approach enables visualization of subcellular locations of specific protein interactions in the normal cellular environment (Hu and Kerppola, 2005).

PART II. MATERIALS AND METHODS

1. Bioinformatic resources

Basic Local Alignment Search Tool (BLAST, Altschul *et al.*, 1990) services provided by the National Center for Biotechnology Information (NCBI, <http://www.ncbi.nlm.nih.gov/>) were used in this study for comparison of nucleic acid and amino acid sequences. The Institute Genomic Research (TIGR, <http://www.tigr.org/tdb/tgi/>) wheat gene index, The Arabidopsis Information Resource (TAIR, <http://www.arabidopsis.org/>), Functional Genomics of Abiotic Stress (FGAS, <http://bioinfo.uwindsor.ca/cgi-bin/abiotic/project.cgi>) wheat ESTs databases are used to identify and analyze the genes used in this study and to help design gene specific primers. European Bioinformatics Institute (EBI, <http://www.ebi.ac.uk/>) ClustalW2 was used for multiple sequences alignment and analysis of sequence structure. The software Primer3 (Rozen and Skaletsky, 2000) was used to design and test all the primers used in this study. KEGG (Kyoto Encyclopedia of Genes and Genomes) website was used to elucidate the biochemical pathways associated with the genes (<http://www.genome.jp/kegg>). CBS (Center for biological sequence analysis) prediction service website was used for signal peptide and protein subcellular localization predictions (<http://www.cbs.dtu.dk/services>).

2. Plant materials

Triticum and *Aegilops* seeds were obtained from Plant Gene Resources of Canada/ Agriculture and Agri-Food Canada. The seeds were for *Triticum urartu*, *T. turgidum*, *T. aestivum*, *Aegilops speltoides* and *A. tauschii*, which include AA, AABB,

AABBDD, BB and DD genomes, respectively (Table 1). Tobacco seeds (*Nicotiana benthamiana*) were obtained from Dr. Francois Laliberté, Institute Armand Frappier, Laval, Canada.

Table (1): *Triticum* and *Aegilops* species used for genome designation.

The Name	AAFC Accession	Genome
<i>Triticum urartu</i>	CN 37663	AA
<i>Triticum turgidum</i>	CN 11002	AABB
<i>Triticum aestivium</i>	CN 31143	AABBDD
<i>Aegilops speltoides</i>	CN 108093	BB
<i>Aegilops tauschii</i>	CN 30817	DD

AAFC: Agriculture and Agri Food Canada germplasm accession number.

3. Plant growth conditions

3.1. Soil preparation

Equal volumes of peat moss, vermiculite and soil were mixed and heat treated at 150°C for 3 hours to reduce the risk of insects and fungus contaminations. Water was added to the autoclaved soil before the plants were planted.

3.2. *Triticum*, *Aegilops* and Tobacco growth conditions

Triticum and *Aegilops* seeds were germinated in the green house (26°C) and plants were grown for 14 days. At the end of this period, the leaves were harvested, then frozen immediately in liquid nitrogen and stored in -80°C. Tobacco (*Nicotiana benthamiana*) seeds were germinated in 10 cm pots in the green house with supplemental light to extend the day length to 16h light / 8h dark at 20°C and grown for 2-4 weeks.

4. Chinese spring *Triticum aestivum* cytogenetic stocks

Cytogenetic stocks of hexaploid *Triticum aestivum* were used to map genes to wheat chromosomes. The selected set included 19- nullisomic-tetrasomic lines (Sears

1966), which have one chromosome pair substituted by a homeologous pair of chromosomes. Furthermore, selected ditelosomic lines which were missing specific chromosome arms (Sears and Sears, 1978) and partial chromosome-arm deletion lines (Endo and Gill, 1996) were used to confirm the chromosome position of the genes and to determine the chromosomal arm for the locus (Table 2).

Table (2): Chinese *Triticum aestivum* cytogenetic stocks used for chromosome mapping.

Line Name	Description
N1AT1D	nulli 1A-tetra 1D
N1BT1D	nulli 1B-tetra 1D
N1DT1B	nulli 1D-tetra 1B
N2BT2D	nulli 2B-tetra 2D
N2DT2A	nulli 2D-tetra 2A
N3AT3D	nulli 3A-tetra 3D
N3BT3D	nulli 3B-tetra 3D
N3DT3B	nulli 3D-tetra 3B
N4AT4D	nulli 4A-tetra 4D
N4DT4B	nulli 4D-tetra 4B
N5AT5D	nulli 5A-tetra 5D
N5BT5D	nulli 5B-tetra 5D
N5DT5B	nulli 5D-tetra 5B
N6AT6B	nulli 6A-tetra 6B
N6BT6A	nulli 6B-tetra 6A
N6DT6B	nulli 6D-tetra 6B
N7AT7D	nulli 7A-tetra 7D
N7BT7D	nulli 7B-tetra 7D
N7DT7B	nulli 7D-tetra 7B
Dt1BL	ditelosomic 1BL
Dt2AS	ditelosomic 2AS
Dt2BL	ditelosomic 2BL
Dt3BL	ditelosomic 3BL
Dt5AL	ditelosomic 5AL
Dt5BL	ditelosomic 5BL
Dt6AS	ditelosomic 6AS
Dt6BL	ditelosomic 6BL
Dt7BL	ditelosomic 7BL
5AL-12*	partial 5AL deletion at (0.35**)
5AL-10*	partial 5AL deletion at (0.57**)
5AL-17*	partial 5AL deletion at (0.78**)
5AL-23*	partial 5AL deletion at (0.87**)

* Each deletion is indicated by the chromosome arm (in this case 5AL, etc.) and a sequential number. This tag is followed by the FL (fraction length**) value, which indicates the percent of the chromosome arm present in each deletion chromosome. For example, deletion 5AL-23 has an FL value of 0.87, indicating

that 87 % of the short arm of chromosome 5A remains (a 13 % deletion of the arm). <http://wheat.pw.usda.gov/mEST/>.

5. Fluorescent organelle markers

Subcellular organelle fluorescent mCherry markers were obtained from ABRC (Arabidopsis Biological Resource Center). The reliability of the fluorescent organelle markers have been established by Nelson *et al.*, (2007) and clones of the fusion proteins are available as binary plasmids for plant transformation via *Agrobacterium* infiltration (Table 3).

Table (3): Organelle markers as red fluorescent-protein fusions.

Organelle	Construct Name	Targeting Protein
Plasma Membrane	PM-rk CD3-1007	The full length of AtPIP2A, a plasma membrane aquaporin.
Endoplasmic Reticulum	ER-rk CD3-959	contains the signal peptide of AtWAK2, wall-associated kinase2, fluorescent at the N-terminus of protein and ER retention signal, His-Asp -Glu-leu, at the C- terminus.
Plastids	Pt- rk CD3-999	The first 79 aa of the small subunit of tobacco rubisco.
Mitochondria	Mt-rk CD3-991	The first 29 aa of yeast cytochrome C oxidase.
Golgi	G-rk CD3-967	The first 49 aa of GmMan1, soybean α -1,2 mannosidase 1.
Peroxisome	Px-rk CD3-983	Peroxisomal targeting signal1, Ser-Lys-Leu, at the C- terminus of fluorescent protein.

PM, Plasma Membrane; **ER**, Endoplasmic Reticulum; **Pt**, Plastids; **Mt**, Mitochondria; **G**, Golgi; **PX**, Peroxisome; **r**, mCherry fluorescent protein; **k**, kanamycin resistance; **aa**, amino acid.

6. Modified plant genomic DNA extraction using CTAB

6.1. Buffers

- **CTAB buffer 100ml**

2.0 g	CTAB (Hexadecyl trimethyl-ammonium bromide)
10.0 ml	1 M Tris pH 8.0
4.0 ml	0.5 M EDTA pH 8.0 (EthylenediaminetetraAcetic acid Di-sodium salt)
28.0 ml	5 M NaCl
40.0 ml	H ₂ O

Adjust to pH 5.0 with HCL and make up to 100 ml with H₂O.

- **1 M Tris pH 8.0**

- **TE buffer**

50mM	Tris-Hcl (pH8.0)
10 mM	EDTA

6.2. DNA extraction procedure

1. 200 mg of plant tissue was ground to a fine paste in approximately 500 µl of CTAB buffer.
2. CTAB/plant extract mixture was transferred to a microfuge tube.
3. The extract mixtures were incubated for approximately 15 min at 55°C.
4. After the incubation, the CTAB/plant extraction mixture was centrifuged at 12000 rpm in a microcentrifuge for 5 min to spin down cell debris.
5. The supernatant was transferred to a clean microfuge tube.
6. To each tube, 250 µl of Chloroform: Iso Amyl Alcohol (24:1) was added and the solutions were mixed by inversion. After mixing, the tubes were centrifuged at 13000 rpm for 3 min.
7. The upper aqueous phase was transferred to a clean microfuge tube.
8. To each tube, 50 µl of 7.5 M Ammonium Acetate was added, followed by 500 µl of ice cold absolute ethanol.

9. The tube was inverted slowly several times to precipitate the DNA, then placed for 2 hr at -20 °C.
10. The DNA was isolated by spinning the tube at 13000 rpm for 3 minutes. The supernatants were removed and 750 µl of ice cold 70 % ethanol was added to the pellet.
11. The DNA pellet was centrifuged at 13000 rpm for 3 min. the supernatant was removed and the DNA pellet was left to dry (approximately 15 min).
12. - The DNA was resuspended in TE buffer, then stored at -20°C.

7. Agarose gel electrophoresis

PCR products were electrophoresed in 1 % Agarose in 1X TAE (Tris-acetate EDTA) with ethidium bromide (1: 20,000) (Sambrook *et al.*, 1989). The size of PCR fragments was measured by comparison to 1 Kb DNA standard ladder (Fermentas, 0.5ug/ul).

8. Gateway cloning system

Gateway technology is a cloning method based on the site-specific recombination properties of bacteriophage lambda. The system provides a rapid and highly efficient way to subclone DNA sequences into multiple vector systems for functional analysis and protein expression (Hartley *et al.*, 2000). Two recombination reactions constitute the basis of Gateway cloning system.

8.1. BP Reaction

BP reaction facilitates recombination of DNA fragment flanked by attB recombination sites with an attP recombination site in a donor vector to create entry

clone with the insert flanked by attL-recombination sites (Figure 3a). This reaction is catalyzed by BP Clonase™ enzyme mix (Invitrogen) and carried out according to the manufacturer's protocol, except the reaction volumes were reduced to a half of those recommended.

8.2. LR Reaction

LR reaction facilitates recombination of an attL substrate (entry clone) with an attR substrate (destination vector) to create an expression clone with the insert flanked by short 22 nt attB recombination sites (Figure 3b). This reaction is catalyzed by LR Clonase™ enzyme mix (Invitrogen) and carried out according to the manufacturer's protocol, except the reaction volumes were reduced to a half of those recommended.

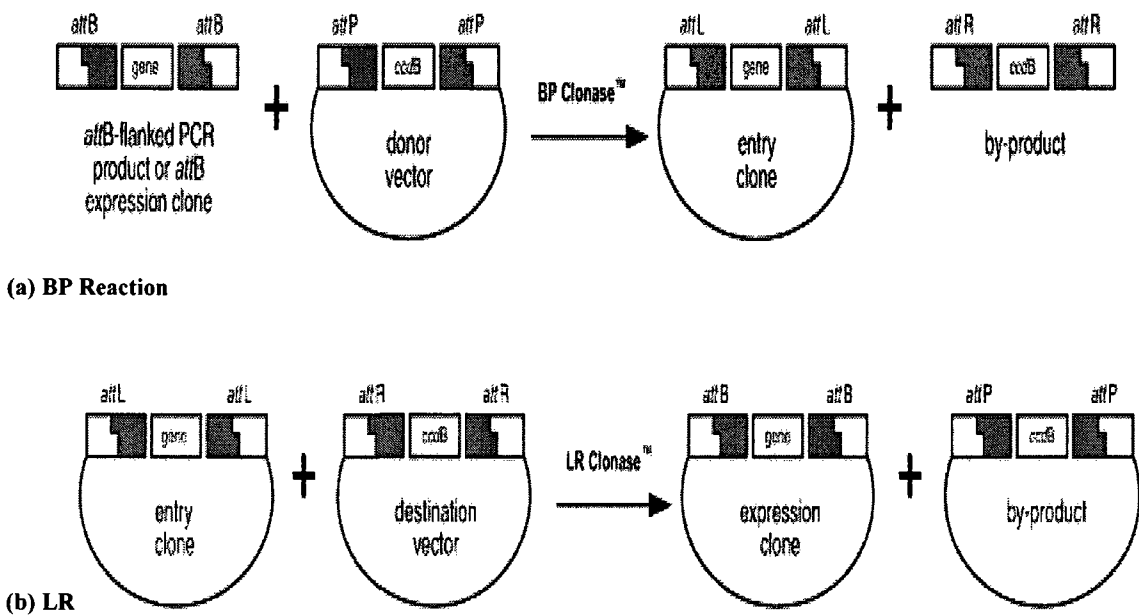


Figure (3): Scheme of Gateway BP and LR recombination reactions.

(The scheme was taken form Invitrogen website)

9. TaPG-PLC cDNA sequencing and analysis

Three homologs of phosphoglycerol specific phospholipase C from *T. aestivum* (TaPG-PLC) were identified from three cDNA clones from the Genome Canada Functional Genomics of Abiotic Stress (FGAS) program. They have FGAS identification codes of WEF038_J09, WEF081_I17 and L6B024_D09 and they encode TaPG-PLC1, TaPG-PLC2 and TaPG-PLC3 respectively. cDNA clones for the three homologs were fully sequenced with specific primers (Table 4) and full coding regions were identified.

10. TaPG-PLC homolog mapping

10.1. TaPG-PLC homolog genome mapping

Triticum and *Aegilops* seeds obtained from Plant Gene Resources of Canada were used to determine in which genome in hexaploid wheat TaPG-PLC1, TaPG-PLC2 and TaPG-PLC3 were mapped. The gene-specific primers of each individual homolog were designed using gene-specific coding regions and 3'UTR sequences, since the latter include highly polymorphic (Table 4). PCR reactions were carried out with the genomic DNA of the diploid and tetraploid progenitors of bread wheat. These include *T. urartu*, *Ae. speltoides* and *Ae. tauschii* *T. turgidum*, *T. aestivum*, which have AA, BB, DD, AABB, and AABBDD genomes respectively. PCR amplification with Taq polymerase was done under the following conditions: 94°C for 5 minutes, followed by 40 cycles of 45 seconds at 94°C, 40 seconds at 56°C, 2 minutes at 72°C; these were followed by 10 minutes at 72°C. The PCR products were then electrophoresed and visualized as described in section 7.

Table (4): Oligo nucleotide PCR primers were used in this study.

Primer Name	Description	Sequence
P1 L6bD024-D09	Forward TaPG-PLC3 (S.)	5'ATGGCCAGAACGTCATTAG 3'
P6 L6bD024-D09	Reverse TaPG-PLC2 and PG-PLC3 (S.)	5'GAGCCGCTCATGACGTT 3'
P7 L6bD024-D09	Reverse TaPG-PLC3 (S.)	5'GTCGTTGGCAGGGAATC 3'
P8 L6bD024-D09	Reverse TaPG-PLC3 (S.)	5'CTGCGTAACGGTTTGCTTCT 3'
P2 WFF081-II7	Forward TaPG-PLC1, PG-PLC2 and PG-PLC3 (S.)	5'CACGGCTTCGAGGACATC3'
P4 WFF081-II7	Forward TaPG-PLC2 (S.)	5'CTGGATACCGCCAACAGATT3'
P5 WFF081-II7	Reverse TaPG-PLC1 and PG-PLC2 (S.)	5'CGTCGTTGGGTGATACTCCT3'
TaPG-PLC1	Forward TaPG-PLC1 (M.)	5'GTTTCAAGTGGAGTTGATTCA3'
TaPG-PLC1	Reverse TaPG_PLC1 in 3' UTR (M.)	5'TCCAACAATCATTATAGTA3'
TaPG-PLC2	Reverse TaPG_PLC2 in 3' UTR (M.)	5'CTTGCAAGATGATGAGCGGT3'
TaPG-PLC3	Reverse TaPG_PLC3 in 3' UTR (M.)	5'TCCCGACAACAGATTCCAGAT3'
pCMVSPORT6	Forward pCMVSPORT6 (C.)	5'CCATAGAAGACACCCGGA 3'
WEF101_A23	Reverse WEF101_A23 TaPI-PLC1 (C.)	5'CAGGTGAAGGGAGCTCTT3'
attB1 pCMVSPORT6	Forward pCMVSPORT6 primer with > gateway attB1 (C.)	5'GGGACAAAGTTTGTACAAAAGCAGGC> >TT CAGCCTCCGGACTTAGC3'
attB2 WEF101_A23	Reverse WEF101_A23 primer with > gateway attB2 (C.)	5'GGGACCACTTTGTACAAGAAAGCTGGG> >TCTCGGTGTAAGTGGTCT3'
attB2 partial TaPI-PLC1	Reverse new extended sequence primer with > gateway attB2 (C.)	5'GGGACCACTTTGTACAAGAAAGCTGGG> >TCAGTCGCTGCTGAGCTGGT3'
attB1 TaPI-PLC1	Forward ORF TaPI-PLC1 with Gateway > attB1 (C.)	5'GGGGACA AGT TTG TACAAAAAGCAG> >GCTTCATGGGCACCTACAAGTGC3'
attB2 TaPI-PLC1	Reverse ORF TaPI-PLC1 with Gateway > attB2 (C.)	5'GGGGACCACTTTGTACAAGAAAGCTG> >GGTCCACAACCTCAAAGCGCATG3'
attB1 TaPI-PLC2 FL	Forward ORF TaPI-PLC2 with Gateway > attB1 (C.)	5'GGGGACAAGTTTGTACAAAAGCAG> >GCATGAGCACGTACAGGGT3'
attB2 TaPI-PLC2 FL	Reverse ORF TaPI-PLC2 with Gateway > attB2 (C.)	5'GGGGACCACTTTGTACAAGAAAGCTGGG> >TCCGAAAACCTCGAAGCGCAT3'

Continued >>

Table (4): Continued

Primer Name	Description	Sequence
attB1 TaPI-PLC2ΔEF-hand	Forward primer from partial part of TaPI-PLC2 starts at PLCX domain with gateway attB1 (C.)	5' GGGGACA AGT TTG TACAAAAAAGCAG> >GCTTCATGGTTCACCATGACAT3'
attB2 TaPI-PLC2ΔC2-2	Reverse primer from partial part of TaPI-PLC2 ends before C2-2 domain with gateway attB2 (C.)	5' GGGGACCACTTTGTACAAGAAAGCTGG> >GTCTGTCTTCACTGGTAGTTT3'
attB2 stop TaPI-PLC1	Reverse ORF TaPI-PLC1 with Gateway attB2 (C.)	5'GGGACCACTTTGTACAAGAAAGCTG> >GGTCTCACACAACAACTCAAAGCGCAT3'
attB1 TaPG-PLC1 FL	Forward ORF TaPG-PLC1 with Gateway attB1(C.)	5'GGGGACAAGTTTGTACAAAAAAGCA> >GGCTTCATGGCCGCCCGGAGAG3'
attB2 TaPG-PLC1 FL	Reverse ORF TaPG-PLC1 with Gateway attB2(C.)	5'GGGGACCACTTTGTACAAGAAAGCTGG> >GTCGAGTTCAGATGACAAGCCGGT3'
attB1 TaPG-PLC2 FL	Forward ORF TaPG-PLC2 with Gateway attB1(C.)	5'GGGGACAAGTTTGTACAAAAAAGCAGG> >CTTCATGGCCGCCCGGAGAG3'
attB2 TaPG-PLC2 FL	Reverse ORF TaPG-PLC2 with Gateway attB2(C.)	5'GGGGACCACTTTGTACAAGAAAGCTGG> >GTCGAGTTCAGATGACAAGCCGGT3'
attB1 TaPG-PLC3 FL	Forward ORF TaPG-PLC3 with Gateway attB1(C.)	5' GGGGACAAGTTTGTACAAGAAAGCAGG> >CTTCATGGCCGCCCGGAGAG3'
attB2 TaPG-PLC3 FL	Reverse ORF TaPG-PLC3 with Gateway attB2(C.)	5'GGGGACCACTTTGTACAAGAAAGCTGGG> >TCAAGCTCTGATGACAAGCCAGT3'
attB1 TaPG-PLC1ΔNT	Forward truncated PG-PLC1 with Gateway attB1(C.)	5'GGGGACAAGTTTGTACAAAAAAGCAGG> >CTTCAGACGGTGGTGGTGGTGC3'
attB1 TaPG-PLC2ΔNT	Forward truncated PG-PLC2 with Gateway attB1(C.)	5'GGGGACAAGTTTGTACAAGAAAGCAGG> >CTTCAGACGGTGGTGGTGGTGC3'
attB1 TaPG-PLC3ΔNT	Forward truncated PG-PLC3 with Gateway attB1(C.)	5'GGGGACAAGTTTGTACAAAAAAGCAGG> >CTTCAGACGGTGGTGGTGGTGC3'
attB1 J822	Forward J822 missing 240 nt with Gateway attB1(C.)	5'GGGGACAAGTTTGTACAAAAAAGCAGG> >CTTCAAATGGTAGCAGATGAGGAAAG3' Continued >>

Table (4): Continued

Primer Name	Description	Sequence
attB2 j822	Reverse J822 missing 240 nt with Gateway attB2 (c.)	5'GGGGACCACTTTGTACAAAGAAAAGCTGGG> >TCAGCTGAAAACGTTGACCTGC3'
attL1	Forward Invitrogen sequencing primer for entry clones (s.)	5' TCGCGTTAACGCTAGCATGGATCTC 3'
attL2	Reverse Invitrogen sequencing primer for entry clones (s.)	5' GTAACATCAGAGATTTTGAGACAC 3'

S: Sequencing M: Mapping C: Cloning

10.2. Chromosome assignment and bin map of TaPG-PLC3

Cytogenetic stocks of hexaploid Chinese spring *Triticum aestivum* which included nullisomic-tetrasomic, ditelosomic and partial chromosome-arm deletion lines were used to map TaPG-PLC3 to a chromosomal region. The same primers and PCR conditions were the same as that described in section 10.1 for TaPG-PLC3 chromosomal assignment. The absence of PCR products in lines with missing chromosomes or parts of chromosomes was taken as an indication of the location of the gene.

11. TaPI-PLC1 full length cDNA cloning

TaPI-PLC1 was represented by FGAS tentative contig, cluster 3141-contig 2; the gene was strongly induced by cold treatment from 1 day to 14 days (Liu, 2005). The original clone was a partial length cDNA (FGAS 030579) with FGAS ID STG1_K11 and GenBank EST accession gi:70971255 and 100% identity with FGAS EST clone WEF101_A23. The later clone had a 1192 nt ORF, however it appeared to lack the 5' end of the cDNA. A pair of primers was designed to isolate the full length of TaPI-PLC1 by PCR amplification from a cDNA library. The forward primer was for the pCMVSPORT, the cloning vector used for the cDNA libraries and reverse primer was gene-specific corresponding to WEF101_A23 (Table 4). Four cDNA libraries made from *T. aestivum*, referred to as L3, L4, L5 and L6 were made available to us by Dr Jean Danyluk, from Université du Québec a Montréal (UQAM). PCR amplification was carried out with 1ul aliquots of these libraries using polymerase pfu enzyme (Fermentas Canada Inc., Burlington, Canada). PCR temperature cycling used was: 94°C for 3 minutes, followed by 40 cycles of 30 seconds at 94°C, 40 seconds at 49°C, 2 minutes at 72°C; this was

followed by 10 minutes at 72°C. The PCR products were then held at 4°C. PCR reactions products were electrophoresed. Another PCR reaction was carried out with the PCR product of L6, the only library that yielded an amplification product, using pairs of gene specific primer sets that also contain Gateway attB recombination sites. The left primer had the attB1 downstream of pCMVSPORT forward primer, while the right primer had attB2 site and WEF101_A23 gene-specific sequence (Table 4). PCR temperature cycling used was: 94°C for 3 minutes, followed by two different types of cycles, 10 cycles of 30 seconds at 94°C, 40 seconds at 53°C, 2 minutes at 72°C; these were followed by 40 cycles of 30 seconds at 94°C, 40 seconds at 69°C, 2 minutes at 72°C; then 10 minutes at 72°C. The PCR products were held at 4 °C and electrophoresed in an agarose gel. The PCR product was subcloned into pDONR 207, Gateway cloning vector, using Gateway ® BP clonase II enzyme mix reaction (section 8) and subsequently transformed into the TOP10 competent *E. coli*. The transformants were selected on LB media with 7 ug/ml gentamycin. Two colonies were cultured in liquid LB media with 7ug/ml gentamycin overnight at 37°C with shaking. The plasmids were purified using QIAprep® Spin Miniprep Kit (QIAGEN) and were sent to the Génome Québec Innovation Centre at McGill University for sequencing. The result of sequencing showed that a part of the original clone was extended, but the start codon of Ta-PIPLC1 was missing. A second round of cloning using a similar strategy was done using attB1 pCMVSPORT primer and attB2 a second gene specific primer for TaPI-PLC1, derived from the new extended sequence. The second set of clones was sent for sequencing. Another pair of primers with attB1 recombination sites was designed to isolate a full length clone of TaPI-PLC1 from library L6 (Table 4). A second cycle of cloning of PCR

amplification products from the library 6 for the full length clones was done using the Gateway cloning system. PCR temperature cycling used was: 94°C for 3 minutes, followed by two different types of cycles, 10 cycles of 30 seconds at 94°C, 40 seconds at 57°C, 2 minutes at 72°C; these were followed by 40 cycles of 30 seconds at 94°C, 40 seconds at 70°C, 2 minutes at 72°C; then 10 minutes at 72°C. The PCR products were held at 4 °C. The PCR product was subcloned into pDONR 207 by Gateway ® BP clonase II Enzyme mix (section 8) and subsequently transformed into the TOP10 competent *E. coli*. Single TaPI-PLC1 colony was purified using QIAprep® Spin Miniprep Kit (QIAGEN) and was sent for sequencing.

12. Subcellular localization of fluorescent protein and in vivo protein-protein interactions

12.1. Generating entry clones

The coding regions of phosphoglycerol specific phospholipase C TaPG-PLC1, TaPG-PLC2 and TaPG-PLC3, of the phosphoinositol specific phospholipase C genes, TaPI-PLC1, TaPI-PLC2 and J822 were cloned as fusions with fluorescent proteins in plant expression vectors using Gateway Cloning System. The gene-specific primers contained attB1 and attB2 extensions were designed for the genes with their stop codons removed to enable fusion to their C termini (Table 4).

PCR reactions were carried out using the full length cDNA clones WEF038_J09, WEF081_I17 and L6B024_D09 cDNA clones which encode TaPG-PLC1, TaPG-PLC2 and TaPG-PLC3, respectively as well as their partial lengths. Both TaPG-PLC1 Δ NT and TaPG-PLC2 Δ NT had the first 48 amino acids removed from the N-terminal end, but with an ATG start codon added. TaPG-PLC3 Δ NT had the first 47 amino acids removed from

the N-terminal end, but with an ATG start codon added. Fusion proteins were also made with TaPI-PLC1 and L3C112_D16 to clone TaPI-PLC1, TaPI-PLC2, TaPI-PLC2 Δ EF-hand (TaPI-PLC2 the EF-hand domain domain from aa 1 to 23 removed) and TaPI-PLC2 Δ C2-2 (TaPI-PLC2 with the C2-2 domain from aa 390 to 586 removed. PCR temperature cycling used was: 94°C for 3 minutes, followed by two different types of cycles, 10 cycles of 30 seconds at 94°C, 40 seconds at (53 to 58°C), 2 minutes at 72°C; these were followed by 40 cycles of 30 seconds at 94°C, 40 seconds at 69°C, 2 minutes at 72°C; then 10 minutes at 72°C. PCR products were electrophoresed the same as described in section 7 to confirm the correct molecular sizes of the PCR products.

The PCR fragments were then subcloned into pDONR 207 via BP reaction Gateway® BP clonase II mix (section8). The entry clones from two colonies of each construct were analyzed by PCR to verify the insert size and then were confirmed by sequencing using, the recommended Invitrogen attL1 and attL2 sequencing primers.

In the case of the G-protein J822, multiple attempts of the cloning were made including carrying out the Gateway PB and LR reactions *in vitro* without the intermediate *E. coli* transformation step. All attempts clone into Gateway the entry vector or expression vectors resulted in truncation products missing various amounts of the 5' end of the J822. One clone was selectes with retained its initial start codon but was missing the following 240 nt and retained its proper reading frame.

12.2. Plant expression clones

Gateway LR reactions were used to transfer the inserts of the entry clones of TaPG-PLCs and TaPI-PLCs to the plant destination binary vector, PK7FWG2, to generate Enhanced Green Fluorescent Protein (EGFP) C-terminal fusions (section 8).

These fusions were downstream of strong constitutive 35S promoter. They were also transferred to Gateway Bimolecular Fluorescent Complimentation (BiFC) binary Yellow Fluorescent Protein (YFP) vector, pBatL-B-sYFP-N to study the possibility of their protein-protein interactions with G-proteins. J822 missing 240 from 5' end was also transferred to pBattL-cYFP. The BiFC vectors were obtained from Alan M. Jones, Departments of Biology and Pharmacology, University of North Carolina. The *E. coli* transformants were selected on LB media with 50 µg/ml spectinomycin. Single colony for each construct was used to inoculate liquid LB media with 50 µg/ml spectinomycin. Plasmid for the expression clones of each construct was purified using QIAGEN Spin Miniprep Kit. Diagnostic PCR reactions were carried out with the expression clones to verify the presence of the full length of the insert in the clones.

12.3. *Agrobacterium* transformation

Electrocompetent *Agrobacterium* strain AGL1 were transformed with expression clones by electroporation and selected on LB agar plates containing 100 µg of ampicillin and 50 µg/ml spectinomycin.

12.4. Agroinfiltration

A loop of *Agrobacterium tumefaciens* colonies transformed with GFP or YFP fluorescent protein fusion expression vectors was grown over night in LB media at 29°C with the appropriate antibiotics. Bacteria were collected by centrifugation at 4000 xg for 15 min at 4°C and resuspended in 10 mM MgCl₂ and 150 µM Acetosyringone at to an OD₆₀₀ of 0.1. The cells were left in this solution for 2 hours at room temperature (English *et al.*, 1996). Equal volumes three *Agrobacterium* culture suspensions containing

expression vectors for the experimental sample, the mCherry fluorescent cellular marker proteins and expression of P19 of tomato bushy stunt virus, used to suppress gene silencing (Voinnet *et al.*, 2003) were mixed. The agroinfiltration solution of transformed *Agrobacterium* was co-infiltrated into the leaf abaxial air space of 2-4 week old *N. benthamina* plants. The plants were incubated in environmental growth chamber under long days (16h light / 8h dark) at 20°C.

12.5. Confocal laser scanning microscopy

The epidermic tissues of tobacco leaves were examined two days after infiltration, using SD2 (Scanning Disk2) confocal microscope, at The Cell Imaging and Analysis Network (CIAN) laboratory, McGill University. GFP was excited at a wavelength of 491 nm by the diode laser and the emitted fluorescence was collected through a 520/535nm band-pass. YFP was excited at the same wavelength laser, and the emitted fluorescence was collected through a 543 nm long-pass filter, while mCherry Red Fluorescent Protein (RFP) was excited at a wavelength of 561 nm and the emitted fluorescence was collected through a 624/640 nm long-pass filter.

PART III. RESULTS

1. PG-PLC1 sequence analyses

Three full length cDNA clones of wheat phosphoglycerol specific phospholipase C were identified from FGAS clones. The identification codes of the three FGAS clones were WEF038-J09, WEF081-I17 and L6B024-D09. They encode three homologs of TaPG-PLC and they are referred to as TaPG-PLC1, TaPG-PLC2 and TaPG-PLC3, respectively. The three cDNA clones were fully sequenced and their coding regions were identified (Appendix 1). The ORF of TaPG-PLC1, TaPG-PLC2 and TaPG-PLC3 are 1626, 1623 and 1623 nt. and encode proteins of 541, 540 and 540 amino acids, respectively (Figure 4); their 3' UTRs are 374, 369 and 364 nt, respectively. The predicted proteins for TaPG-PLC homologs have the molecular weight of 60.16, 60.13 and 60.03 KDa. The identity between the amino acid (aa) sequences of TaPG-PLC1 and TaPG-PLC2 was 97%, whereas the identity between TaPG-PLC1 and TaPG-PLC3; TaPG-PLC2 and TaPG-PLC3 were 96%. In Arabidopsis and rice the PG-PLC gene families have 6 and 7 members, respectively (Table 5). The six Arabidopsis PG-PLCs were reported by Nakamura *et al.*, (2005). They were referred to as non specific Phospholipase C (NPC). The Arabidopsis gene AT1G07230, PG-PLC1, is the most similar Arabidopsis gene to TaPG-PLC1 with 69% aa sequence identity. The rice PG-PLCs are numbered chronologically in the order that sequences were submitted into GenBank (Table 5). The rice gene OsPG-PLC1 (GenBank GI:15042826) was the most similar to TaPG-PLC1 with 88% aa sequence identity. The phylogram constructed with all Arabidopsis, rice sequences and the wheat TaPG-PLC1, 2 and 3 showed that the three

wheat genes are more similar to each other than to the genes from the other two species (Figure 5).

```

TaPG-PLC1      MAAAGERRLLVGLLLLALMVSAHCLDGAGHHGPRVKKRRKKREIHEFVETVVVVVMMENRS 60
TaPG-PLC2      MAAAGERRLLACLALLLAMI SAHCLDGAGHHGPRVKKRRKKREIHEFVKTIVVVVMMENRS 60
TaPG-PLC3      MAAAGERRLLVGLLLLALVVAHCLDG-GHHGPRMKRRRKKREIHEFVETVVVVVMMENRS 59
                ***** . ***** : ***** ***** : ***** ***** *****

TaPG-PLC1      FDHVLGNLRAGRPDIDGLTGTEENKLNASDPSPSEIIFVYDRAQYVDSDFGHGPFEDIREQI 120
TaPG-PLC2      FDHVLGNLRAGRPDIDGLTGTEENKLNASDPSPSEIIFVYDRAQYVDSDFGHGPFEDIREQI 120
TaPG-PLC3      FDHVLGNLRAGRPDIDGLTGTEENKLNASDPSPSEIIFVYDRAQYVDSDFGHGPFEDIREQI 119
                ***** . ***** : ***** ***** : ***** ***** *****

TaPG-PLC1      FGSADTSAVPPPNMGGFAQARQMLQHAQNVNSGFAPDSVVFYAAALADEFAVFDKWFASV 180
TaPG-PLC2      FGSADTSAVPPPNMGGFAQARQMLQHAQNVNSGFAPDSVVFYAAALADEFAVFDKWFASV 180
TaPG-PLC3      FGSADTSAVPPPNMGGFAQARQMLQHAQNVNSGFAPDSVVFYAAALADEFAVFDKWFASV 179
                ***** ***** ***** ***** ***** ***** *****

TaPG-PLC1      FTSTQFNRLFVHSATSHGLTFNARKDLINGFPQTIIFDSLEEDGLSFGIYYQIIPATLFT 240
TaPG-PLC2      FTSTQFNRLFVHSATSHGLTFNARKDLINGFPQTIIFDSLEEDGLSFGIYYQIIPATLFT 240
TaPG-PLC3      FTSTQFNRLFVHSATSHGLTFNARKDLINGFPQTIIFDSLEEDGLSFGIYYQIIPATLFT 239
                ***** ***** ***** ***** ***** ***** *****

TaPG-PLC1      QSLRRLKHLKFKHQYSLRFKLDARQNLPHYVVIQRVYFCRZFFANDQHFSDHWARGQR 300
TaPG-PLC2      QSLRRLKHLKFKHQYSLRFKLDARQNLPHYVVIQRVYFCRZFFANDQHFSDHWARGQR 300
TaPG-PLC3      QSLRRLKHLKFKHQYSLRFKLDARQNLPHYVVIQRVYFCRZFFANDQHFSDHWARGQR 299
                ***** : ***** : ***** : ***** ***** ***** *****

TaPG-PLC1      FVREYVETLRASPQWNETALIITYDEHGGFYDHVETFPVVGVPQPDGIGDFYIFKFDRL 360
TaPG-PLC2      FVREYVETLRASPQWNETALIITYDEHGGFYDHVETFPVVGVPQPDGIGDFYIFKFDRL 359
TaPG-PLC3      FVREYVETLRASPQWNETALIITYDEHGGFYDHVETFPVVGVPQPDGIGDFYIFKFDRL 359
                ***** ***** ***** ***** ***** ***** *****

TaPG-PLC1      GVRVPSFLISPWVEKGTVIHEPNGPEGTSQYEHSSIPATVKKLFNLRANYLTKRDWAGT 420
TaPG-PLC2      GVRVPSFLISPWVEKGTVIHEPNGPKEDSQYEHSSIPATVKKLFNLRANYLTKRDWAGT 419
TaPG-PLC3      GVRVPSFLISPWIEKGTATHEPNGPFENSRYEHSSIPATVKKLFNLRANYLTKRDWAGT 419
                ***** : ***** . ***** * : ***** ***** ***** *****

TaPG-PLC1      FESYLKVRKTPRTDCPEKLPVTKSLRPFGANEDKSLSEFQVELIQLASQLNGDHVLNSY 480
TaPG-PLC2      FDSYLKVRKTPRTDCPEKLPVTKSLRPFGANEDKSLSEFQVELIQLASQLNGDHVLNSY 479
TaPG-PLC3      FENYLKVRKTPRTDCPEKLPVTKSLRPFGANEDKSLSEFQVELIQLASQLNGDHVLNSY 479
                * : ***** ***** ***** ***** ***** ***** *****

TaPG-PLC1      PDIGKTMSVGEANRYAEDAVSRFLEAGRIALRAGANESALVTMRPALTSRAAMSTGLSSE 540
TaPG-PLC2      PDIGKTMSVGEANRYAEDAVSRFLEAGRIALRAGANESALVTMRPALTSRAAMSTGLSSE 539
TaPG-PLC3      PDIGKTMSVGEANRYAEDAVSRFLEAGRSALRAGANESALVTMRPALTSRAAMSTGLSSE 539
                ***** ***** ***** ***** ***** ***** *****

TaPG-PLC1      L 541
TaPG-PLC2      L 540
TaPG-PLC3      L 540
                *

```

Figure (4): The multiple amino acids sequence alignments for the three homologs of TaPG-PLC using Clustal W2. The functional phosphoesterase domain of PG-PLC is highlighted in gray.

Table (5): PG-PLC genes in Arabidopsis and rice.

Isoform Name	Gene Name	Accession No.	Ch. No.	Molecular Mass	Amino Acid Residues	Localization*
At-PG-PLC1	AT1G07230	NP_172203	Ch.1	60 KD	533 aa	Secretory
At-PG-PLC2	AT2G26870	NP_180255	Ch.2	58 KD	514 aa	Secretory
At-PG-PLC3	AT3G03520	NP_187002	Ch.3	59 KD	523 aa	Others
At-PG-PLC4	AT3G03530	NP_566206	Ch.3	61 KD	538 aa	Others
At-PG-PLC5	AT3G03540	NP_566207	Ch.3	59 KD	521 aa	Others
At-PG-PLC6	AT3G48610	NP_190430	Ch.3	58 KD	520 aa	Secretory
Os-PG-PLC1		AAK82449	Ch.3	61 KD	545 aa	Secretory
Os-PG-PLC2		EAY77273	Ch.1	57 KD	520 aa	Secretory
Os-PG-PLC3		EAZ18936	Ch.11	43 KD	395 aa	Others
Os-PG-PLC4		NP_001041746	Ch.1	58 KD	528 aa	Secretory
Os-PG-PLC5		NP_001051927	Ch.3	58 KD	527 aa	Others
Os-PG-PLC6		NP_001068198	Ch.11	58 KD	535 aa	Others
Os-PG-PLC7		BAB62632	Ch.1	65 KD	593 aa	Secretory

At, *Arabidopsis thaliana*; Os, *Oryza setiva*; Ch. NO., Chromosome Number

* The prediction of localizations was by TargetP. Secretory genes have putative signal peptides for the secretory pathway.

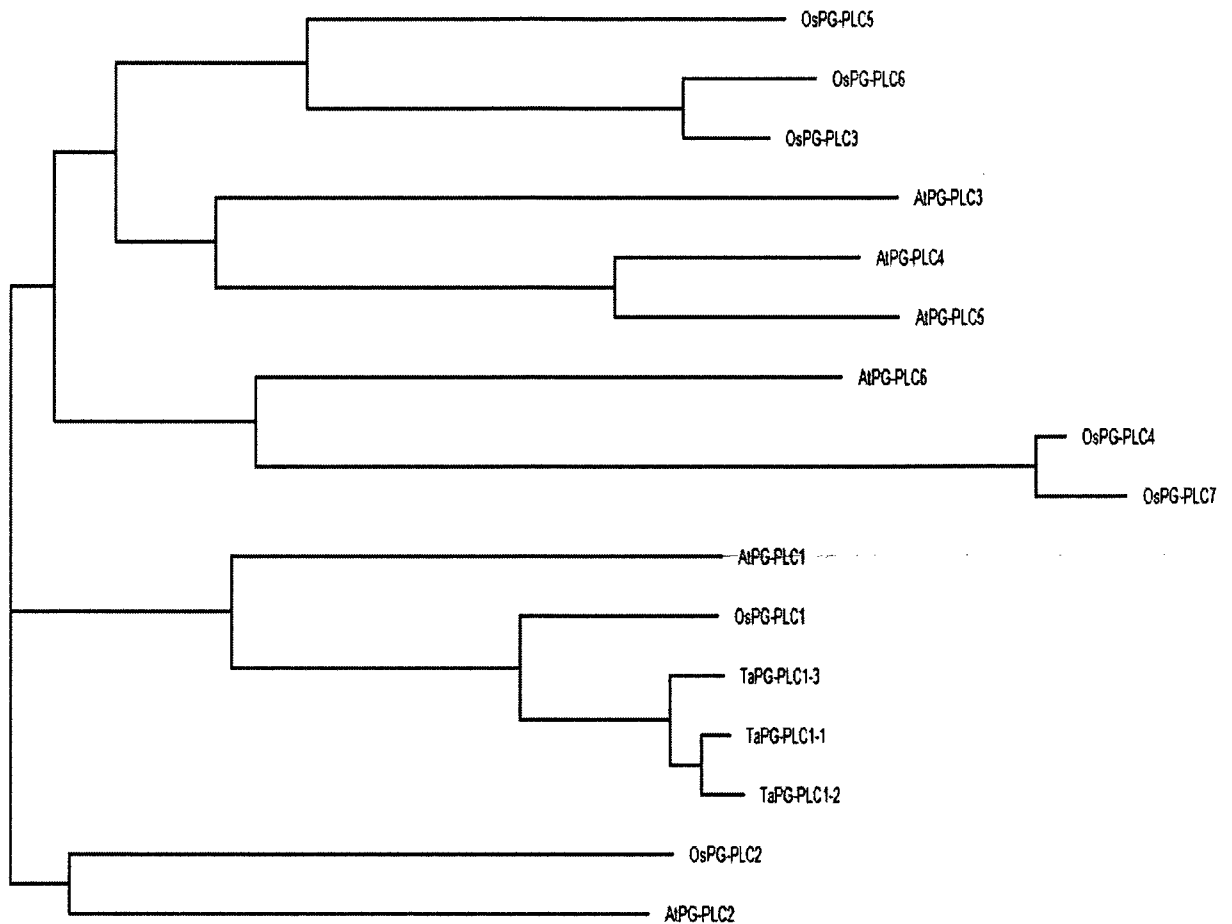


Figure (5): Phylogram of PG-PLCs in wheat (Ta), Arabidopsis (At) and rice (Os). Ta, *Triticum aestivum*; At, *Arabidopsis thaliana*; Os, *Oryza setiva*

2. Mapping of TaPG-PLC homologs

2.1. TaPG-PLC genome mapping

The mapping of the three TaPG-PLC homologs to A, B, D genome was done with pairs of gene-specific primer for each homolog (Table 4). PCR amplification was done with the genomic DNA of *T. urartu*, *T. turgidum*, *T. aestivium*, *Ae. speltoides* and *Ae. tauschii* which include AA, AABB, AABBDD, BB and DD genomes, respectively

(Figure 6). The expected molecular size of TaPG-PLC1, TaPG-PLC2 and TaPG-PLC3 PCR products were 584, 313 and 519 bp, correspondingly. PCR amplification with the gene specific primer pair for TaPG-PLC3 gave a product when the DNA template was from *T. urartu* (AA), *T. turgidum* (AABB) and *T. aestivium* (AABBDD) but they did not yield a product with *Ae. speltoides* (BB) and *Ae. tauschii* (DD), indicating that TaPG-PLC3 is likely in the A genome. Gene specific primers for TaPG-PLC1 gave a product of 584bp with a DNA template from in *T. turgidum* (AABB), *T. aestivium* (AABBDD), *Ae. speltoides* (BB) and *Ae. tauschii* (DD) and did not yield a product with DNA from *T. urartu* (AA). This indicates that there are copies of TaPG-PLC1 like genes in both the B and D genomes. In addition, TaPG-PLC2 specific primers gave products with *T. urartu* (AA), *T. turgidum* (AABB), *T. aestivium* (AABBDD), and *Ae. speltoides* (BB), and did not yield products with *Ae. tauschii* (DD). This suggests copies of TaPG-PLC2 like genes in the A and B genomes (Figure 6).

2.2. Chromosome assignment and bin map of TaPG-PLC3

In order to map TaPG-PLC3 in the A genome, the same gene-specific primers that were used before for genome mapping of TaPG-PLC3 were applied for PCR screening of chromosomal deletion stocks which include nullisomic-tetrasomic, ditelosomic and partial chromosome-arm deletion lines (Table 2). In this case, the genetic stocks that did not give any PCR product indicate that the desired gene is present on the missing chromosome or chromosome part. The absence of PCR product from N5AT5D stock and the presence of the PCR amplification in DT5AL indicates that TaPG-PLC3 is located on the long arm of chromosome 5A (Figure 7). In order to determine in which segment of chromosome 5A TaPG-PLC3 is localized, stocks for four deletions in long

arm of 5A were used. The deletions from terminal to internal part of 5AL (long arm of chromosome 5A) were 5AL-23, 5AL-17, 5AL-10 and 5AL-12, respectively (Figure 7). The PCR results revealed no band in any of the deletion stocks, which indicates that TaPG-PLC3 is located on the terminal segment of the long arm of chromosome 5A.

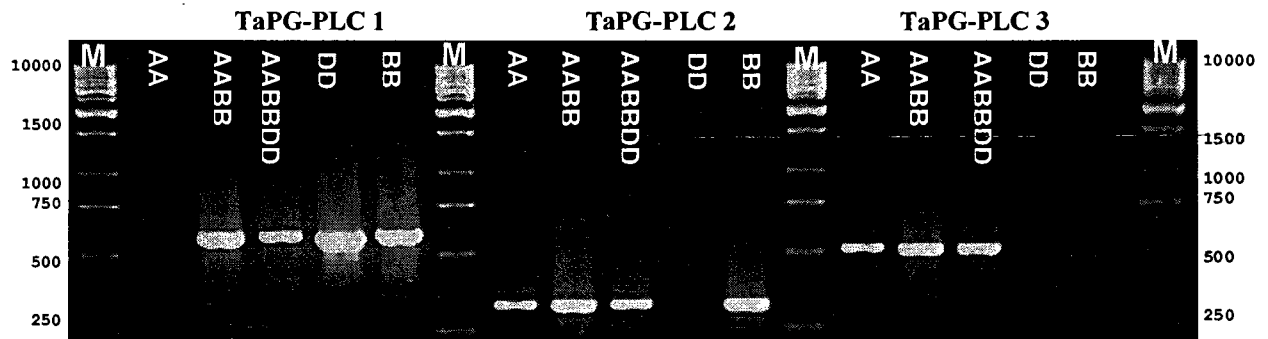


Figure (6): Genome mapping of TaPG-PLC1, TaPG-PLC2 and TaPG PLC3. AA, *Triticum urartu*; AABB, *Triticum turgidum*; AABBDD, *Triticum aestivium*; DD, *Aegilops tauschii*; BB, *Aegilops speltoides*; M, 1KB DNA ladder; * The expected molecular size of TaPG-PLC1, TaPG-PLC2 and TaPG-PLC3 PCR products were 584, 313 and 519 bp, respectively.

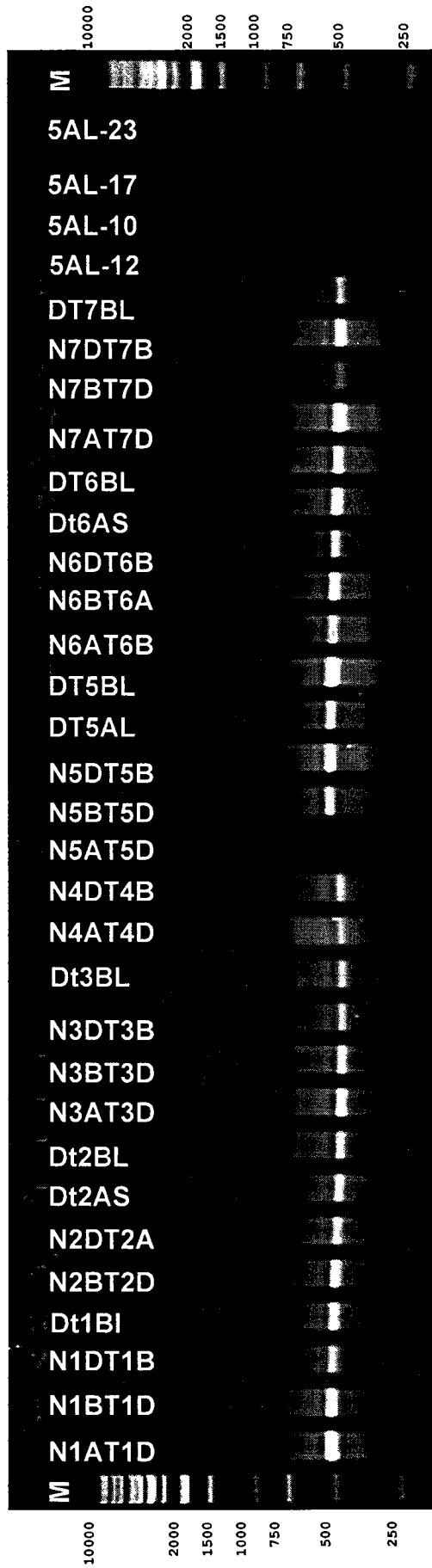


Figure (7): Mapping of TaPG-PLC3 using cytogenetic stocks of hexaploid Chinese spring wheat after PCR amplification with gene-specific primer. A, B and D, AA, BB and DD genomes; 1, 2, 3, 4, 5, 6 and 7, the number of wheat chromosomes; N, Nullisomic; T, Tetrasomic; DT, Detilosomic; L, Long arm of the chromosome; S, Short arm of the chromosome, M, 1KB DNA ladder; * The expected molecular size of TaPG-PLC3 was 519bp.

3. *Triticum aestivum* full-length TaPI-PLC1 and TaPI-PLC2 cDNA clones

The partial length of TaPI-PLC1 (FGAS ID STG1_K11 and GB GI:70971255) was strongly induced by cold treatment in wheat from 1 day to 14 days (Liu, 2005). STG1_K11 was 100% identical with WEF101_A23, another FGAS clone. The WEF101_A23 clone encodes 396 amino acids of the C-terminal part of TaPI-PLC1 and is missing the N-terminus. A pair of primers was designed to clone the full length TaPI-PLC1. The 5' UTR and the 5' end of the coding region TaPI-PLC1 were isolated after two rounds of PCR cloning. The ORF of the full length TaPI-PLC1 is 1521 nt and the 3' UTR has 214 nt (Figure 8). TaPI-PLC1 encodes 506 amino acids and the predicted protein has a molecular weight of 57 KDa. The amino acid sequence of TaPI-PLC1 is 80% identical to *O. sativa* PI-PLC1, (GenBank AAK01711) (Song and Goodman, 2002). Figure (9) shows the multiple amino acid sequence alignments of TaPI-PLC1, OsPI-PLC1 from rice (Song and Goodman, 2002), ZmPI-PLC from maize (NM_001114647), and AtPI-PLC6 from Arabidopsis (NP_850327). The common aspect of these genes is that they do not have an EF-hand calcium binding domain, as is found in other PI-PLCs.

TaPI-PLC2 is a full length cDNA clone, (FGAS ID L3C112_D16) initially identified as an EST sequence (GI: 39562842) (Appendix 2). The ORF of TaPI-PLC2 is 1761 nt and encodes a 586 aa protein. It has 59% amino acid identity to TaPI-PLC1 and contains an EF-hand calcium binding domain.

cagtctcccctacggatacatcgccgacgacccaagcaagcaagccgcccagcag
caacaaaccaaccaaccaatccctgcccggccaaactccaaacttccaaagcc
█ggcactacaagtgcctcgtcttcaagcgcggcccccaggtccaccacgacatg 60
M G T Y K C C L V F K R R P Q V H H D M
Tcccagcccctctcccactactcgtctacacgggccacaactcgtacctcaccggcaac 120
S Q P L S H Y Y V Y T G H N S Y L T G N
Cagctcagcagcgactgcagcgcagctccccatcatcaaggccctgcagcgcggcgtccgg 180
Q L S S D C S D V P I I K A L Q R G V R
Gtcaatcgagctcgacatgtggcccaactccgccaaggacgacatcagcatcctccatggc 240
V I E L D M W P N S A K D D I S I L H G
Agactttgaccaccccgtttcgtgctgaaatgcttgaatccatcaaagactatgct 300
R T L T T P V S L L K C L K S I K D Y A
Ttcgctcgcgtctccctaccggttatcatcacactcgaagaccaccttacacccgagctg 360
F V A S P Y P V I I T L E D H L T P E L
Caggacaaagttgccaagatggtccttgaagtgtttggcaccatactgtactaccctgaa 420
Q D K V A K M V L E V F G T I L Y Y P E
Gaagaacatcccaaagagctcccttcacctgagtcctcaagggtcgcgtgctcctatca 480
E E H P K E L P S P E S L K G R V L L S
Acaaagcccccaaggagtagcttgaagccaaggatggtggtgcccggaaagacggtgat 540
T K P P K E Y L E A K D G G A A K D G D
Gcggagcagaatcctggcaaaggaactgacgatgatgcccgttggggaacagaagtcca 600
A E Q N P G K G T D D D A A W G T E V P
Gatttcaagactgaaatccaatctgctaaacaggaagatgatgcctctgagaaccgtaga 660
D F K T E I Q S A K Q E D D A S E N R R
Gacggcgtagggacgacgatgaggacgaacagaaaatgcaacagcatctagctcca 720
D G D E D C D D D E D E Q K M Q Q H L A P
Cagtataagcgccttattactataagagcaggaagccaaaggggggtactacgtctgat 780
Q Y K R L I T I R A G K P K G G T T S D
Gccttgaagtgtgaccgcaacaagttaggcggctcagtttgagcagcaacagcttgcc 840
A L K C D P N K V R R L S L S E Q Q L A
Aaagctgtagttaatcattggcaccgaaatagtgaggtttacacagaggaatctactgagg 900
K A V V N H G T E I V R F T Q R N L L R
Atatacccaaagggcactcgggttacttcatccaactacaatccattttattggtgggtg 960
I Y P K G T R V T S S N Y N P F I G W V
Catggtgctcagatggttagccttcaatatgcagggatatggaagagctctttggttaatg 1020
H G A Q M V A F N M Q G Y G R A L W L M
Catggattttataaagccaatggtggctgtggctacgtgaagaaccggatttcttgatg 1080
H G F Y K A N G G C G Y V K K P D F L M
Cagtccgagccggaaagtttctgatccaaaaagcctcagcctgttaagaaaaaccttgaag 1140
Q S E P E V F D P K K P Q P V K K T L K
Gtgaaagtgtacatgggagatggttggcggatggacttcaagcagactcactttgaccaa 1200
V K V Y M G D G W R M D F K Q T H F D Q
Tattctcctccagatttttacgcacgggtcgggatcgccggcgtcccggcggactcgggtg 1260
Y S P P D F Y A R V G I A G V P A D S V
Atgaagaagaccaagggcgggtggaggacaactgggtgcccgggtgtggggggaggagtctcg 1320
M K K T K A V E D N W V P V W G E E F S
Ttcgacctgacggtgcccggagctggcgctgctgcgggtggaggcgcacgagtacgacatg 1380
F D L T V P E L A L L R V E A H E Y D M
Tcggagaaggacgactttgcccggcagacggtgctgccggtgctcggagcttcagcccggg 1440
S E K D D F A G Q T V L P V S E L Q P G
Atccgcgcccgtggcgtgttcgaccgcaaggggaacaagctccccaacgtcaagctcctc 1500
I R A V A L F D R K G N K L P N V K L L
Atcgcgtttgagtttggtttggaatggtttggtttggtttgagagatgatggcgtg 1560
M R F E F V -
Tcggcggccatggttgggtacttgggtgctcgtgcattctttggttcatcctgtacatacgtg 1620
Atcgggtctgtgtaatacggagtgtacggttgtatgtgagtcagttgtgtagacacg 1680
Agaattcatcaaccctgtatttgggtgagtgccgtaataaggtattttaccatcaaaaa 1740

Figure (8): Nucleotide sequence of TaPI-PLC1 full length cDNA and predicted amino acid sequence. The red letters are the deduced amino acid sequence; The blue nucleotides are 3' UTR sequence and green nucleotides are 5'UTR; The red highlights are start and stop codons of TaPI-PLC1.

4. Generating Gateway TaPG-PLC, TaPI-PLC and J822 fluorescent fusions

The ORF of the phosphoglycerol specific phospholipase C and phosphoinositol specific phospholipase C wheat cDNA clones TaPG-PLC1, TaPG-PLC2, TaPG-PLC3, TaPI-PLC1, TaPI-PLC2 and J822 respectively as well as their subdomains were used in this study to determine their subcellular localization. Figure (10) illustrates the PCR products of TaPG-PLC homologs and their truncations with attB flanking sites. The expected PCR molecular sizes were 1684, 1681, 1681, 1543, 1540 and 1540 bp for TaPG-PLC1, TaPG-PLC2, TaPG-PLC3, TaPG-PLC1 Δ NT, TaPG-PLC2 Δ NT and TaPG-PLC3 Δ NT, respectively. On the other hand, the expected molecular size of TaPI-PLC1, TaPI-PLC2, TaPI-PLC2 Δ EF-hand (TaPI-PLC2 without EF-hand domain) and TaPI-PLC2 Δ C2-2 (TaPI-PLC2 without C2-2 domain) were 1579, 1819, 1498 and 1436 bp, respectively (Figure 11). The PCR fragments of TaPG-PLCs, TaPI-PLCs and J822, the latter starting at aa 81, were cloned. Sequencing of the entry clones confirmed that they were intact and without mutation. They were then transferred into PK7FWG2, EGFP binary Gateway vector and two Gateway BiFC binary Yellow Fluorescent Protein YFP vectors, pBatL-B-sYFP-N and pBattL-cYFP using LR Gateway reaction (Table 6).

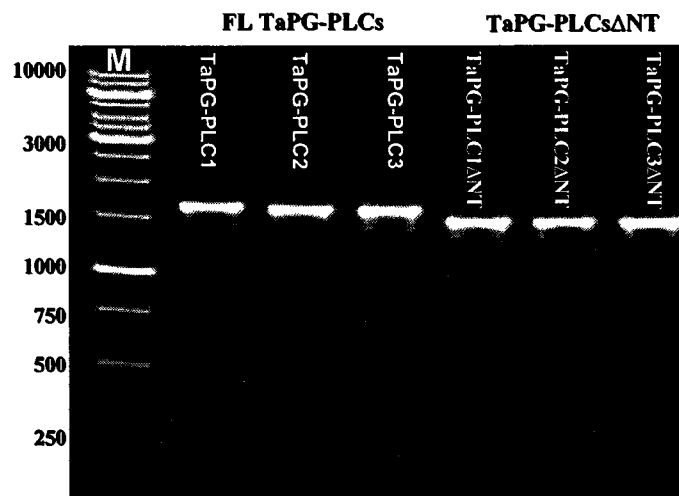


Figure (10): PCR products of PG-PLC homologs and their truncations. The expected molecular size for TaPG-PLC1, TaPG-PLC2, TaPG-PLC3, TaPG-PLC1 Δ 144NT, TaPG-PLC2 Δ 144NT and TaPG-PLC3 Δ 141NT were 1684, 1681, 1681, 1543, 1540 and 1540bp. **FL**, Full Length; **M**, Marker; **bp**, base pair; Δ , lacked; **NT**, N-terminal.

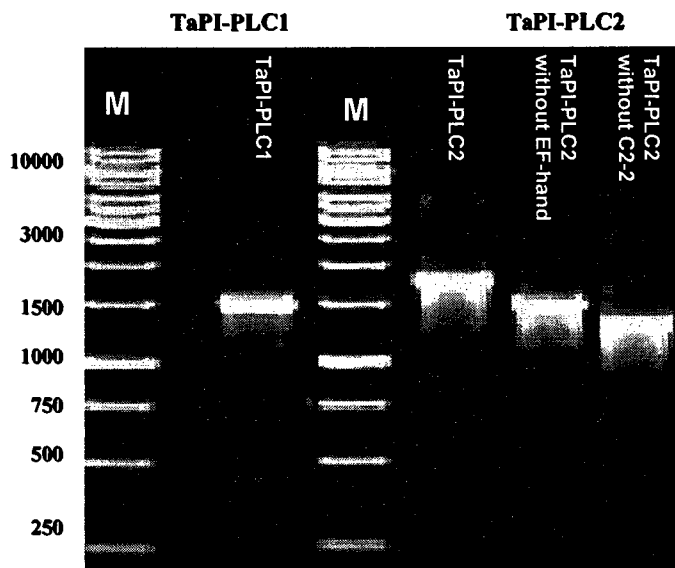


Figure (11): PCR products of TaPI-PLC1 and TaPI-PLC2 and some truncations of TaPI-PLC2. The expected molecular size of TaPI-PLC1, TaPI-PLC2, TaPI-PLC2 Δ EF-hand and TaPI-PLC2 Δ C2-2 were 1579, 1819, 1498 and 1436bp. **FL**, Full Length; **M**, Marker; **bp**, base pair.

5. Subcellular localization of TaPG-PLC and TaPI-PLCs

5.1. Subcellular localization of TaPG-PLCs

The full length cDNA of TaPG-PLC1, TaPG-PLC2 and TaPG-PLC3 and their truncations were used to study their subcellular localization. PSORT, TargetP, Predotar and signalP are programs which predict the localization of the proteins from their amino acid sequences and their conserved motifs. Because of the high identity between TaPG-PLC homologs, they showed the same predictions (Table 7). TaPG-PLC1, TaPG-PLC2 and TaPG-PLC3 are predicted to be localized in the endoplasmic reticulum (ER) with 0.82 and 0.98 probabilities using PSORT and Predotar prediction programs, respectively. Moreover, TargetP indicates that TaPG-PLC1, TaPG-PLC2 and TaPG-PLC3 have secretory pathway targeting signals (Table 7).

Experimental expression of the three TaPG-PLC::GFP constructs in tobacco epidermal tissue showed ER localization for these proteins (Figure 12). The ER localization is evident from the network structure that is seen in the upper focal plains of the cell. In addition, TaPG-PLC1::GFP fusion was co-localized with control fluorescent mCherry organelle associated (Nelson *et al.*, 2007). The co-localization with mCherry organelle markers showed that TaPG-PLC1 was co-localized with, ER, PM and golgi, while it was not co-localized with, plastids (Pt), mitochondria (Mt), nor Peroxisome (PX) (Figure 13).

Table (6): The Gateway entry clones and GFP fusion constructs for expression in *N. benthamiana*.

The Name of clone	Description
En.TaPG-PLC1	The entry clone of TaPG-PLC1 full length
En.TaPG-PLC2	The entry clone of TaPG-PLC2 full length
En.TaPG-PLC3	The entry clone of TaPG-PLC1 full length
En.TaPG-PLC1ΔNT	The entry clone of truncated TaPG-PLC1 which missed 144 nucleotides of N- terminal TaPG-PLC1
En.TaPG-PLC2ΔNT	The entry clone of truncated TaPG-PLC2 which missed 144 nucleotides of N- terminal TaPG-PLC2
En.TaPG-PLC3ΔNT	The entry clone of truncated TaPG-PLC3 which missed 141 nucleotides of N- terminal TaPG-PLC3
En.TaPI-PLC1	The entry clone of TaPI-PLC1 full length
En.TaPI-PLC2	The entry clone of TaPI-PLC2 full length
En.TaPI-PLC2ΔEF-hand	The entry clone of truncated TaPI-PLC2 which missed EF-hand domain
En.TaPI-PLC2ΔC2-2	The entry clone of truncated TaPI-PLC2 which missed C2-2 domain
Ex.TaPG-PLC1::GFP	The GFP expression clone of TaPG-PLC1 full length
Ex.TaPG-PLC2::GFP	The GFP expression clone of TaPG-PLC2 full length
Ex.TaPG-PLC3::GFP	The GFP expression clone of TaPG-PLC1 full length
Ex.TaPG-PLC1ΔNT::GFP	The GFP expression clone of truncated TaPG-PLC1 which missed 144 nucleotides of N-terminal TaPG-PLC1
Ex.TaPG-PLC2ΔNT::GFP	The GFP expression clone of truncated TaPG-PLC2 which missed 144 nucleotides of N-terminal TaPG-PLC2
Ex.TaPG-PLC3ΔNT::GFP	The GFP expression clone of truncated TaPG-PLC3 which missed 141 nucleotides of N-terminal TaPG-PLC3
Ex.TaPI-PLC1::GFP	The GFP expression clone of TaPI-PLC1 full length
Ex.TaPI-PLC2::GFP	The GFP expression clone of TaPI-PLC2 full length
Ex.TaPI-PLC2ΔEF-ha::GF	The GFP expression clone of truncated TaPI-PLC2 which missed EF-hand domain
Ex. TaPI-PLC2ΔC2-2::GF	The GFP expression clone of truncated TaPI-PLC2 which missed C2-2 domain
Ex. TaPG-PLC1::GFP	The GFP expression clone of TaPG-PLC1 full length

Continued>>

Table (6): Continued

The Name of clone	Description
Ex.TaPG-PLC1::NT-YFP	The N-half YFP expression clone of TaPG-PLC1 full length
Ex.TaPI-PLC1::NT-YFP	The N-half YFP expression clone of TaPI-PLC1 full length
Ex.TaPI-PLC2::NT-YFP	The N-half YFP expression clone of TaPI-PLC2 full length
EX.J822::CT-YFP	The C-half YFP expression clone of j822 missing 240nt of 5' end

En., Entry; Ex., Expression; Δ, missed

Table (7): The prediction of subcellular localization of candidate proteins with 4 prediction algorithms.

The Name of the gene	PSORT	TargetP	Predotar	SignalP
TaPG-PLC1	ER (0.82)	Secretory pathway	ER (0.98)	Yes
TaPG-PLC2	ER (0.82)	Secretory pathway	ER (0.98)	Yes
TaPG-PLC3	ER (0.82)	Secretory pathway	ER (0.98)	Yes
TaPI-PLC1	N (0.3)	Mitochondria	None	No
Ta PI-PLC2	Mt (0.6)	Mitochondria	Mt (0.55)	No

ER, endoplasmic reticulum; Mt, mitochondria; N, Nucleus

* The number between the brackets shows the probability of the prediction

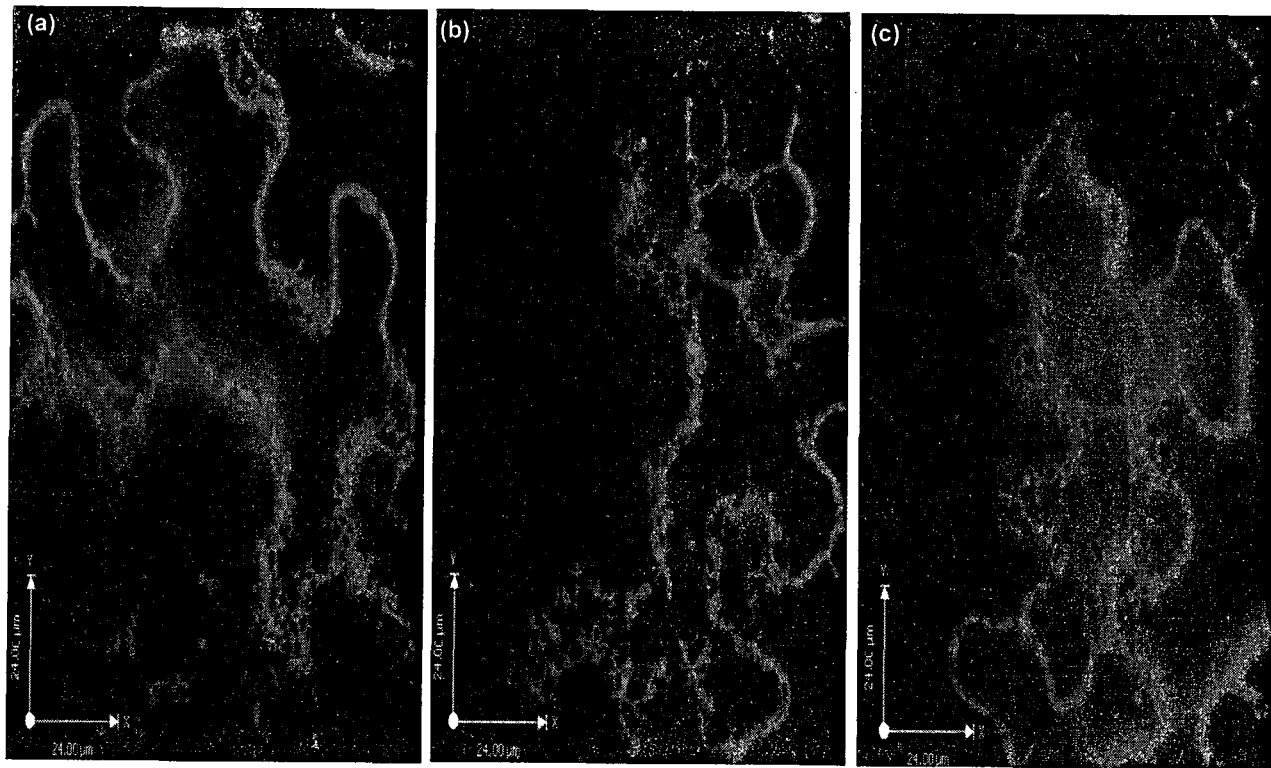


Figure (12): Transient expression of TaPG-PLC::GFP fusion proteins in tobacco leaf epidermal cells. The endoplasmic reticulum network structure is seen in each homolog. (a) TaPG-PLC1::GFP, (b) TaPG-PLC2::GFP and (c) TaPG-PLC3::GFP fusions. Scale bar = 24 μ M

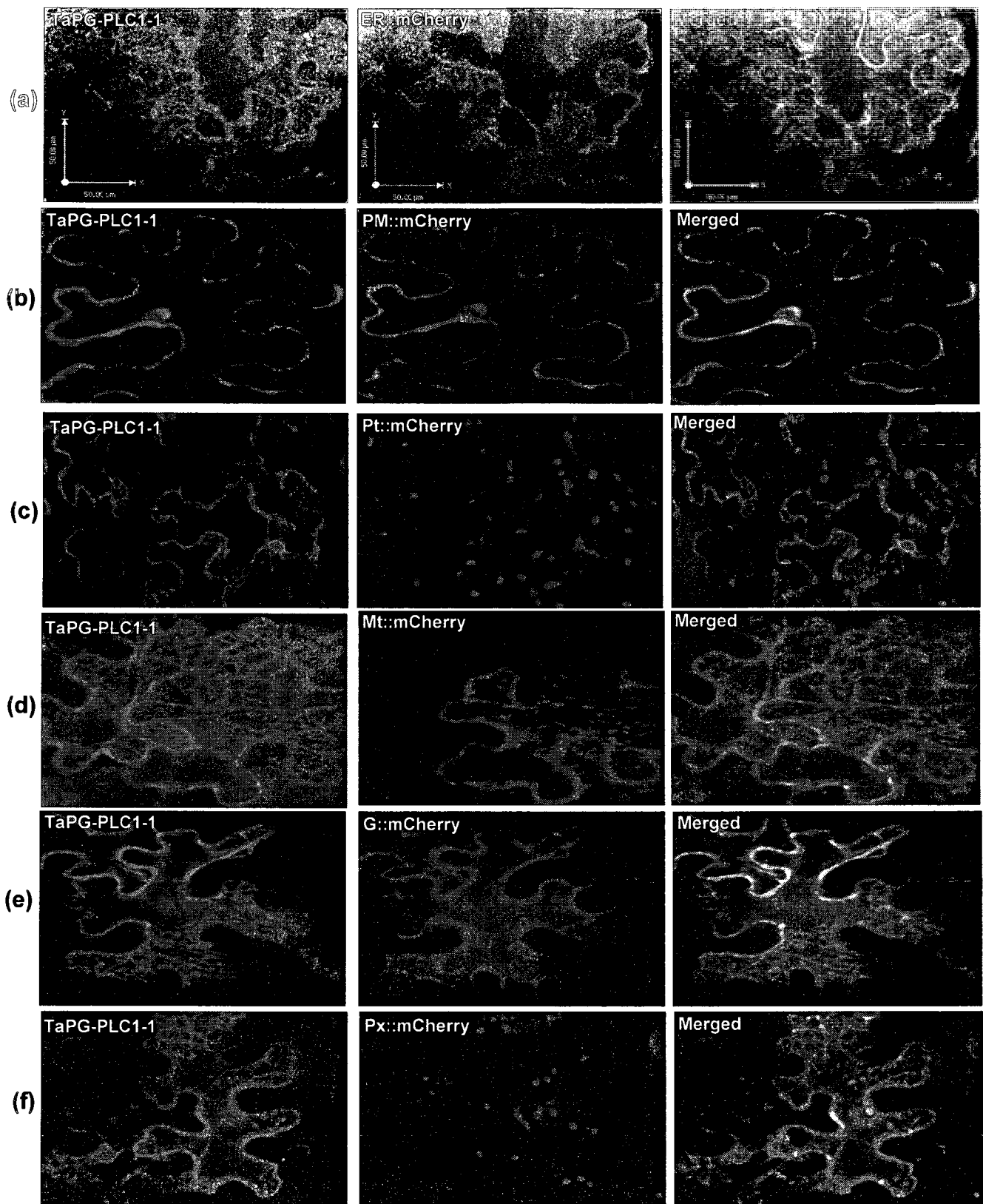


Figure (13): Co-localization of TaPG-PLC1::GFP with six mCherry organelle markers in tobacco leaf epidermal cells. (a)TaPG-PLC1 with ER (Endoplasmic Reticulum); (b)TaPG-PLC1 with PM (Plasma Membrane); (c)TaPG-PLC1 with Pt (Plastide); (d) TaPG-PLC1 with Mt (Mitochondria); (e) TaPG-PLC1 with G (Golgi); (f) TaPG-PLC1 with PX (Peroxisome); Scale bar = 50 µM.

The SignalP prediction program indicated that the TaPG-PLC homologs have signal peptides which consist of 24 amino acids. To study the effect of signal peptides on their localization, TaPG-PLC1, TaPG-PLC2 and TaPG-PLC3 truncations were made in which the first 48 codons were deleted from the N-terminal region and the resulting ORF was fused with GFP (Table 6). In contrast to the full length TaPG-PLC1 the shortened TaPG-PLC1 Δ NT was only localized to the PM (Figure 14).

5.2. Subcellular localization of TaPI-PLCs

The amino acid identity between TaPI-PLC1 and TaPI-PLC2 was 59%. TaPI-PLC2 has an EF-hand domain in its N-terminal region, while TaPI-PLC1 does not. No signal peptide was identified in TaPI-PLC1 or TaPI-PLC2 with the signalP detection algorithm (Table 7). PSORT predicted that TaPI-PLC1 and TaPI-PLC2 would be localized in the nucleus and mitochondria with low, 0.3 and 0.6, probabilities, while TargetP program indicated that both TaPI-PLC1 and TaPI-PLC2 have predicted mitochondria target sequences (Table 7). However, experimental subcellular localization of TaPI-PLC1 and TaPI-PLC2 GFP fusions revealed that TaPI-PLC1 was localized to the ER (Figure 15), whereas TaPI-PLC2 was found on the PM (Figure 16). The co-localization results with control markers confirmed that TaPI-PLC1 was co-localized with ER and PM (Figure 17) and was not localized with the other organelle markers. Similarly, TaPI-PLC2 did not localize with any other subcellular marker beside the PM marker (Figure 18).

To study the effect of EF-hand and C2-2 domains on TaPI-PLC2 targeting to PM two truncated versions were tested. TaPI-PLC2 Δ EF-hand::GFP which lacked the EF-hand domain and the other one was TaPI-PLC2 Δ C2-2::GFP fusions without the C2-2

domain (**Table 6**). TaPI-PLC2 Δ EF-hand::GFP was detected on the PM, like the full length construct, however the level of expression appeared to be lower than the full length version of TaPI-PLC2 (**Figure 19**). The level of the expression of TaPI-PLC2 Δ C2-2::GFP was high and it was not localized on PM but was found in the ER (**Figure 20**).

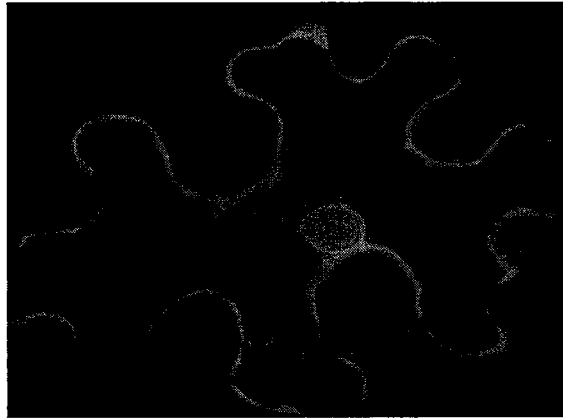


Figure (14): Subcellular localization of TaPG-PLC1 Δ NT::GFP truncation in epidermic tobacco tissues. Scale bar = 24 μ m.

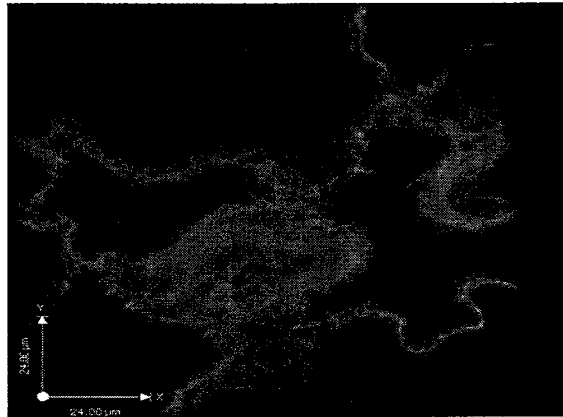


Figure (15): Endoplasmic reticulum like structure of TaP1-PLC1::GFP fusion in epidermic tobacco tissues. Scale bar = 24 μ m

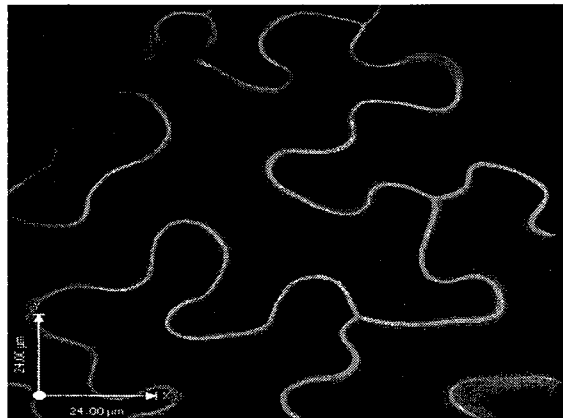


Figure (16): Plasma membrane like structure of TaP1-PLC2::GFP fusion in epidermic tobacco tissues. Scale bar = 24 μ m

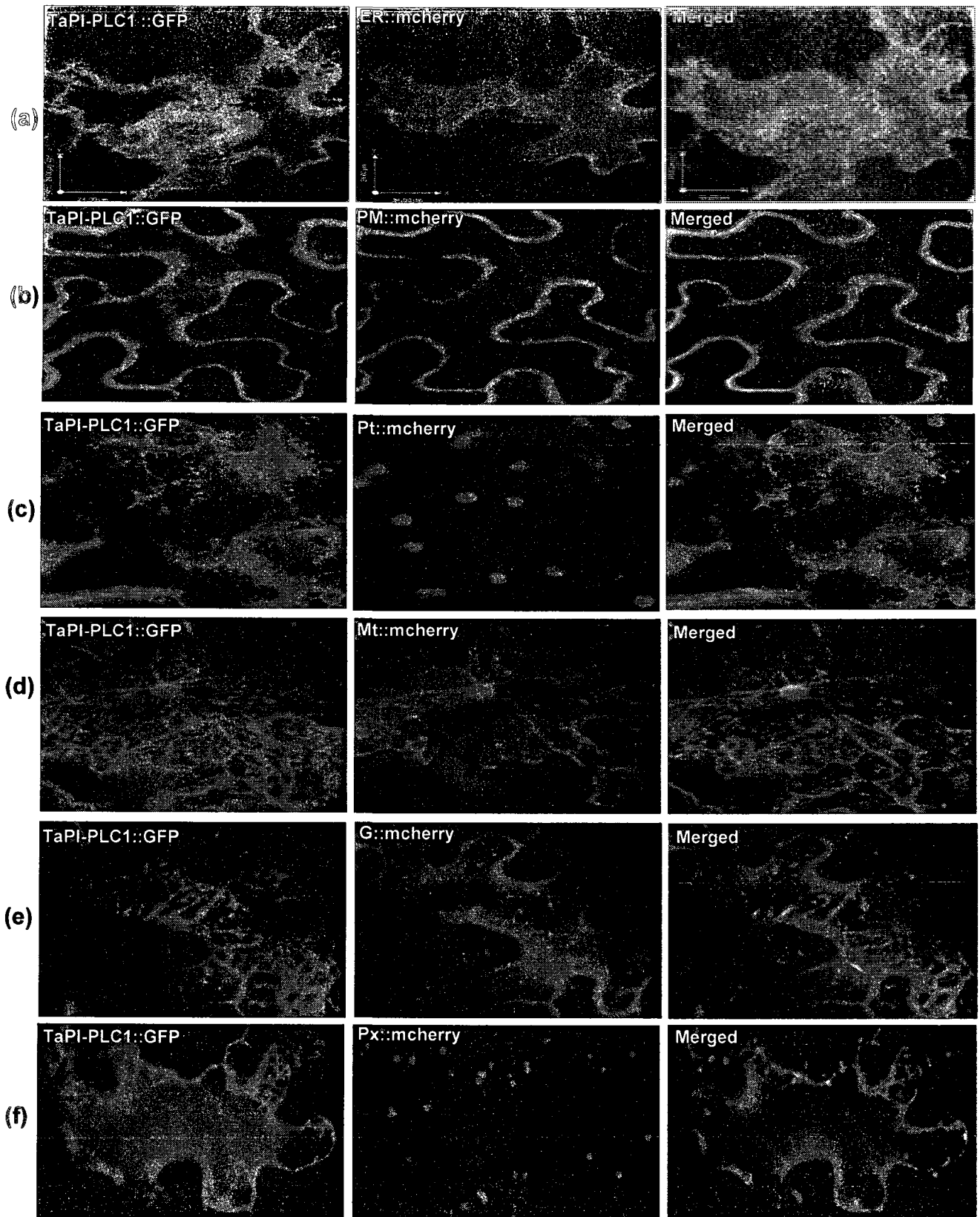


Figure (17): Co-localization of TaPI-PLC1::GFP with six mCherry organelle markers in tobacco leaf epidermal cells. (a)TaPI-PLC1 with ER (Endoplasmic Reticulum); (b)TaPI-PLC1 with PM (Plasma Membrane); (c)TaPI-PLC1with Pt (Plastide); (d) TaPI-PLC1 with Mt (Mitochondria); (e) TaPI-PLC1 with G (Golgi); (f) TaPI-PLC1 with PX (Peroxisome); Scale bar = 50 µM.

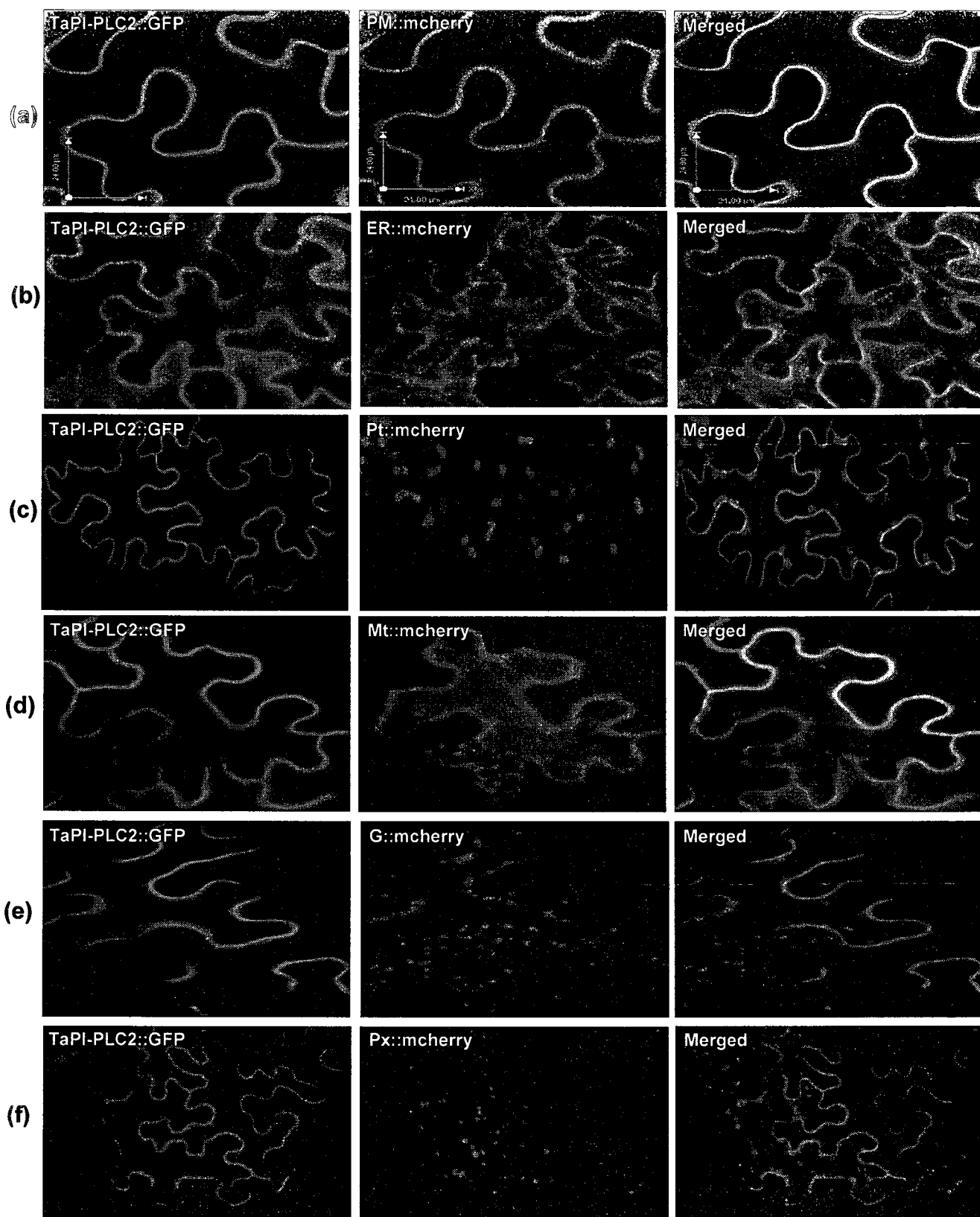


Figure (18): Co-localization of TaPI-PLC2::GFP with six mCherry organelle markers.
 (a) TaPI-PLC2 with PM (Plasma Membrane); (b) TaPI-PLC2 with ER (Endoplasmic Reticulum);
 (c) TaPI-PLC2 with Pt (Plastide); (d) TaPI-PLC2 with Mt (Mitochondria); (e) TaPI-PLC2 with G (Golgi);
 (f) TaPI-PLC2 with PX (Peroxisome); Scale bar = 50 μm.

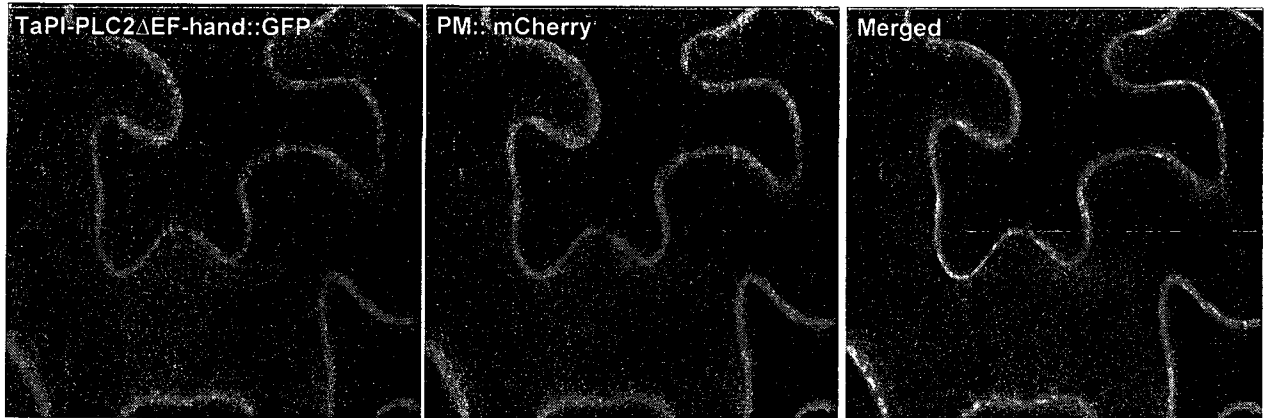


Figure (19): Co-localization of TaPI-PLC2 Δ EF-hand::GFP with PM (Plasma Membrane) mCherry marker in epidermic tobacco tissues. Scale bar = 24 μ M.

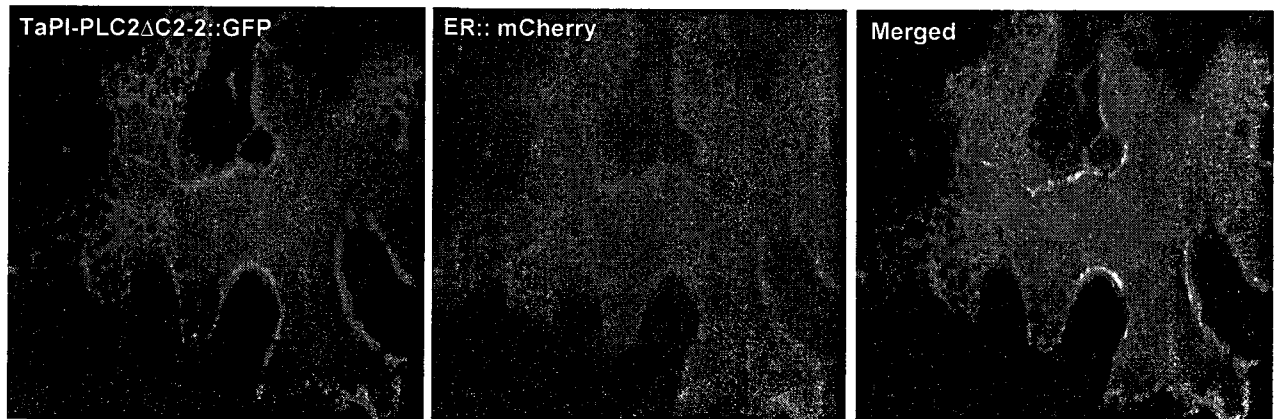


Figure (20): Co-localization of TaPI-PLC2 Δ C2-2::GFP with ER (Endoplasmic Reticulum) mCherry marker in epidermic tobacco tissues. Scale bar = 24 μ M.

6. *In vivo* interactions between wheat PLC genes and GTP-binding proteins

6.1. *In vivo* interactions between wheat PLC genes and Gα using BiFC

To study the involvement of TaPG-PLC1, TaPG-PLC2, TaPG-PLC3 homologs, TaPI-PLC1 and TaPI-PLC2 in signal transduction in plant cells, two BiFC constructs containing the heterotrimeric G protein α subunit, wheat G α , prepared by Zhejun Wang in our laboratory (data not shown), were tested for interaction with wheat PLC genes in tobacco. These included an intact version of TaG α and a mutated form with constitutive GTP binding due to inactivated GTPase active site, TaG α -Q223L. This is the same mutation used by Oki *et al.*, (2005) in the rice G α (RGA1) rQ223L. In BiFC assay, candidate protein interaction partners are fused to one or the other half of the split YFP fluorescent protein. Interaction between the proteins would reconstitute the YFP that is detected in transformed *N. benthamiana* leaf cells (Bracha-Drori *et al.*, 2004; Walter *et al.*, 2004). BiFC experiments were performed to study the interactions between wheat PLC- N-terminal half YFP constructs with wheat G α C-terminal half YFP constructs. The experiment was supported by positive and negative controls to confirm the accuracy of the interactions. Positive controls included AtRGS1 N-terminal-YFP, Arabidopsis regulator of G-protein signaling protein 1, and AtGPA1 C-terminal-YFP, Arabidopsis G α , which showed clear interaction in the PM (data not shown), (Grigston *et al.*, 2008). In the negative control pair, no interaction was observed between AtPIS-C-terminal, Arabidopsis PtdIns synthase, and AtHVA22d-N-terminal-YFP, an Arabidopsis ABA-responsive protein (Dr Hugo Zheng, McGill University).

BiFC interaction showed a positive interaction between TaPI-PLC1 and both TaG α and TaG α -Q223L which were localized on ER and PM. The two interacting pairs were co-localized with PM and ER mCherry organelles markers (Figure 21). Moreover, the BiFC results showed a higher level of yellow fluorescence from the interaction between TaPI-PLC1 and TaG α -Q223L than the level of signal from the interaction between Ta PI-PLC1 and TaG α . The level of yellow fluorescence was seen to be higher as judged relative to the level of fluorescence of the organelle marker which was co-transformed with the interacting proteins. In contrast none of the three homologs of TaPG-PLC nor TaPI-PLC2 showed any interaction with the TaG α nor TaG α -Q223L in BiFC assays.

6.2. *In vivo* interactions between wheat PLC genes and the wheat J822 G-protein using BiFC

A guanine nucleotide binding protein J822 does not have significant sequence similarity to heterotrimeric G proteins and was hypothesized to be a non canonical G-protein (Liu, 2005). BiFC interaction showed the same results as G α as a positive interaction between TaPI-PLC1 and J822 was reported and localized on ER and PM (Figure 22). J822 did not show interaction with the three homologs of TaPG-PLC and TaPI-PLC2.

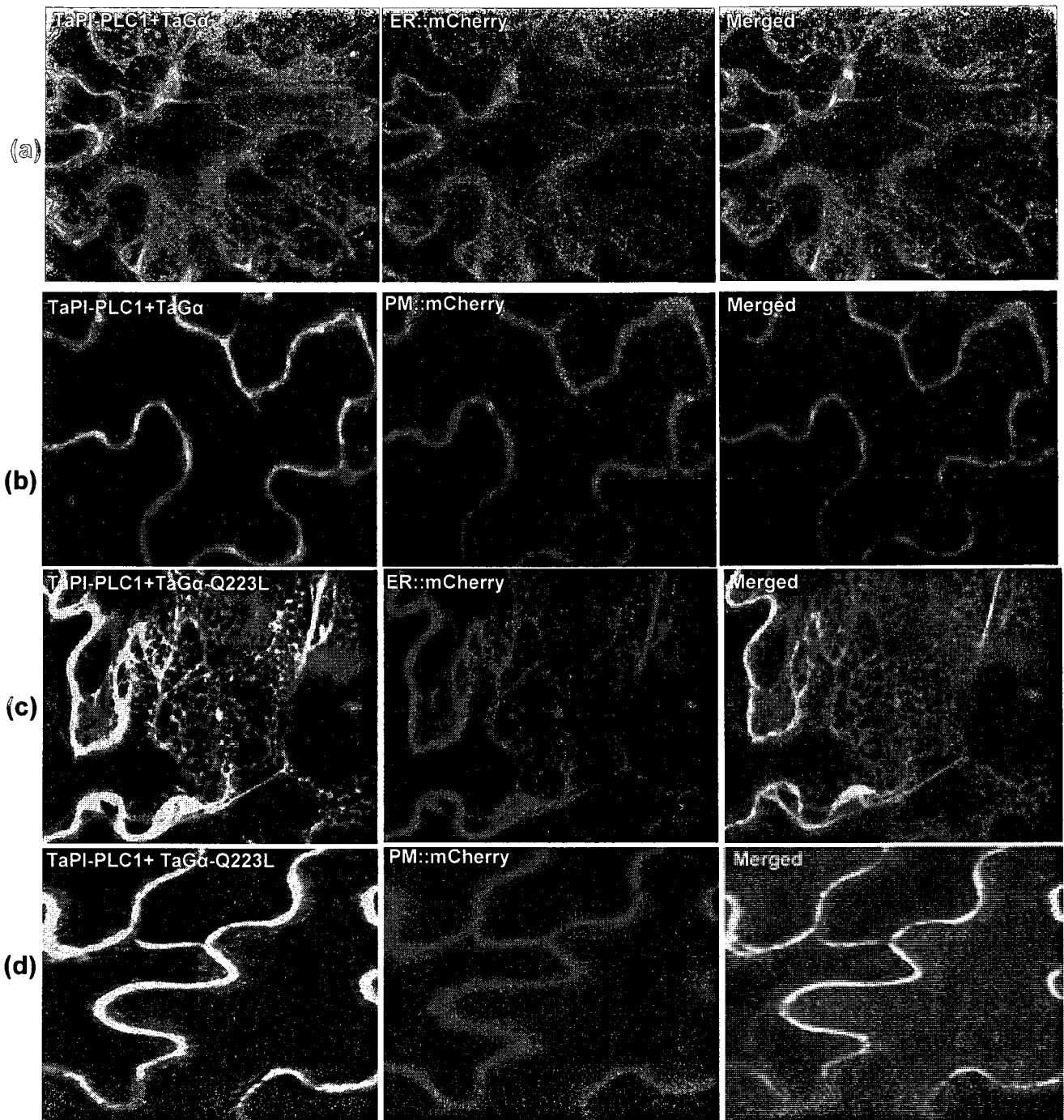


Figure (21): BiFC visualization of TaPI-PLC1 and TaG α interaction in epidermic tobacco tissues. (a)Co-localization of TaPI-PLC1 and TaG α with ER (Endoplasmic Reticulum) mCherry marker; (b)Co-localization of TaPI-PLC1 and TaG α with PM (Plasma Membrane) mCherry marker; (c)Co-localization of TaPI-PLC1 and TaG α -Q223L with ER (Endoplasmic Reticulum) mCherry marker; (d)Co-localization of TaPI-PLC1 and TaG α -Q223L with PM (Plasma Membrane); Scale bar = 24 μ M.

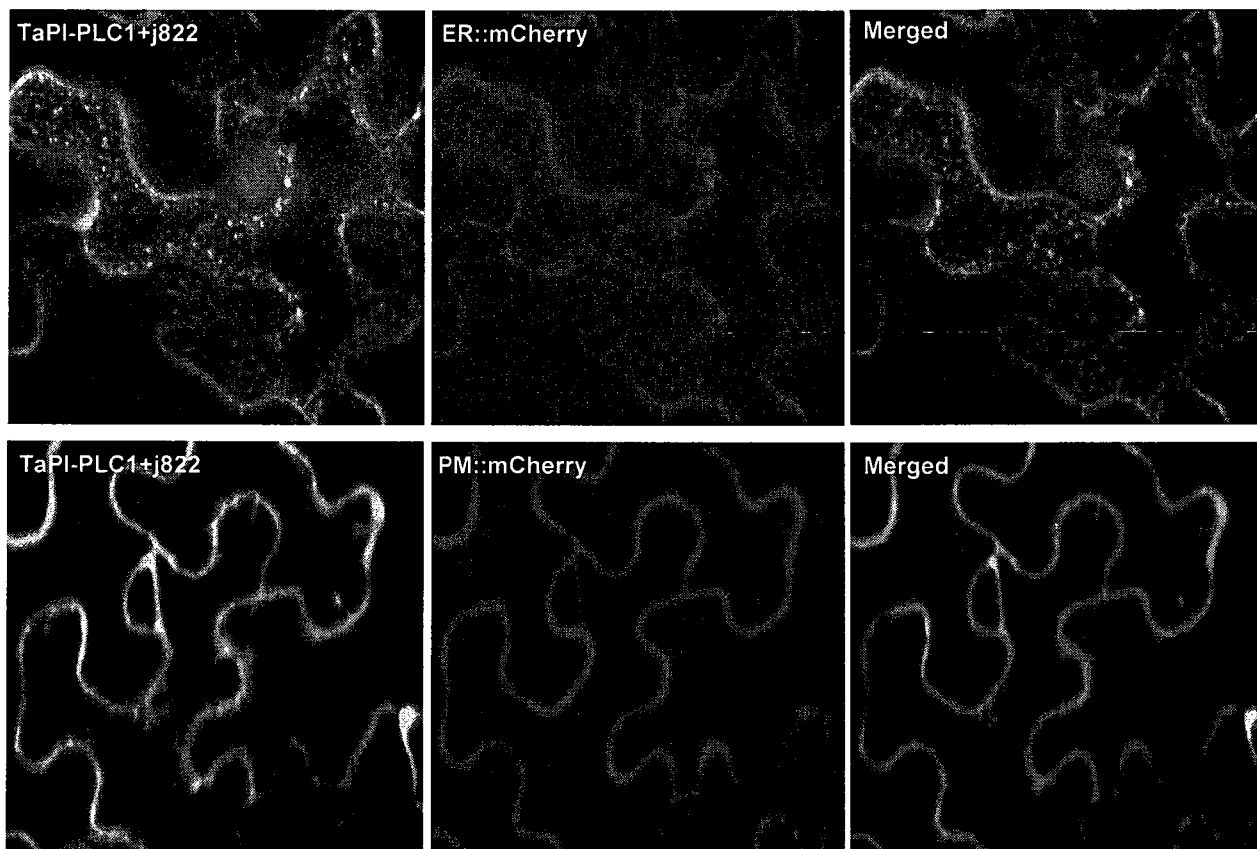


Figure (22): BiFC visualization of TaPI-PLC1 and J822 in epidermic tobacco tissues. (a)Co-localization of TaPI-PLC1 and J822 with ER (Endoplasmic Reticulum) mCherry marker; **(b)**Co-localization of TaPI-PLC1 and J822 with PM (Plasma Membrane) mCherry; Scale bar = 24 μ M.

PART IV. DISCUSSION

1. TaPG-PLC annotation

Phosphoglycerol specific phospholipases, phosphoesterases and non specific phospholipases in Arabidopsis and rice are gene families which include several isoforms that share the same phosphoesterase domain structure. Kyoto Encyclopedia of Genes and Genomes (KEGG) website is a database of biological systems that contains diagrams of biochemical pathways and interrelation networks (KEGG pathway). PG-PLC or plcC (EC 3.1.4.3) in KEGG website plays various roles in different pathways; i.e., glycerophospholipid metabolism (ec00564), inositol phosphate metabolism (ec00562), and ether lipid metabolism (ec00565), glycine, serine and threonine metabolism (ec00260) (Appendix 3a, b, c and d).

In the current study, three homologs of TaPG-PLC1, TaPG-PLC2 and TaPG-PLC3, from wheat were identified and fully sequenced. The sequence identity between the three homologs was between 96% and 93%. Homeologous gene copies in *T. aestivum* are expected to be approximately 97-95% identical within the coding region. In addition, similarity between *T. aestivum* genes and the orthologous genes from a diploid progenitor are expected to be close to 99% identical (eg. Farajalla and Gulick, 2007). TaPG-PLC homologs were found to be most similar to OsPG-PLC1 and AtPG-PLC1 in rice and Arabidopsis (Figure 5).

2. TaPG-PLC mapping on wheat genome

The hexaploid wheat *T. aestivum* is derived from two relatively recent polyploidization events between three diploid species. The first event involves *T. urartu* and a species closely related to *Ae. speltoides* which occurred about 0.5 million years ago, and led to the appearance of hard wheat *T. dicoccoides*. The second polyploidization event took place about 9000 years ago, between *T. dicoccoides* (tetraploid) and a third diploid *Ae. tauschii* (Feuillet and Muehlbauer 2009), thus most genes are expected to exist in 3 copies in wheat due to polyploidy events. Moreover, gene copy number can also be affected by gene duplications and deletions. Amplification with gene specific primers for TaPG-PLC3 indicates a single gene copy on A genome progenitor (Figure 11). In contrast, amplification with gene specific primers for TaPG-PLC1 and TaPG-PLC2 yielded products from both the B and D genome progenitors as well as the AB genome tetraploid progenitor. This would indicate copies of the genes in both the B and D genomes, and implies four gene copies detected with these primers. The reverse primers correspond to regions of insertion/deletion in the 3' UTR so it is unlikely that there were non-specific amplifications. The experiments were repeated with a second set of primers (data not shown) with the same results. Though Southern blot data often detects multiple gene copies in both diploid and polyploidy plant species (Qi, 2004) it is surprising that gene copies on the B and D genomes would retain such high sequence similarity especially in non-coding regions.

TaPG-PLC3 is a single copy gene copy in the A genome progenitor. PCR amplification with DNA from *T. urartu*, the A genome progenitor, 5A nullitetrasonic and ditelosomic lines as well as the 5AL segmental deletion lines was in agreement with this

map location. The chromosomes from homeologous group 5 in wheat carry important genes associated with domestication (Q), grain quality (Ha), plant responses to seasonal changes (Vrn1 and Vrn2), frost tolerance (Fr1 and Fr2), regulation of homeologous chromosome pairing (Ph1), salt and dehydration tolerance (Esi2, Esi4, Esi14, Esi28, Esi32, Esi47, Dhn2, and Dhn1), heat tolerance (Hsp16.9) and numerous resistance genes to pathogens (e.g., Tsn1, Lr18, Snb3, and Sr30) (McIntosh *et al.*, 2003). Linkiewicz *et al.*, (2004) observed statistically significant colinearity between low-copy-number ESTs from wheat homeologous group 5 and rice chromosomes 12 (88 ESTs), 9 (72 ESTs) and 3 (84 ESTs). OsPG-PLC1, the rice gene most similar to TaPG-PLC1, was mapped on rice chromosome 3 (Table 5). Wheat Binmap Viewer (<http://wheat.pw.usda.gov/wEST/binmaps/>) is a graphical interface to the wheat ESTs mapped in Chinese Spring deletion lines; Figure (23) taken from this site illustrates the colinearity between the distal part of chromosome 5L in wheat and chromosome 3 in rice.

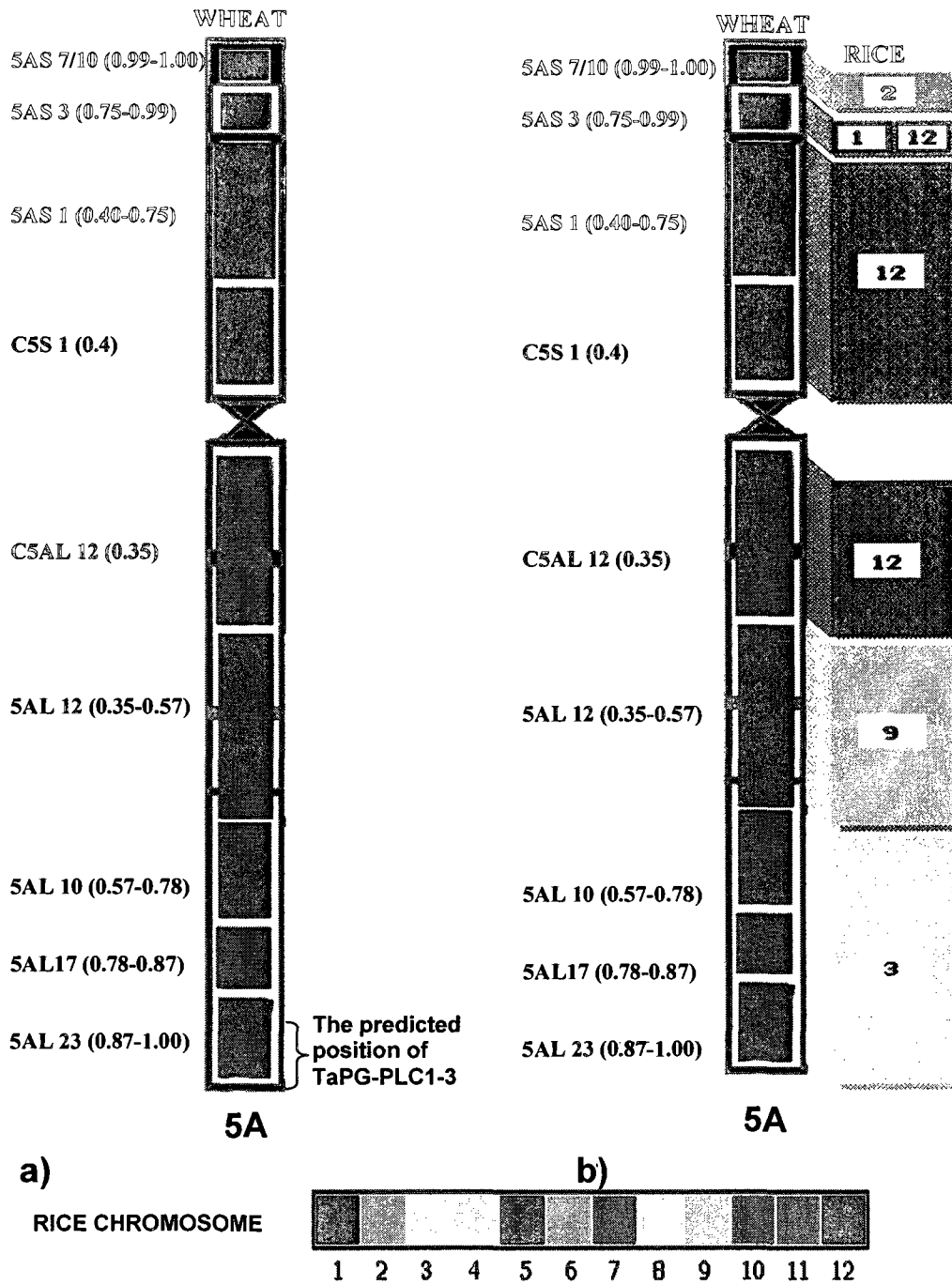


Figure (23): Chromosome bin map of 5A in wheat; the predicted position of TaPG-PLC3 in wheat the colinearity between chromosome 5A in wheat and its relative to rice genome. (http://wheat.pw.usda.gov/wEST/binmaps/wheat5_rice.html).

3. TaPI-PLC sequence analyses

Based on amino acid sequence comparisons, plant PI-PLCs are most closely related to the δ PLC subfamily (Shi 1995). Plant PI-PLCs all contain X and Y domains that are necessary for the phosphoesterase activity and a C2-2, a Ca^{2+} - binding domain. The X domain of TaPI-PLC1 contains four conserved histidine residues (Figure 8). The most similar gene in rice, OsPI-PLC1, has five histidine residues (Song and Goodman, 2002). Histidine residues have been shown to be essential for enzyme activity (Cheng *et al.*, 1995 and Ellis *et al.*, 1995). There are nine PI-PLCs identified in Arabidopsis. Arabidopsis PI-PLC1, PI-PLC2, PI-PLC3, PI-PLC4, PI-PLC5 and PI-PLC7 each have an EF-hand domain, consisting of a core of four alpha helices which is important for enzyme function (Otterhag *et al.*, 2001), while Arabidopsis PI-PLC6, PI-PLC8 and PI-PLC9 do not. Among the nine AtPI-PLC isoforms in Arabidopsis, AtPI-PLC2 has the highest amino acid sequence identity to TaPI-PLC1 with 65% amino acid sequence identity; however, AtPI-PLC6 with 64% identity is more likely the actual ortholog to TaPI-PLC1. Both TaPI-PLC1 and AtPI-PLC6 lack the EF-hand domain whereas AtPI-PLC2 includes this domain. Within the X domain, the identity between TaPI-PLC1 and AtPI-PLC6 is 74%, while the identity between TaPI-PLC1 and AtPI-PLC2 is 70%. C2-2 domain of TaPI-PLC1 has 72% identity with AtPI-PLC6 whereas it shares only 69% identity with AtPI-PLC2. Overall, structural conservation suggests that TaPI-PLC1 is closely related to AtPI-PLC6 and we predict that they have similar activity.

4. The relationship between the isoforms of PI-PLCs and the environmental stress tolerance

PI-PLC produces IP3 by its hydrolysis activity with PIP2. IP3 which is soluble in the cytosol triggers transient increases of cytosolic Ca²⁺. Knight (2000) reported that cold stress has been shown to elicit rises in cytosolic free calcium levels. Moreover, the relation between PI metabolism and cytosolic calcium level has been reported (Zhu, 2002 and Xiong *et al.*, 2002). TaPI-PLC1 was expressed at very low level under normal conditions, while it was strongly induced by cold acclimation from 1 day to 14 days (Liu, 2005) and (Table 8). OsPI-PLC1 which is the most closely related gene to TaPI-PLC1 was induced by various chemical and biological inducers of plant defense pathways (Song and Goodman, 2002) and (Table 8).

The effects of the environmental changes on the Arabidopsis PI-PLCs are varied (Table 8). Till now, there has been no study with AtPI-PLC6 in relationship to environmental stresses. There have been three reports that AtPI-PLC1 is highly inducible by environmental stresses (Hirayama *et al.*, 1995; Hunt *et al.*, 2004; Sanchez and Chua 2001). Transgenic Arabidopsis lines expressing antisense AtPI-PLC1 constructs accumulated less IP3 after being treated with ABA and showed decreased induction of ABA responsive genes compared with such induction in control plants (Sanchez and Chua, 2001) which suggests that IP3 acts in signal transduction for up regulated genes in response to ABA.

Table (8): PI-PLCs of wheat, rice and Arabidopsis involvement in environmental stress.

Gene	Accession No.	Evidence for involvement in abiotic stress	reference
TaPI-PLC1		* Up-regulation by environmental stress, protein interaction with J822, a novel cold induced GTP-binding protein gene in wheat.	(Liu, 2005)
OsPI-PLC1	AAK01711.1	* Molecular cloning and characterization of a rice phosphoinositide-specific phospholipase C gene, OsPI-PLC1, that is activated in systemic acquired resistance.	(Song and Goodman, 2002)
AtPI-PLC1	NP_568881	* A gene encoding a phosphatidylinositol-specific phospholipase C is induced by dehydration and salt stress in Arabidopsis thaliana.	(Hirayama et al., 1995)
		* Arabidopsis PLC1 is required for secondary responses to abscisic acid signals	(Sanchez and Chua, 2001)
		* Gene-specific expression and calcium activation of <i>Arabidopsis thaliana</i> phospholipase C isoforms	(Hunt et al., 2004)
AtPI-PLC4	Q944C1	* Gene-specific expression and calcium activation of <i>Arabidopsis thaliana</i> phospholipase C isoforms	(Hunt et al., 2004)
AtPI-PLC5	Q944C2	* Gene-specific expression and calcium activation of <i>Arabidopsis thaliana</i> phospholipase C isoforms	(Hunt et al., 2004)

Ta, *Triticum aestivum*; Os, *Oryza sativa*; At, *Arabidopsis thaliana*

5. The localization of TaPG-PLC in plants

5.1. TaPG-PLC1 localized in ER, Golgi and PM

In general, PG-PLC hydrolyzes the glycerolphosphate ester linkage of phosphatidyleglycerol (PG) to DAG and glycerol-3-phosphate (Simockova *et al.*, 2008) or the glycerolphosphate ester linkage of phosphatidylcholine (PC) (Nakamura *et al.*, 2005), so it is logic to predict that it will localize on plasma membrane and plastids. Although, the computational methods of predicting protein subcellular localization sometimes are not precise, some programs are supported by a confidence number as a measure of the accuracy of their predictions. In this study, PSORT and Predotar prediction programs predicted that TaPG-PLC homologs would be localized in the ER. Nakamura *et al.*, (2005) used TargetP to predict the localization of six Arabidopsis PLCs referred to as Non Specific Phospholipase Cs (NPC) which have the same phosphoeesterase domain structure as TaPG-PLC1; NPC1, NPC2 and NPC6 are predicted to enter the secretory pathway, but NPC3, NPC4 and NPC5 were not (Table 5). In addition, they showed that the subcellular localization of the NPC4 protein (AT3G03530) in Arabidopsis was highly enriched in plasma membrane using cell fractionation and western blotting. Experimental localization of TaPG-PLC1::GFP has shown its localization in the ER, PM and golgi (Figure 13).

5.2. TaPG-PLC homologs and the secretion pathway

Plant cells are highly compartmentalized and each compartment has a specific role, therefore the distributions and localizations of proteins are intrinsically bound to their functions. ER is the entry point for most membrane and soluble proteins into the secretory pathway. Nascent proteins destined for secretion are delivered to the ER and then

transported to the golgi apparatus, where they are further sorted for translocation to the cell exterior, or to cellular compartments such as protein storage vacuoles, lytic vacuoles, the plasma membrane, or the cell wall (Sebastian and Raikhel, 1992). TargetP revealed that TaPG-PLC homologs would enter into the secretory pathway. The TaPG-PLC1::GFP fusion co-localized with ER, PM and golgi which suggests that it enters the ER and is tranlocated to golgi, then to PM.

In eukaryotes, proteins that are targeted to the ER membrane are mediated by signal peptides that target the protein either co-translationally or post translationally to Sec61, a membrane protein translocator. The ER signal peptides are cleaved from exported protein after export into the ER lumen by SPC, Signal Peptidase Complex (Paetzel *et al.*, 2002). SignalP prediction program showed that TaPG-PLC homologs have signal peptides which consist of 24 amino acids. The most important aspect of the signal peptides of secretory proteins is that they include a positively charged amino-terminal n-region, a hydrophobic core and a carboxyl-terminal specificity c-region (Table 9). TaPG-PLC1 Δ NT truncation::GFP fusion which was missing the signal peptide from N-terminal region of the TaPG-PLC1 was localized on PM.

Table (9): The deduced amino acid sequences of TaPG-PLC1 signal peptides.

Homologs Name	The amino acid sequences of TaPG-PLC1 signal peptides		
	n-region	h-region	c-region
TaPG-PLC1	M AAA GERR	LLVGLLLL ALM	V SAHC
TaPG-PLC2	M AAA GERR	LLACLELL ALM	I SAHC
TaPG-PLC3	M AAA GERR	LLVGLLLL ALV	V SAHC

n-rigion, a positively charged N-terminal region; **h-region**, hydrophobic region; **c-region**, carboxyl-terminal region

6. Subcellular localization of TaPI-PLCs in plants

6.1. TaPI-PLC1 and TaPI-PLC2 were localized on ER and PM, respectively

Based on *in vitro* enzyme activity assays, two types of PI-PLC have been identified in higher plants; one is predominantly present in the cytosolic fraction and the other is localized in plasma membrane (Mueller-Roeber and Pical, 2002). Table (10) lists the subcellular localization of PI-PLCs in different plants. The four prediction programs that were mentioned before for subcellular localization did not give predictions with high confidence scores for TaPI-PLC1 or TaPI-PLC2. The subcellular localization of TaPI-PLC::GFP fusions showed that TaPI-PLC1 was localized on ER and PM, while TaPI-PLC2 was localized on PM (Figures 17a and 18a). AtPLC2 was also found to be predominantly localized in plasma membrane using a polyclonal antibody raised against a synthetic polypeptide specific for Arabidopsis AtPLC2 isoform (Otterhag *et al.*, 2001). Furthermore, *Vigna radiata* VrPI-PLC3::GFP fusion was localized primarily to the plasma membrane of transgenic Arabidopsis protoplasts (Kim *et al.*, 2004).

Table (10): The localization of higher plant PI-PLCs.

Gene	localization	Plant	Experimental evidence	reference
OsPI-PLC	Plasma membrane	<i>Oryza sativa</i>	Plasma membrane purification	(Yotsushima <i>et al.</i> , 1993)
AsPI-PLCs	Plasma membrane and Cytosol	<i>Avena Sativa</i>	Cell fractionation	(Huang <i>et al.</i> , 1995)
GmPI-PLC	Plasma membrane and Cytosol	<i>Glycine max</i>	Western blot and cell fractions	(Shi,1995)
AtPI-PLC1	Plasma membrane	<i>A. thaliana</i>	Suspension cells	(Mueller and Pical, 2002)
BnPI-PLC	Plasma membrane	Brassica napus	Subcellular fractions of hypocotyls of young plants	(Novotna <i>et al.</i> , 2003)
VrPI-PLC3	Plasma membrane	<i>Vigna radiate</i>	GFP fusion	(Kim <i>et al.</i> , 2004)
NtPI-PLC3	Plasma membrane	<i>Nicotiana tabacum</i>	YFP fusion	(Helling <i>et al.</i> , 2006)

6.2. The effect of EF-hand and C2-2 domains on TaPI-PLC2 targeting to PM

Different signals raise cytosolic calcium concentration which in turn is thought to regulate cellular and developmental processes via Ca^{2+} -binding proteins. Three out of the four classes of Ca^{2+} -binding proteins in plants contain Ca^{2+} -binding EF-hand motifs. The number of EF-hands in each protein varies from one to six (Day *et al.*, 2002). Some PI-PLCs in plants have EF-hand and others do not have (Kopka *et al.*, 1998). TaPI-PLC2 has four EF-hand motifs in the N-terminal region of its ORF. TaPI-PLC2 Δ EF-hand::GFP in which the four EF-hands were deleted was localized in PM, as was the intact PI-PLC2::GFP fusion

The C2 domain is thought to be involved in calcium-dependent phospholipid binding (Brose *et al.*, 1995) and in membrane targeting processes such as subcellular localization. TaPI-PLC2 Δ C2-2::GFP in which C2-2 was deleted, failed to localize to the PM. Kim *et al.*, (2004) made a truncation *Vigna radiata* Vr-PLC which the C2 domain was deleted, and found that the C2 domain was essential for Vr-PLC3 to be targeted to the plasma membrane.

7. TaPI-PLC1 and TaG α and their relations in signal transduction

BiFC studies found interaction between TaPI-PLC1 and TaG α on both the ER and PM. This is the same location for the full length TaPI-PLC1 expressed as a GFP fusion. TaG α was also detected in the PM and ER (data not shown). It has been reported in Arabidopsis that phospholipase D (PLD α 1) interacts with G protein α subunit (Zhao and Wang, 2004). Misra *et al.*, (2007) reported the interaction between G α and PI-PLC in *Pisum* and the interaction was mapped to the C2 domain. The TaPI-PLC1 from *Pisum* has

approximately 67% amino acid sequence identity. $G\alpha$ and PI-PLC interaction has been demonstrated with *in vitro* and *in vivo* studies in Pisum (Misra *et al.*, 2007), but to date, there has been no direct evidence for the localization of the $G\alpha$ and PLC interaction in plants. In this study, the interaction was seen clearly in the network structure of the ER in the upper focal planes of the cell as well as by co-localization with the ER marker. The interaction was seen in the plasma membrane that is readily viewed in the mid focal planes of the cell as well as by co-localization with the PM marker. In the mid cell focal plane the ER and the PM are in close proximity, never the less it was possible to distinguish ER from PM in this focal plane in most images for example (Figure 18b) which shows PI-PLC2 in the PM which is distinct from the location of the ER marker.

The localization of the GFP protein fusions and the BiFC YFP fusions were in agreement. The level of fluorescence seen in the interaction between TaPI-PLC1 and Ta $G\alpha$ -Q223L was higher than TaPI-PLC1 and Ta $G\alpha$ interaction. This suggests that PI-PLC1 preferentially interacts with the GTP bound form of $G\alpha$, in agreement with the classical model of PI-PLC and $G\alpha$ interaction and signaling. The effect of this interaction on the regulation of PI-PLC warrants further investigation. .

The expression system used in this study employed heterologous expression of genes derived from the monocot wheat in the cells of *N. benthamiana*, a dicot. The expression vectors give high levels of expression under the control of the constitutive 35S promoter, and the bacteria *Agrobacterium* was used for infiltration for transient expression. In spite of the possible compounfounding effects of these factors the specificity of protein localization and interaction appear to be maintained as evidenced by the lack of interaction of other candidate gens, namely The PG-PLCs.

8. TaPI-PLC1 and j822 non canonical GTP-binding protein interaction

J822 is a novel cold regulated gene in wheat which encodes a guanine nucleotide binding protein and was identified in a previous study of gene expression by microarray analyses (Gulick *et al.*, 2005). BiFC showed a positive interaction between TaPI-PLC1 and J822 was on both the ER and PM. Both TaPI-PLC1 and J822 were strongly induced by cold stress during the first 14 days of cold treatment. Yeast two-hybrid screening and BiFC showed that J822 interacts with proteins derived from partial length cDNA clones of PI-PLC1 and PG-PLC1 (Tardif *et al.*, 2007). In our data, a version of J822 starting with amino acid 81 interacts with the full length of TaPI-PLC1, while it did not show any interaction with TaPG-PLCs or TaPI-PLC2. In contrast to animals, plants seem to have only one or two heterotrimeric G α protein encoded in their genomes, so it is possible that plants have additional non-canonical GTP binding protein. The interaction of J822 with PI-PLC1 suggests that J822 is one of these non canonical G-proteins.

9. Future Studies

To date, there is just one or two G α in plants. It is possible that G α has multiple signaling functions through multiple interacting proteins or there are different G proteins that activate PI-PLC in the presence of different external signaling. The interaction between G α in plants with other proteins has been localized to the PM, (Assmann 2002). In our data, we found interaction between TaG α and TaPI-PLC in both PM and ER. The G protein (j822) showed a positive interaction with TaPI-PLC1 in the PM and ER as well.

My results raise several questions: Does the localization of the G-protein and TaPI-PLC1 interactions at the PM and ER has different signaling functions? Do the interactions of TaPI-PLC1 both G α and j822 have the same signaling pathway or not? Is G α in the

heterotrimeric G protein complex associated with the ER? If it is, is the complex different from the protein complex it is associated with in the PM? Does PI-PLC associate with $G\alpha$ as a monomer or in a complex? These questions could be addressed by the isolation of the membrane fractions and subsequently of the protein complexes associated with $G\alpha$ through TAP-tagging methods or by (GST). These complexes could be characterized by mass spectroscopy. Does the interaction between $G\alpha$ and PI-PLC activate PI-PLC? Is the interaction between $G\alpha$ and PI-PLC dependent on the GTP binding state of the protein and is $G\alpha$ and J822 interaction with PI-PLC competitive? This could be investigated by in vitro interaction studies with the proteins expressed and purified from E. coli. This has been started. Is the interaction between $G\alpha$ and PI-PLC1 due to $G\alpha$ that has been retained in the ER during its movement to the PM or does it relocate to the ER after localization to the PM?

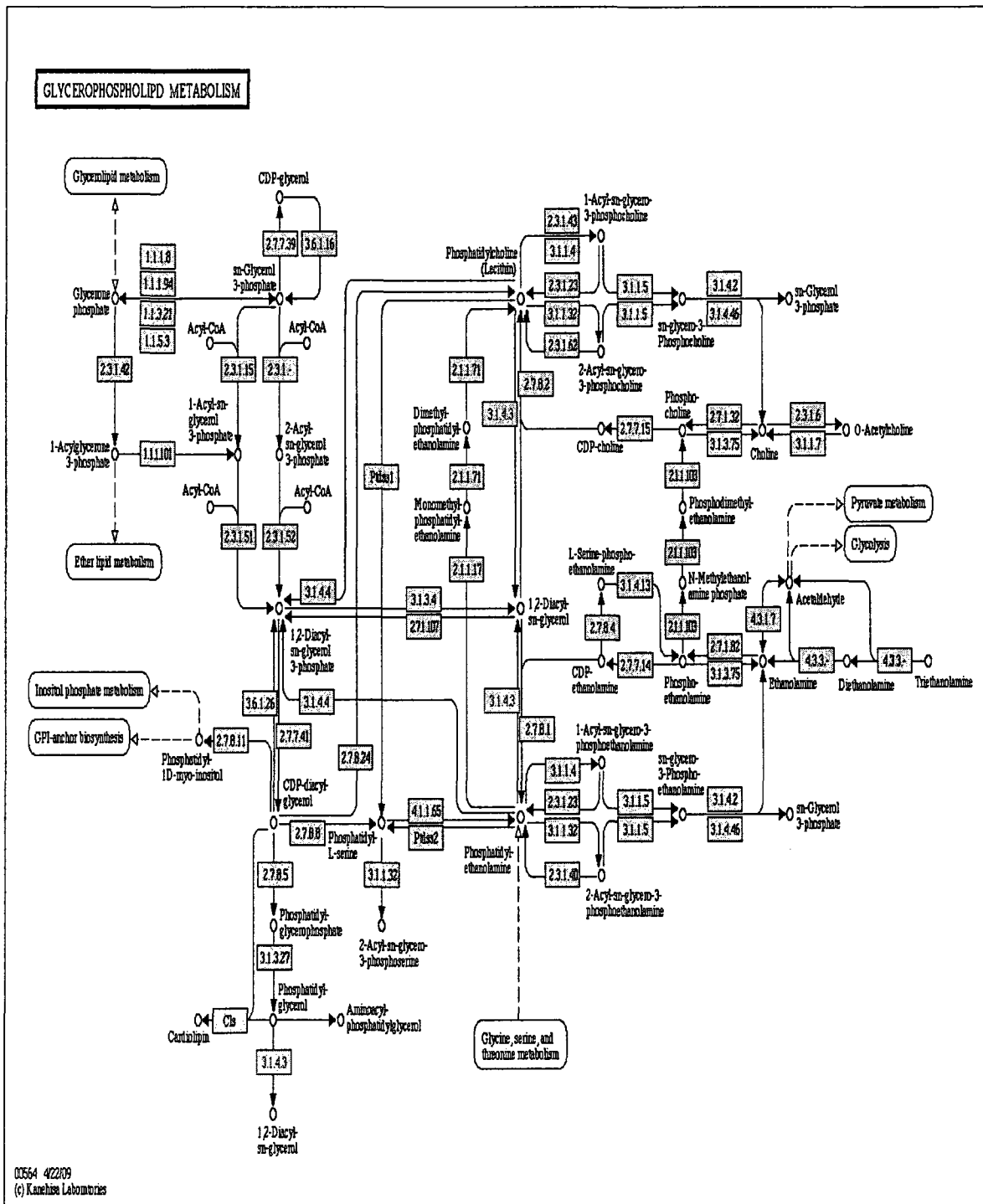
Appendix 2

T. aestivum PI-PLC2 ORF (FGAS code L3C112_D16)

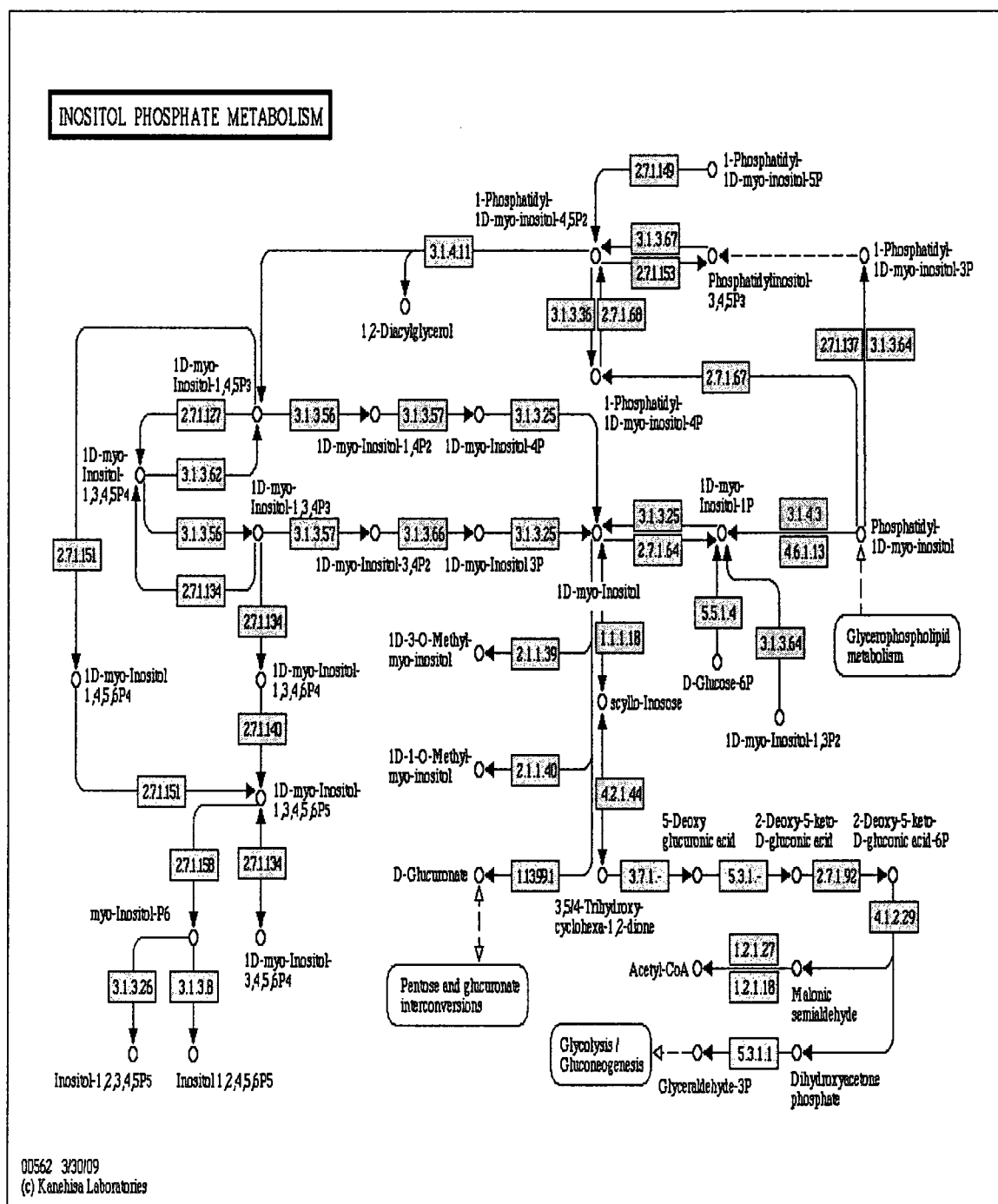
ACGACGTACAGGGTGTGCTGCTTCCTCCGGCGGTTCCGGCCGGCGTCCAACGAGCCGTCCGAGGCCATCGGGGACG
TGTTTCGAGGCGTACGCCGGCGCCGACGGCAGCGGCAGCGCGCTCGGGGAGGAGGCGCTCAGGAGGTTCCCTCCGGGAGGT
GCAGGGGGAGGCCGGCGACGACGACGTGAGGCGGGCGGAGGGAGGTCCTGGCCTTCGCGGCGGAGCACCGGTTGCTC
AAGAAGGGCGGGGGCTCACCGTTCGAGGGCTTCCACCGGTGGCTCTGCAGCGACGCCAACGCCGCCCTCCATCCTCGCC
GTGGGGTTACCATGACATGGGGCTGCCGCTGTGCGACTACTTCATCTACACGGGCCACAACCTCGTACCTGACCGGGAA
CCAGTGTAGCAGCGGGTGCAGCGAGGGCCCATCGCCAAGGCGCTTCGCGACGGCGTCAGGGTCATCGAGTTCGACCTC
TGGCCAATGCCGCCAAGGACGACGTGAGGTCCTCCACGGCAGGACATGGACGTGCGCGGTGGACCTGATGAAATGCC
TGGAGACCGTCAAGGAGCACGCCTTCGTCTCCTCCCCATACCCCGTTATCCTCACCCCTCGAAGATCACCTCACTCCGCA
TCTTCAAGCCAAAGTAGCAAAGATGGTCAAGGAGACATTCGGAGACTTGCTCCACCTCTCGGAGTCCGAGGCAATGCC
GTATTCCTTCCCCGAGGACCTCAGGGGCAAGATCATAATATCAACCAAACCGCCAAAAGAGTACCTTGAACCAAGA
GTAGCAAGGAGGAGGCCAAAATGGTAGCGCAGAGGAGGAGAGTGTGTGGGGGACGAGATCCCCGACAACAAGGCTCA
GGTGGCTACTGCTCGCCAGGTTTTCAGAGAAGGACACAGAGCGGTATGTGGAAGAGGATGAAGAGATGGAGAAGAAGGTA
CAACAGGGGGTTAACGGGGAGTATAAAAGTCTCATCTCAATCAGCCTCACCCGGAGAAAGCACGACATGGATCAGGATC
TCAAGGTTGATCCCGAGAAAGTGTCTCGGATGAGCTTGGGGGAGGGCGCATACGAGAAGGCCACCATTAATCATGGATC
TGAATATATAAAGTTTACACAGAGGAACCTTGCTACGGATTTTCCCAAAGACAACGCGCATTAATTCGTCCAATTACAAT
CCGCTGATGGGCTGGAGATATGGAGCTCAGATGGTTCAGCAAACATGCAGGGCCATGGAAGGAAACTATGGCTGACTC
AAGGATGTTCCGGGCAAATGGCGGTTGTGGTTATGTGAAAAGCCTGATTTTCTTATGAACACGGATAAAATGTTTGA
CCCTAGATCCAACTACCAAGTGAAGACAAGGCTCAAGGTGACTGTCTACATGGGAGACGGATGGCGATTCGACTTCCGT
AAGACGCATTTTCGACAAGTGCTCGCCACCAGACTTCTACGCAAGGGTGGGTATAGCAGGAGTGGTTGCAGACACAATGA
TGAAGGAGACCAAGGTGATCATGGACAACCTGGATACCGACGTGGGACCAGAGTTCGAGTTCCTCGCTGTCCGTGCCGGA
GCTCGCTCTGCTGCGGCTCGAGGTGCACGAGTCAGACAACCACGAAAGGACGACTTCGCGGCCAGACCTGCCTGCCG
GTCTGGGAGCTCCGGTCCGGGATACGCTCCGTACGGCTCTACGCCCGGATGGCGAGGTGCTGCGCTCGGTAAGCTGC
TAATGCGCTTCGAGTTTTCG

Appendix 3

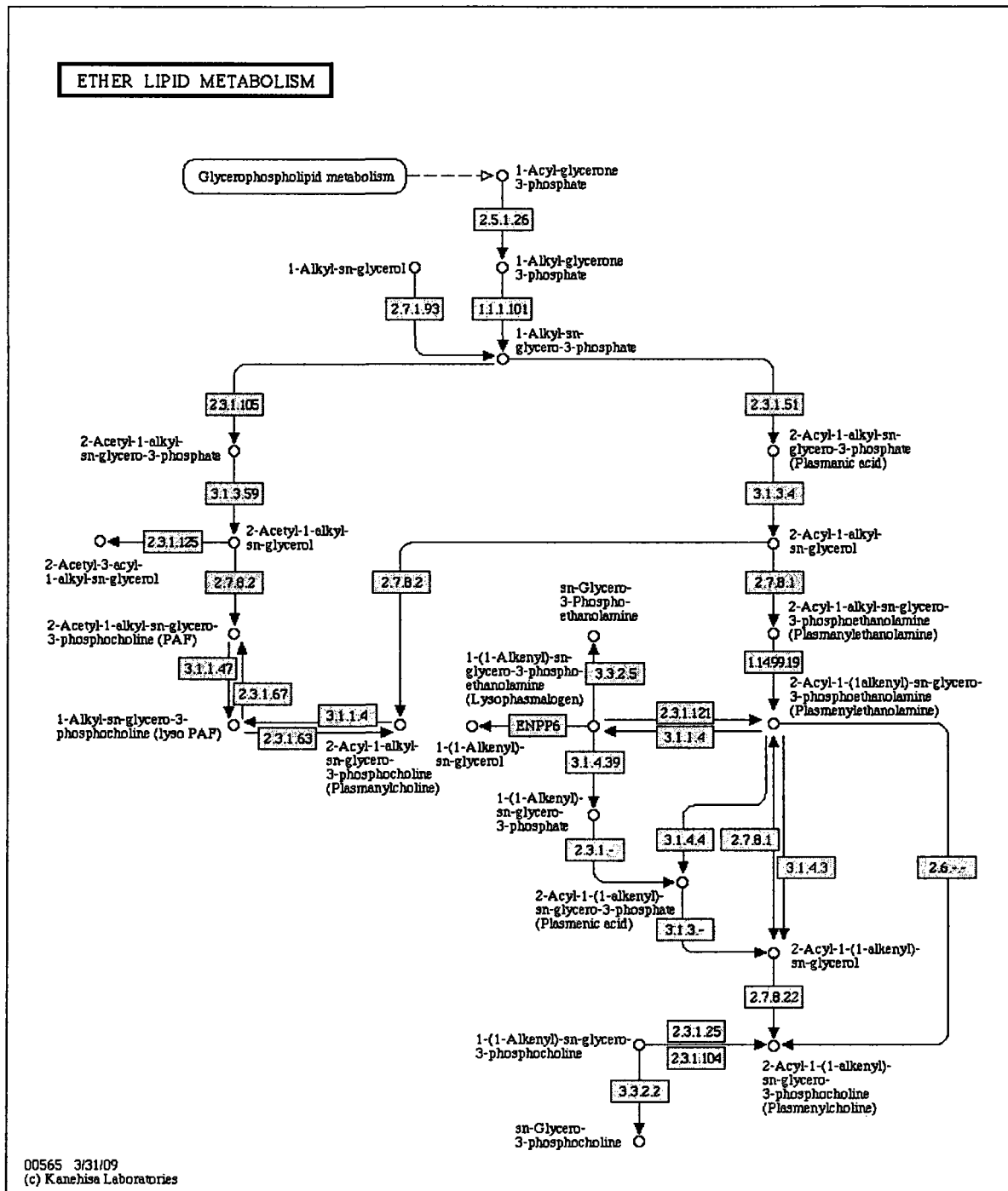
3.a. Glycerophospholipid metabolism:



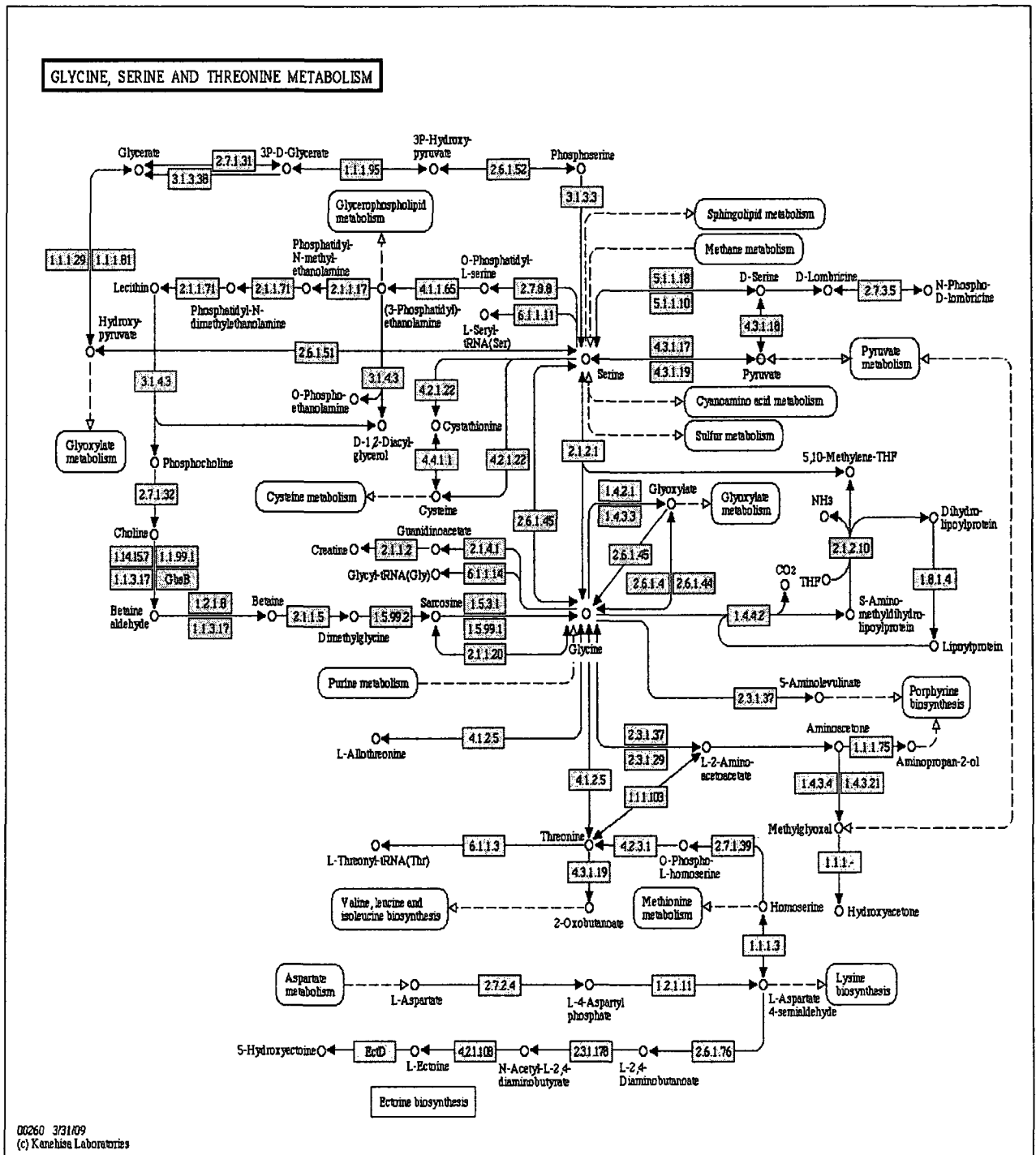
3.b. Inositol phosphate metabolism:



3.c. Ether lipid metabolism:



3.d. Glycine, serine and threonine metabolism:



REFERENCES

- Aiyar N., J. Disa, J. Stadel and P. Lysko (1999).** Recombinant calcitonin gene-related peptide (CGRP) human receptor independently stimulates 3',5'-cyclic adenosine monophosphate and Ca²⁺ signaling pathways. *Mol. Cell. Biochem.* 197: 179–185.
- Altschul S. F. , W. Gish , W. Miller , E. W. Meyersand, D. J. Lipman (1990).** Basic local alignment search tool. *J. Molec. Biol.* 215: 403-410.
- Baulcombe D. C., S. Chapman and S. Santa (1995).** Jellyfish green fluorescent protein as a reporter for virus infections. *Plant J.* 7: 1045-1053.
- Bokman S. H. and W. W. Ward (1981).** Renaturation of Aequorea green fluorescent protein. *Biochem. Biophys. Res. Commun.*, 101: 1372-1380.
- Bolwell G. P., Coulson V., Rodgers M. W., Murphy D. L., Jones D. (1991).** Modulation of the elicitation response in french bean cells and its implication for the mechanism of signal transduction. *Phytochemistry*, 30: 39-405.
- Boyer J.S. (1982).** Plant productivity and environment. *Science*, 218: 443–448.
- Brose N. A., G. Petrenko, T. C. Südhof and R. Jahn (1992).** Synaptotagmin: a Ca²⁺ sensor on the synaptic vesicle surface. *Science.* 256:1021–1025.
- Chalfie M., Y. Tu, G. Euskirchen, W. W. Ward and D. C. Prasher (1994).** Green fluorescent protein as a marker for gene expression. *Science*, 263:725-888.
- Cheng H. F., M. J. Jiang, C. L. Chen, S. M. Liu, L. P. Wang, J. W. Losmasney and K. King (1995).** Cloning and identification of amino acid residues of human phospholipase C δ 1 essential for catalysis. *Journal of Biochemical Chemistry*, 270: 5495-5505.
- Chiu W. L., Y. Niwa, W. Zeng, T. Hirano, H. Kobayashi and J. Sheen (1996).** Engineered GFP as a vital reporter in plants. *Curr. Biol.*, 6: 325-330.
- Day, I. S., V. S. Reddy, G. S. ali and A. S. N. Reddy (2002).** Analysis of EF-hand containing protein in arabidopsis. *Genome Biol.*, 3: 1-24.
- De Nisi P. and Zocchi G. (1996).** The role of calcium in the cold shock responses. *Plant Sci.*, 121: 161-166.
- Ding J. P., B. G. Pickard (1993).** Mechanosensory calcium-selective cation channels in epidermal cells. *Plant J.*, 3: 83–110.
- Ellis M. V., S. U. Katan and M. katton (1995).** Mutations within a highly conserved sequence present in the X region of phosphoinositide-specific phospholipase C δ 1. *Biochemical J.*, 307: 69-75.

- Endo T. R., Y. Mukai, M. Yamamoto and B. S. Gill (1991).** Physical mapping of a male-fertility gene o common wheat. *Japan J. Genet.*, 66: 291-295.
- Endo T.R. and B.S. Gill (1996).** The deletion stocks of common wheat. *J. Heredity*, 87: 295-307.
- English j. j., E. Mueller and D. C. Baulcombe (1996).** Suppression of virus accumulation in transgenic plants exhibiting silencing of nuclear genes. *Plant Cell*, 8: 179-188.
- Evans N. H., M. R. McAinsh and A. M.Hetherington (2001).** Calcium oscillations in higher plants. *Curr. Plant Biol.*, 4: 415-420.
- Farajalla M. R. and P. Gulick (2007).** Members of the α -tubulin gene family in wheat (*Triticum aestivum* L.) have differential expression during cold acclimation. *Genome*, 50: 502-510.
- Feuillet C. and M. J. Gary (2009).** Genetics and Genomics of the Triticeae. *Corp and models*, Vol. 7 (Ed.),2009.
- Galvez Susana, O. Roche, E. Bismuth, S. Brown, P. Gadai and M. Hodges (1998).** Mitochondrial localization of a NADR-dependent isocitrate dehydrogenase isoenzyme by using the green fluorescent protein as a marker. *Porc. Natl Acad. Sci.*, 95: 7813-7818.
- Garg P., V. Sharma, , P. Chaudhari and N. Roy (2008).** SubCellProt: Predicting Protein Subcellular Localization Using Machine Learning Approaches. *In Silico Biology. In Silico Biology*, 9.
- Gill, K. S., B. S. Gill and T. R. Endo (1993).** A chromosome region specific mapping strategy reveals gene-rich telomeric ends in wheat. *Chromosome*, 102: 374-381.
- Grebenok R. J., E. Pierson, G. M. Lambert, Gong, C. L. Afonso, R. Haldeman-Cahill, J. C. Carrington and D. W. Galbraith (1997).** Green-fluorescent protein fusions for efficient characterization of nuclear targeting. *Plant J.*, 11: 573-586.
- Gu X. and D. P. S. Verma (1997).** Dynamics of phragmoplastin in living cells during cell plate formation and uncoupling of cell elongation from the plane of cell division. *Plant Cell*, 9: 157-169.
- Gulick P. J., S. Drouin, Z. H.Yu, J. Danyluk, G. Poisson, A. F. Monroy, F. Sarhan (2005).** Transcriptome comparison of winter and spring wheat responding to low temperature. *Genome*, 48: 913-923.
- Hartley J. L., G. F. Temple and M. A. Brasch (2000).** DNA cloning using in vitro site-specific recombination. *Genome Res.*, 10: 1788-1795.
- Hartweck L. M.,D. J. Llewellyn, E. S. Dennis (1997).** The Arabidopsis thaliana genome has multiple divergent forms of phosphoinositol-specific phospholipase C. *Gene*, 202:151-156.

Heim R. and R. Y. Tsien (1996). Engineering green fluorescent protein for improved brightness, longer wavelengths and fluorescence resonance energy transfer. *Curr. Biol.*, 6: 178-182.

Heim R., D. C. Prasher and R. Y. Tsien (1994). Wavelength mutations and posttranslational autooxidation of green fluorescent protein. *Proc. Natl. Acad. Sci.*, 91: 12501-12504.

Heinlein M., B. L. Epel, H. S. Padgett and R. N. Beachy (1995). Interaction of tobamovirus movement proteins with the plant cytoskeleton. *Science*, 270: 1983-1985.

Helling D, Possart A, Cottier S, Klahre U, Kost B (2006) Pollen tube tip growth depends on plasma membrane polarization mediated by tobacco PLC3 activity and endocytic membrane recycling. *Plant Cell*, 18: 3519-3533.

Henriksson K. N. and A. J. Trewavas (2003). The effect of short-term low-temperature treatments on gene expression in Arabidopsis correlates with changes in intracellular Ca²⁺ levels. *Plant Cell Environ.*, 26: 485-496.

Hepler J. R., Gilman A. G. (1992). G proteins. *Trends Biochem. Sci.*, 17: 383-387.

Hirayama T, C. Ohto, T. Mizoguchi and K. A. Shinozaki (1995). Gene encoding a phosphatidylinositol-specific phospholipase C is induced by dehydration and salt stress in Arabidopsis thaliana. *Proc Natl Acad Sci.*, 92 (9):3903-3907.

Hu C. D. and T. K. Kerppola (2005). Direct visualization of protein interactions in living cells using bimolecular fluorescence complementation analysis. *Protein-Protein Interactions* (ed. P. Adams and E. Golemis), Cold Spring Harbor Laboratory Press, 34: 1-20.

Huang H., F. Tate, C. Crain and G. Cote (1995). Multiple phosphoinositide-specific phospholipases C in oat roots: characterization and partial purification. *Plant J.*, 8: 257-267.

Huang S., A. Sirikhachornkit, J. D. Faris, X. Su, B. S. Gill, R. Haselkorn and P. Gornicki (2002). Phylogenetic analysis of the acetyl-CoA carboxylase and 3-phosphoglycerate kinase loci in wheat and other grasses. *Plant Mol. Biol.*, 48:805-820.

Hunt L., L. Otterhag, J. C. Lee, T. Lasheen, J. Hunt, M. Seki, K. Shinozaki, M. Sommarin, D. J. Gilmour, C. Pical and J. E. Gray (2004). Gene-specific expression and calcium activation of Arabidopsis thaliana phospholipase C isoforms. *New phytologist*, 643-654.

Joung J., E. Ramm and C. Pabo (2000). A bacterial two-hybrid selection system for studying protein-DNA and protein-protein interactions. *Proc Natl Acad Sci.*, 13: 7382-7394.

Joyard J., E. marechal, C. Miege, M. A. Block, A. J. Dorne and R. Douce (1998). Structure, distribution and biosynthesis of glycerolipids from higher plant chloroplasts. *Lipids in photosynthesis. Kluwer academic publishers*, pp.21-52.

Kim W. Y., N. Y. Cheong, D. C. Lee, D. Y. Bahk, J. D. Je, M. J. Cho and S. Y. Lee (1995). Cloning and sequencing analysis of full length cDNA encoding a G-protein α subunit, SGA1, from soybean. *Plant Physiol.*, 108: 1315-1316.

Kim Y., K. Jee, L. Jae, L. Myoung, J. Ho, B. Young, H. Byung, H. Inhwan, K. Woo (2004). The Vr-PLC3 gene encodes a putative plasma membrane-localized phosphoinositide specific phospholipase C whose expression is induced by abiotic stress in mung bean *Vigna radiata* L. *FEBS Letters*, 556: 127-136.

Knight H. (2000). Calcium signaling during abiotic stress in plants. *International Rev. Cytol.*, 195: 269-325.

Knight H., A. J. Trewavas and M. R. Knight (1996). Cold calcium signaling in *Arabidopsis* involves two cellular pools and a change in calcium signature after acclimation. *Plant Cell*, 8: 489-503.

Knight M. R., A. K. Campbell, S. M. Smith and A. J. Trewavas (1991). Transgenic plant aequorin reports the effects of touch and cold-shock and elicitors on cytoplasmic calcium. *Nature*, 352: 524-526.

Kohler R.H., W. R. Zipfel, W. W. Webb and M. R. Hanson (1997). The green fluorescent protein as a marker to visualize plant mitochondria in vivo. *Plant J.*, 11: 613-621.

Kopka J., C. Pical, J. E. Gray and B. Muller (1998). Molecular and enzymatic characterization of three phosphoinositide-specific phospholipase C isoforms from potato. *Plant Physiol.*, 116: 239-250.

Krebs J. A., Y. Wu, H. S. Chang, T. Zhu, X. Wang and J. Harper (2002). Transcriptome changes for *Arabidopsis* in response to salt, osmotic, and cold stress. *Plant Physiol.*, 130: 2129-2141.

Krinke O., N. Zuzana, V. Olga and M. Jan (2007). Inositol triphosphate receptor in higher plants: is it real? *Journal of Experimental Botany*, 58: 361-376.

Laxalt A. M. and T. Munnik (2002). Phospholipid signalling in plant defence. *Curr. Opin. Plant Biol.*, 5: 332-338.

Linkiewicz A. M., L. L. Qi, B. S. Gill, A. Ratnasiri, B. Echalié, S. Chao, G. R. Lazo, D. D. Hummel, O. D. Anderson, E. D. Akhunov, J. Dvorák, M. S. Pathan, H. T. Nguyen, J. H. Peng, N. L. V. Lapitan, Miftahudin, J. P. Gustafson, C. M. La Rota, M. E. Sorrells, K. G. Hossain, V. Kalavacharla, S.F. Kianian, D. Sandhu, S. N. Bondareva, K. S. Gill, E. J. Conley, J. A. Anderson, R. D. Fenton, T. J. Close, P. E. McGuire, C. O. Qualset, and J. Dubcovsky (2004). A 2500-locus bin map of wheat homoeologous group 5 provides insights on gene distribution and colinearity with rice. *Genetics*, 168: 665-676.

Liu W. (2005). Characterization J822, a novel cold induced GTP-binding protein gene in wheat (*Triticum aestivum*). *Thesis*.

- Lundberg G. A. and M. Sommarin (1992).** Diacylglycerol kinase in plasma membranes from wheat. *Biochim. Biophys. Acta*, 1123: 177–183.
- Ma H., M. F. Yanofsky and E. M. Meyerowitz (1990).** Molecular cloning and characterization of GPA1, a G-protein α subunit gene from Arabidopsis. *Proc. Natl. Acad. Sci.*, 87: 3821-3825.
- Marcotte E. M., I. Xenarios, A. M. Blik, and D. Eisenberg (2000).** Localizing proteins in the cell from their phylogenetic profiles. *Proc. Natl. Acad. Sci.*, 97: 12115-12120.
- McIntosh R. A., Y. Yamazaki, K. M. Devos, J. Dubcovsky, W. J. Rogers and R. Appels (2003).** Catalogue of gene symbols for wheat (MacGene 2003) Int. *Wheat Genet. Symp.*, 4: 312-320.
- Meijer H. J. G. and T. Munnik (2003).** Phospholipid-based signaling in plants. *Annu. Rev. Plant Biol.*, 54: 265–306.
- Misra S., W. Yuliang, V. Gayatri, K. S. Sopory and T. Narendra (2007).** Heterotrimeric G-protein complex and G-protein-coupled receptor from a legume (*Pisum sativum*): role in salinity and heat stress and cross-talk with phospholipase C. *The plant J.*, 51: 656-669.
- Monroy A. F. and R. S. Dhindsa (1995).** Low-temperature signal transduction: induction of cold acclimation-specific genes of alfalfa by calcium. *Plant Cell*, 7: 321-331.
- Mueller-Roeber B. and C. Pical (2002).** Inositol phospholipid metabolism in *Arabidopsis*. Characterized and putative isoforms of inositol phospholipid kinase and phosphoinositide-specific phospholipase C. *Plant Physiol.*, 130:22–46.
- Mukai Y. and T. R. Endo (1992).** Physical mapping of a fertility- restoring gene against *Aegilops kotschy* cyto-)lasm in wheat. *Japan J. Genet.*, 67: 199-207.
- Munnik T. (2001).** Phospholipid-derived second messengers in plants - Differences and similarities. FEBS Advanced Course: Lipid-mediated signalling in cellular functions, June 23, *Santa Maria Imbaro*, Italy.
- Munnik T., R. F. Irvine and A. Musgrave (1998).** Phospholipid signalling in plants. *Biochem. Biophys. Acta.*, 1389: 222–272.
- Murata N. and D. A. Los (1997).** Membrane fluidity and temperature perception. *Plant Physiol.*, 115: 875–879.
- Nakamura Y., K. Awai, T. Masuda, Y. Yosshioka, K. Takamiya and H. Ohta (2005).** A Novel phosphatidylecholine- hydrolyzing phospholipase C induced by phosphate starvation in Arabidopsis. *The Journal of Biological Chemistry*, 280:7469-7476.
- Nelson K. B., C. Xue and N. Andreas (2007).** A multicolored set of in vivo organelle markers for co-localization studied in Arabidopsis and other plants. *The plant J.*, 51: 1126-1136.

Niedz R. P., M. R. Sussman and J. S. Satterlee (1995). Green fluorescent protein: an in vivo reporter of plant gene expression. *Plant Cell*, 14: 403-406.

Novotná Z. , J. Martinec, B. Profotová, S Zaroová, J.C. Kader and O. Valentová (2003). In vitro distribution and characterization of membrane-associated PLD and PI-PLC in *Brassica napus*, *J Exp. Bot.*, 54: 691–698.

Ohlrogge J. and J. Browse (1995). Lipid biosynthesis. *Plant Cell*, 7: 957-970.

Otterhag L., M. Sommarin and C. Pical (2001). N-terminal EF-hand-like domain is required for phosphoinositide-specific phospholipase C activity in *Arabidopsis thaliana*. *FEBS Letters*, 497: 165–170.

Paetzel M., R. E. Dalbey And N. C. J. Strynadka (2002). Crystal structure of a bacterial signal peptidase apoenzyme. *J Biol Chem* 277, 9512–9519.

Peng, J. H. , G. R. Lazo, J. P. Gustafson, S. Chao, O. D. Anderson, L. L. Qi, B. Echalié, R. A. Greene, M. E. Sorrells, E. D. Akhunov, J. Dvorak, A. M. Linkiewicz , J. Dubcovsky, K. G. Hossain, V. Kalavacharla, S. F. Kianian, A. A. Mahmoud, Miftahudin, E. J. Conley, J. A. Anderson, M. S. Pathan, H. T. Nguyen, P. E. McGuire, C. O. Qualset and N. L. V. Lapitan (2004). Chromosome bin map of expressed sequence tags in homoeologous group 1 of hexaploid wheat and homoeology with rice and *Arabidopsis*. *Genetics*, 168: 609-623.

Phizicky E. M. and F. Stanley (1995). Protein-protein interactions: methods for detection and analysis. *American Society for Microbiology*, 59(1): 94-123.

Plieth C. (2005). Calcium: Just another regulator in the machinery of life? *Ann. Bot. Lond.*, 96: 1-8.

Prasher D. C., V. K. Eckenrode, W. W. Ward, F .G. Prendergrast and M. J. Cormier (1992). Primary structure of the *Aequorea victoria* green fluorescent protein. *Gene*, 111: 229-233.

Qi L. L. (2004). A chromosome bin map of 16,000 expressed Sequence Tag loci and distribution of genes among the threegenomes of polyploidy wheat. *Genetics*, 168: 701-712.

Qi L. L., and B. S. Gill (2001). High-density physical maps reveal that the dominant male-sterile gene Ms3 is located in a genomic region of low recombination in wheat and is not amenable to map-based cloning. *Theor. Appl. Genet.* 103: 998–1006.

Rozen S, H. J. Skaletsky (2000). Primer3 on the WWW for general users and for biologist programmers. In: Krawetz S, Misener S (eds) *Bioinformatics Methods and Protocols: Methods in Molecular Biology*. *Humana Press, Totowa, NJ*. pp 365-386.

Sambrook J.; E. F. Fritsch and T. Maniatis (1989). *Molecular Cloning: a laboratory manual*. 2nd ed. N.Y., Cold Spring Harbor Laboratory, *Cold Spring Harbor Laboratory Press*, pp:1659- 1671.

Sanchez J. P. and N. H. Chua (2001). *Arabidopsis* PLC1 is required for secondary responses to abscisic acid signals. *Plant Cell*, 13:1143-1154.

- Scott M. S., D. Y. Thomas, and M. T. Hallett (2004).** Predicting subcellular localization via protein motif co-occurrence. *Genome Res.*, 14: 1957-1966.
- Sears E. R. (1966).** Nullisomic-tetrasomic combinations in hexaploid wheat, in *Chromosome Manipulations and Plant Genetics*, edited by R. RILEY and K. R. LEWIS, /Oliver & Boyd, Edinburgh, pp. 29–45
- Sears E. R. and L. M. S. Sears (1978).** The telocentric chromosomes on common wheat. In proceeding of 5th international wheat genetic symposium, Indian society of genetics and plant breeding. pp: 389-407.
- Sebastian Y., B. and N. V. Raikhell (1992).** Intracellular trafficking of secretory proteins. *Plant Mol. Biol.*, 20: 133-150, 1992.
- Shcherban A. B., E. K. Khlestkina, and E. A. Salina (2004).** Analysis of the DNA Marker Specific to the Wheat G Genome. *Russian Journal of Genetics*, 40: 288-294.
- Sheen J., S. B. Hwang, Y. Niwa, H. Kobayashi and D. W. Galbraith (1995).** Green fluorescent protein as a new vital marker in plant cells. *Plant J.*, 8: 777-784.
- Shi J., R. A. Gonzales, M. K. Bhattacharyya (1995).** Characterization of plasma membrane-associated phosphoinositide-specific phospholipase C from soybean. *The Planta J.*, 8: 381-390.
- Siegenthaler P. A. (1998).** Molecular organization of acyl lipids in photosynthetic membranes of higher plants. Lipids in photosynthesis. *Kluwer academic publishers*, pp.119-144.
- Simockova M., R. Holic, D. Tahotna, J. Patton and P. Griac (2008).** Yeast Pgc1p (YPL206c) controls the amount of phosphatidylglycerol via a phospholipase C-type degradation mechanism. *J. Biol. Chem.*, 283:17107–15.
- Singh K., M. Ghai, M. Garg, P. Chhuneja, P. Kaur, T. Schnurbusch · B. Keller, H. S. Dhaliwal (2007).** An integrated molecular linkage map of diploid wheat based on a *Triticum boeoticum* × *T. monococcum* RIL population. *Theor. Appl. Genet.*, 115: 301–312
- Song F. and M. R. Goodman (2002).** Molecular cloning and characterization of a rice phosphoinositide-specific phospholipase C gene, OsPI-PLC1, that is activated in systemic acquired resistance. *Physiological and Molecular Plant Pathology*, 61: 31-40.
- Staci M., S.A. Mabon and N. Stewart (1997).** Applications of green fluorescent protein in plants. *BioTechniques*, 23: 912-918.
- Subbaiah C. C., D. S. Bush and M. M. Sachs (1998).** Mitochondrial contribution to the anoxic Ca²⁺ signal in maize suspension-cultured cells. *Plant Physiol.*, 118: 759-771.
- Tardif G., A. K. Ndjido, A. Helene, L. Louisette, M. Genevive, G. Partic, S. Fathy and L. Jean-Francois (2007).** Interaction network of proteins associated with abiotic stress response and development in wheat. *Plant Mol. Biol.*, 63: 703-718.

- Tsien R. Y. (1998).** The Green Fluorescent Protein. *Annu. Rev. Biochemistry*, 67: 509-544.
- Vergnolle C., M. N. Vaultier , L. Taconnat , J. P. Renou , J. C. Kader , A. Zachowski, E. Ruelland (2005).** The Cold-Induced Early Activation of Phospholipase C and D Pathways Determines the Response of Two Distinct Clusters of Genes in Arabidopsis Cell Suspensions. *Plant Physiol.*, 139: 1217-1233.
- Voinnet O., S. Rivas, P. Mestre and D. C. Baulcombe D.C. (2003).** An enhanced transient expression system in plants based on suppression of gene silencing by the p19 protein of tomato bushy stunt virus. *Plant J.*, 33: 949–956
- Wang C., C. A. Zien, M. Afithile, R. Welti, D. F. Hildebr and X. Wang (2000).** Involvement of phospholipase D in wound-induced accumulation of jasmonic acid in Arabidopsis. *Plant Cell*, 12: 2237–2246.
- Wang X. (2001).** Plant phospholipases. *Ann. Rev. Plant Mol. Biol.*, 52: 211-231.
- Wang X. (2002).** Phospholipase D in hormonal and stress signaling. *Curr. Opin. Plant Biol.*, 5: 408–414.
- Wang X. Q, H. Ullah, A. M. Jones, S. M. Assmann (2001).** G protein regulation of ion channels and abscisic acid signalling in Arabidopsis guard cells. *Science*, 292: 2070–2072.
- Ward W. W., H. J. Prentice, A. F. Roth, C. W. Cody and S. C. Reeves (1982).** Spectral perturbations of the Aequoreagreen fluorescent protein. *Photochem. Photobiol.*, 35: 803-808.
- Welti R., W. Li, M. Li, Y. Sang, H. Biesiada, H. E. Zhou, C. B. Rajashekar, T. D. Williams, X. Wang (2002).** Profiling membrane lipids in plant stress responses. Role of phospholipase D alpha in freezing-induced lipidchanges in Arabidopsis. *J. Biol Chem.*, 277: 31994-32002.
- Werner J. E., T. R. Endo and B. S. Gill (1992).** Toward a cytogenetically based physical map of wheat genome. *Proc. Natl. Acad. Sci.*, 89: 11307-11311.
- Willemot, C., and L. Pelletier (1980).** Influence of light and temperature on the content of linolenic acid and the resistance to frost of winter wheat. *Can. J. Plant Sci.*, 60: 349–355.
- Williams R. L. (1999).** Mammalian phosphoinositide-specific phospholipase C. *Biochim. Biophys. Acta.*, 1141: 255-267.
- Xiong, L., H. Lee, M. Ishitani, and J. K. Zhu (2002).** Regulation of osmotic stress-responsive gene expression by the *LOS6/ABA1* locus in Arabidopsis. *J. Biol. Chem.* 277, 8588–8569.
- Yamamori M., T. Nakamura, T. R. Endo, and T. Nagamine (1994).** Waxy protein deficiency and chromosomal location of coding genes in common wheat. *Theor. Appl. Genet.*, 89: 179-184.

Yang T. T., L. Z. Cheng and S. R. Kain (1996). Optimized codon usage and chromophore mutations provide enhanced sensitivity with the green fluorescent protein. *Nucleic Acid Res.*, 24: 4592-4593.

Yotsushima, K., Mitsui, T., Takaoka, T., Hayakawa, T. und Gaue, I. (1993). Purification and Characterization of Membrane-Bound Inositol Phospholipid. Specific Phospholipase C from Suspension-Cultured Rice (*Oryza sativa* L) Cells - Identification of A Regulatory Factor. *Plant Physiology* 102: 165-172.

Zhang C. and C. L. Guy (2005). Co-immunoprecipitation of Hsp101 with cytosolic Hsc70. *Plant Phy. and Bioch.*, 43:13-18.

Zhao, J. and X. Wang. (2004). Arabidopsis phospholipase D α 1 interacts with the heterotrimeric G-protein α -subunit through a motif analogous to the DRY motif in G-protein-coupled receptors. *J. Biol. Chem.* 279:1794-1800.

Zhu J. K. (2002). Salt and drought stress signal transduction in plants. *Annu. Rev. Plant Biol.*, 53: 247-273.